STUDIES ON THE CATALYTIC MECHANISM OF

CYTOCHROME BC_1 COMPLEX

By

SHAOQING YANG

Bachelor of Science in Biochemistry
Jilin University
Changchun, P.R.China
1996

Master of Science in Biochemistry & Molecular Biology
Nankai University
Tianjin, P.R.China
1999

Submitted to the Faculty of the
Graduate College of the
Oklahoma State University
in partial fulfillment of
the requirements for
the Degree of
DOCTOR OF PHILOSOPHY
July, 2008

STUDIES ON THE CATALYTIC MECHANISM OF

CYTOCHROME BC_1 COMPLEX

Dissertation Approved:

Dr. Chang-An Yu
Thesis Advisor

Dr. Linda Yu

Dr. Robert Burnap

Dr. Robert Matts

Dr. Michael Massiah

Dr. A.Gordon Emslie
Dean of the Graduate College

ACKNOWLEDGEMENTS

I wish to express my sincere appreciation to my major advisor, Dr. Chang-An Yu for his intelligent supervision, constructive guidance, and inspiration. I am also equally grateful to Dr. Linda Yu for her encouragement and guidance during my study. I want to express my thanks to them and the Department of Biochemistry and Molecular Biology for providing financial support and research opportunity.

My sincere appreciation also extends to my committee members, Dr. Robert Matts, Dr. Robert Burnap and Dr. Michael Massiah for their advice and guidance. My sincere gratitude also extends to students and postdoctorates, both former and current, in Dr. Yu's lab for their assistance, hospitality and stimulating discussions.

I would like to thank my family for their love and constant support. I would like dedicate this thesis to my sisters, my parents, my wife and my newborn son. Without their love and support, I don't think I can go this far.

TABLE OF CONTENTS

Chapter Page

Chapter Page

LIST OF TABLES

LIST OF FIGURES

Figure Page

Figure Page

NOMENCLATURE

ADP	Adenosine diphosphate
ATP	Adenosine triphosphate
bc_1	Cytochrome bc_1 complex
β-ME	β-Mercaptoethanol
Cyt.	Cytochrome
DM	*N*-Dodecyl- β -D-Maltopyranoside
DNA	Deoxyribonucleic acid
E. coli	Escherichia coli
EPR	Electron Paramagnetic Resonance
ICM	Intra-Cytoplasmic Membrane
ISP	Iron Sulfur Protein
kDa	kilodaltons
kb	kilo base pairs
LB	Lennox L. Broth
MCLA	6-(4- methoxyphenyl)-2-methyl-3,7-dihydroimidazo[1,2-a] pyrazin-3 (7H) – one hydrochloride
NAD+	Nicotinamide adenine dinucleotide
NADH	Nicotinamide adenine dinucleotide (reduced form)
Ni-NTA	Nickel-Nitrilo Triactic Acid
OG	*N*-octyl-β-D-Gluocopyranoside
PAGE	Polyacrylmide gel electrophoresis
PCR	Polymerase Chain Reaction

PMSF	Phenylmethylsulfonyl fluoride
Pi	Phosphate
Q	Ubiquinone
QH_2	Ubiquinol
$Q_0C_{10}Br$	2,3-dimethoxy-5-methyl-6-(10-bromo)-decyl-1,4-benzoquinone
R.S.	*Rhodobacter sphaeroides*
Ru_2D	$[Ru(bpy)_2]_2(qpy)(PF_6)_4$; qpy, 2,2':4',4":2",2"'–quaterpyridine
SDS	Sodium Dodecyl Sulfate
UHDBT	5-*n*-undecyl-6-hydroxyl-4,7-dioxobenzothiazole
UV	Ultra Violet

CHAPTER I

INTRODUCTION

All living organisms need energy to support their lives. For most energy-consuming biological processes, adenosine triphosphate (ATP) is the direct fuel. In eukaryotic cells, more than 95% of ATP is produced in a process called oxidative phosphorylation. Oxidative phosphorylation occurs in the mitochondrial intermembrane and is carried out by the electron transfer chain and ATP synthase. Driven by a proton gradient across the inner membrane, ATP synthase can synthesize ATP from ADP and Pi. The generation of a proton gradient across mitochondrial inner membrane is carried out by the electron transfer chain (Figure I-1) which is composed of four complexes, called complex I (also known as NADH-ubiquinone oxidoreductase), complex II (also known as succinate ubiquinone reductase), complex III (also known as ubiquinol-cytochrome c reductase) and complex IV(also known ascytochrome *c* oxidase). These four complexes, as well as ATP synthase, are located in the mitochondrial inner membrane. The molar ratio of these five components in living bovine mitochondria is $1.1 \pm 0.2 : 1.3 \pm 0.1 : 3 : 6.7 \pm 0.8 : 3.5 \pm 0.2$ (1). All complexes in the electron transfer chain are enzymes catalyzing electron transfer from reductant to oxidant. Table I-1 shows the characteristics of these complexes.

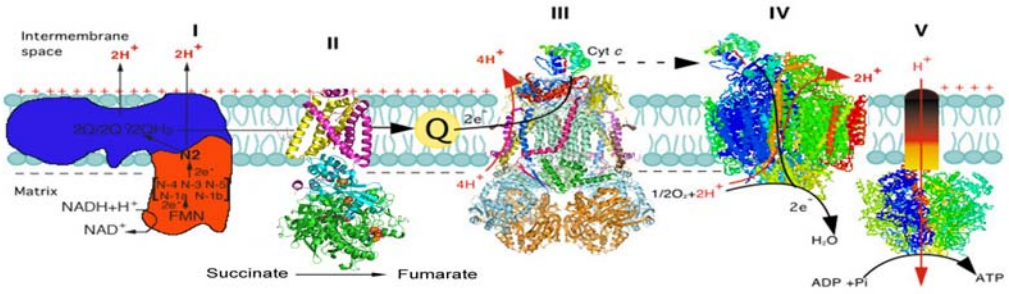

Figure I-1: Electron transfer chain in mitochondria. For more details, see the context

Table I-1: Properties of Bovine Heart Mitochondiral Electron Transfer Complexes

Complex	Other names	Subunits	Proton Pumping	M.W. (monomer) (kDa)	Prosthetic groups	Em (mV)
$I^{(2)}$	NADH-UQ reductase (NQR)	43	Yes	907	FMN	-245~335
					[2Fe2S]N-1a	-375
					[2Fe2S]N-1b	-250
					[2Fe2S]N-2	-150
					[2Fe2S]N-3,4	-250
					[2Fe2S]N-5,6	-260
$II^{(3-5)}$	Succinate-UQ reductase (SQR)	5	No	127	FAD	-40
					[2Fe2S]S-1	0
					[4Fe4S]S-2	-270
					[3Fe4S]S-3	130
					b_{560}	-185
$III^{(6)}$	UQH_2-cytochrome *c* reductase (QCR)	11	Yes	248	b_{562} (b_H)	30
					b_{566} (b_L)	-30
					c_1	230
					2Fe2S	280
$IV^{(7)}$	Cytochrome *c* oxidase (CcO)	13	Yes	204	a	210
					Cu_A	245
					Cu_B	340
					a_3	385

Among these four complexes in the electron transfer chain, complexes I, III and IV are redox-linked proton pumps. Unlike these three complexes, complex II only catalyzes the electron transfer from succinate to ubiquinone, without concomitant proton pumping.

Although these three complexes can pump protons from the matrix to the intermembrane space, they adopt different mechanisms to perform proton pumping. In recent decades, different groups have solved the structures of complexes II, III, IV and ATP synthase through crystallization. These crystallographic structures have not only largely supported previous works, but also provided new information to help us to understand the catalytic mechanism of these complexes.(8).

Our group has been working on complex III for a couple of decades and has made some contributions in the structure and catalytic mechanism of complex III. However, there are still a lot of things remaining unclear. Understanding previous work will help us to develop new ideas.

I. Overviews of Cytochrome bc_1 Complex

Cytochrome bc_1 complex, also called complex III or ubiquione-cytochrome *c* oxidoreductase, is the third complex of the electron transfer chain in the mitochondria. It catalyzes the electron transfer from ubiquinol to cytochrome *c* with concomitant proton translocation across the mitochondrial innermembrane. Cytochrome bc_1 complex can be found in various species, each containing a different number of subunits. Table I-2 shows the numbers of subunits of bc_1 complexes from different sources (9).

Table I-2: The number of subunits in bovine bc_1 complexes from different species(9)

Species	Number of subunits	Relative Specific Activity (%)
Bovine	11	100
Potato	10	N/A
Chicken	10	N/A
Yeast	10	50
Rhodobacter sphaeroides	4	2
Rhodobacter capsulatus	3	1

Table I-3: Em of redox prosthetic groups of cytochrome bc_1 from different species

	Heme b_L	Heme b_H	Iron-sulfur cluster	Heme c_1	Heme c (c_2)
Yeast	-30[10], -20[11]	120[10],62[11]	285[10]	270[11]	260[12]
bovine	-100[13],-20[14]	75[13]	290[14-18]	227[19],250[14]	260[12]
R.Sphaeroides	-87[20,21]	41[20,21]	290[22]	228[23],290[24]	340[25]

Although bc_1 complexes from different sources have a different number of subunits, they share three common subunits: cytochrome *b*, cytochrome c_1 and ISP. These three common subunits house four redox prosthetic groups: hemes b_L, b_H, c_1, and iron-sulfur cluster. Table I-3 shows these four prosthetic groups' Em in bc_1 complexes from different species. These three common subunits are the most important subunits for bc_1 complex catalysis. Other supernumerary subunits contribute to the stability of the bc_1 complexes, and prevent electron leak during electron transfer(26,27).

Our group has been working on cytochrome bc_1 crystallizaiton since 1991 (28). In 1997 our group crystallized the bc_1 complex. With the cooperation of Deisenhofer group, we solved bovine bc_1 complex's crystallographic structure (29). This 3-D structure strongly supports the hypothesis of "Q-cycle", which elucidates the catalytic mechanism of the bc_1 complex. Since then, workers from other groups have solved bc_1 complexes structure from other species such as: chicken, yeast and bacteria (30-33).

II. Bovine Cytochrome bc_1 Structure(29)

The bovine mitochondrial bc_1 complex is in a dimeric form (Figure I-2). It is pear-shaped with a maximal diameter of 130Å and a height of 155Å(29,34). The height consists of three regions: the inner membrane region (38Å), the transmembrane region (42Å) and the matrix region (75Å). Bovine mitochondrial bc_1 complex contains total 11 subunits. These 11 subunits can be divided in three different regions: The intermembrane space region consists of the extramembranous domains of cytochrome c_1, ISP, and subunit 8. The transmembrane region consists of cytochrome *b*, helix domains of cytochrome c1, ISP and subunit 7, 10 and subunit 11. The matrix region primarily

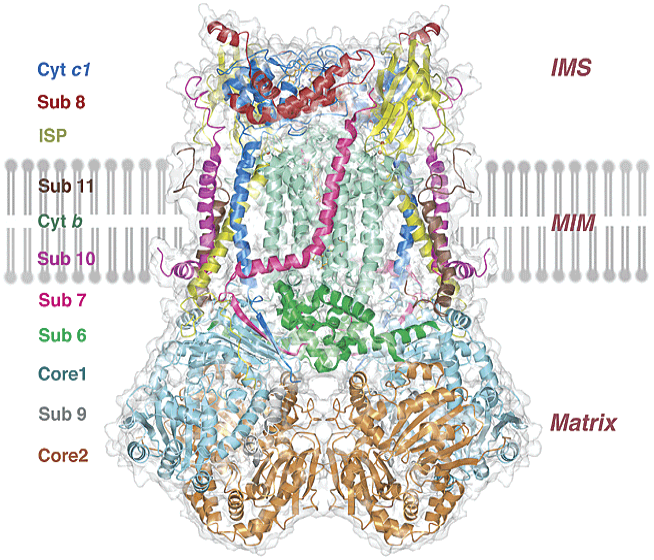

Figure I-2: Cytochrome bc_1 complex crystallographic structure(35,36). The color code for each subunit is given on the side bar. The two parallel lines indicate the membrane-spanning regions. The mitochondrial inter-membrane space (IMS), the membrane spanning region (TM), and the matrix are as labeled

consists of core 1 and core 2, subunit 6, subunit 9 and N-terminal part of subunit 7 and C-terminal of ISP.

1. Structure of Cytochrome *b* (Figure I-3):

Cytochrome *b* is one of the three core subunits of various bc_1 complexes. QH_2 oxidation and rereduction of Q are performed in it. Cytochrome *b* subunit has 8 membrane-spanning helices, named as A-H. These eight helices form 2 groups: helices A,B,C,D,E are in group I and F,G,H in group II. These two groups contact in the matrix side and are separated on the intermembrane space side. These eight helices are connected by four long loops (AB, CD, DE, and EF) and three short loops (BC, FG, and GH). The DE loop is located on the matrix side and the other three loops are on the other side. The CD loop has two short helices, named cd1 and cd2, which are close to the proposed Q_P binding sites, and contact with ISP head domain if ISP is at the *b* position. A helical bundle formed by helices A,B,C,D host heme b_L and b_H. (29). Heme b_L and b_H are ligated by H83/H182, and by H97/H196 on helices B and D, repectively. The closest distance of these two hemes is 8.2Å, facilitating to the efficient electron transfer between them. Cytochrome *b* is the Q-binding subunit, which contains two Q-binding site: Q_P and Q_N. The Qp pocket is on the side of intermemebrane space and the QN pocket is on the side of matrix.

Q_P Pocket (35,37): Reduced QH_2 is oxidized at the Qp pocket . The Qp pocket is proposed in the hypothesis of "Q-cycle"(38), but the exact location of the Q_P pocket remains unclear, even after the resolution of X-ray crystal structure of bc_1 complexes from various species. The oxidation of QH_2 at the Qp pocket is bifurcated. So far, there is no any native Q occupant found in the "Q_P" site in all of those published X-ray bc_1

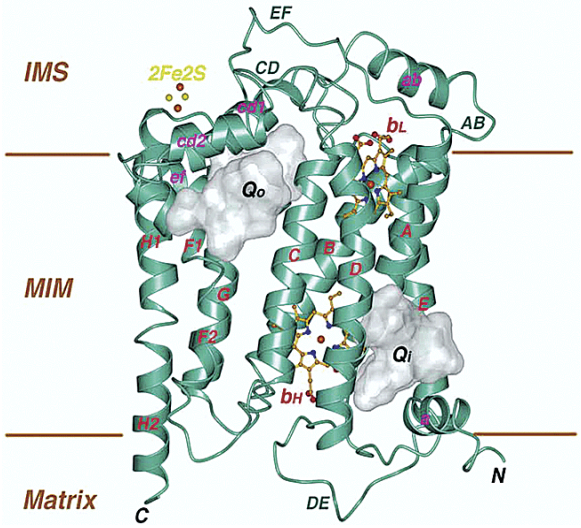

Figure I-3: Q_P and Q_N pockets in the cyt. *b* subunit of bc_1(39). The eight TM helices are labeled A-H. Four prominent surface loops are labeled as AB, CD, DE, and EF. The helices within the surface loops are labeled as ab, cd1, cd2, and ef. Hemes b_L and b_H are shown as stick mode with carbon atom in yellow, nitrogen atom in blue and oxygen in red. The two substrate binding pockets, Q_P and Q_N are labeled. Adopted from reference (5,39)

complex structures. Therefore, scientists only can presume the location of the Qp pocket based on the X-ray structure of bc_1 complexes with inhibitors and on the extrapolation by inference to involvement of ligands that interact with these inhibitors. Based on crystal structures of bc_1 complexes with different Q_P inhibitors, Myxothiazol and MOA-stilbene bind close to the heme b_L, UHDBT binds close to the FeS, and stigmatellin overlaps both binding sites(35).

The binding pocket of stigmatellin in bc_1 complexes is formed by the C-terminal end of helix C, helix cd1, ef linker (including the highly conserved sequence PEWY and helix ef) and the N-terminal end of helix F. Compared to the positions in the native structure, residues P271, F275 and M125 of cytochrome *b* are moved and are near stigmatellin. Meanwhile, residues126-129 of helix C and residues 140-147 of the linker cd are also close by bound stigmatellin.

Myxothiazol also binds bc_1 complex at the Qp pocket. Its binding pocket overlaps that of stigmatellin with a slight displacement towards the center of the memebrane and heme b_L. Both of stigmatellin and myxothiazol are close to P271, but stigmatellin reaches outward from P271 toward the Rieske protein whereas myxothiazol reaches toward Y132 and F129 in helix, close to heme b_L

Q_N Pocket(39): the QN pocket is the site in which the oxidized Q or semiquinone receives electron from heme b_H and take up one proton from the matrix(38). Q_N is located near the matrix side of the membrane, and its entrance is accessible from the center of the membrane bilayer. The Q_N pocket is nearly vertical toward the matrix side of the membrane. This pocket is formed by helices A, D, E, and the amphipatic surface helix a, the A loop and the DE Loop. Table I-4 shows the residues which contribute to the

Table I-4: Residues contributing to the formation of Q_N pocket(39)

Helices	Residues
Helix A	Trp^{31}, Asn^{32}, Gly^{34}, Ser^{35}
Helix D	Ala^{193}, Met^{194}, Leu^{197}, His^{201}
Helix E	Tyr^{224}, Lys^{227}, Asp^{228}
Amphipatic surface helix a	Phe^{18}
Loop A	Ile^{27}
Loop DE	Ser^{205}, Phe^{220}

Note: superscript number of each amino acid residue indicate the position of this residue in the subunit

formation of the Q_N pocket in each helix and loop. These residues are identified based on the X-ray crystal structure of bc_1 complexes with antimycin A, NQNO, and ubiquinone.

2. Structure of ISP(40)

ISP is the subunits housing the prosthetic group of the iron-sulfur cluster (Figure I-4). It can be divided into three domains: tail, neck and head domains. The tail domain is a membrane spanning N-terminal domain, consisting of residues 1-62. The neck domain is flexible and composed of residues 63-72. The head domain, located in the C-terminus of ISP, consisting of residues 73-196, is a rigid, compact and flat-spherical-shaped structure (40). This head domain is composed of three layers of antiparallel beta sheets comprising 10 β-strands (β1- β10). Between the strands β3 and β4, there are a α-helix and a long loop. The iron-sulfur cluster is located at the tip of the head domain. This cluster-binding fold is comprised of 46 amino acids. [2Fe-2S] cluster is coordinated by two cysteine and two histidine residues: Cysteine 139 and Histidines 141 in the loop β4-β5 are one of ligands of Fe-1 and Fe-2 respectively. Likewise, cysteine 158 and histidine 161 in the loopβ6-β7 are the other one of ligands of Fe-1 and Fe-2, respectively. The cysteines 144 in the loop β4-β5 and 169 in the loop β6-β7 are highly conserved and form a disulfide bond to bring these two loops together and stabilize this region. This cluster is also stabilized by multiple hydrogen bonds. All sulfur atoms are involved in two hydrogen bonds in the form of NH-S or OH-S except for the S^{γ} of Cys158, which only form a single hydrogen bond with the N-atom of Cys160.

Compared to other Iron-sulfur clusters, [2Fe-2S] has a much higher Em. There are some factors contributing to this high potential: a) the overall charge of the cluster; b)

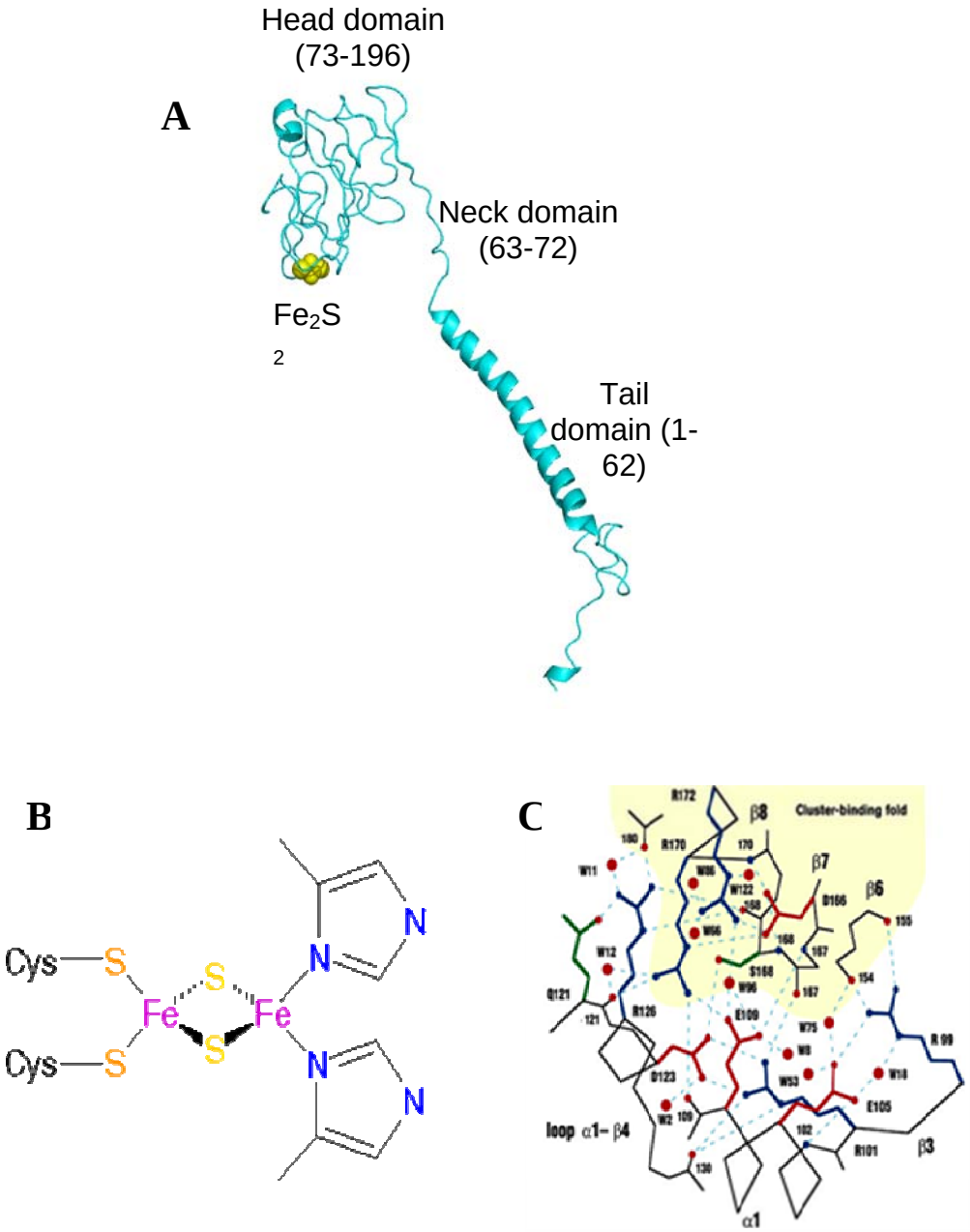

Figure I-4: Structure of Rieske iron-sulfur protein (ISP). (A) The overall structure of ISP; (B) the ligands for Fe_2S_2 cluster; (C) the hydrogen bond network around the 2Fe2S cluster.

the electronegativity of the histidine ligands; c) the complex hydrogen bond network around the cluster; d) the solvent exposure of the Fe(II) (40).

Cytochrome bc_1 crystallographic structures indicated the mobility of ISP head domain and the flexibility of the neck domain of ISP (29,30). Due to its movement between cytochrome *b* interface and cytochrome c_1 interface, the head domain of ISP is considered to have two docking positions: "*b*" position and "c_1" position.(41). Later, workers demonstrated that the mobility of ISP head domain is functionally required for bc_1 catalysis (29,35,37,42,43). Tian et al (37,42-44) proved that decreasing the flexibility of neck domain of ISP will decrease the bc_1 activity. Later, Xiao et al (42) showed stronger evidence to confirm the requirement of the mobility of ISP in the bc_1 catalysis. They fixed the head domain of ISP in the b position with an artificial disulfide bond, which makes the iron-sulfur cluster close to QH_2 and far away from heme c_1. The ISP-fixed bc_1 shows little activity, however, the bc_1 complex will recover most of its activity once ISP is released by β-mercaptoethanol.

3. Structure of Cytochrome c_1 (30):

Cytochrome c_1 is the subunit housing the redox prosthetic group heme c_1 (Figure I-5). It is an all-α helix-type protein like other members of the cytochrome *c* family. Cytochrome c_1 contains seven helices, including the C-terminal membrane helix. The heme c_1 is coordinated with His41 and Met160. In addition, heme c_1 is also covalently linked to Cys37 and Cys40. In this subunit, there are three docking sites for cytochrome *c*, ISP and subunit 8, respectively. The docking site of cytochrome *c* is most likely at the heme c_1 crevice (45). Heme c_1 crevice is surrounded by 10 acidic amino acids in the helix α_1' and loop α_3-β_1. Many of these 10 acidic residues point to the intermembrane

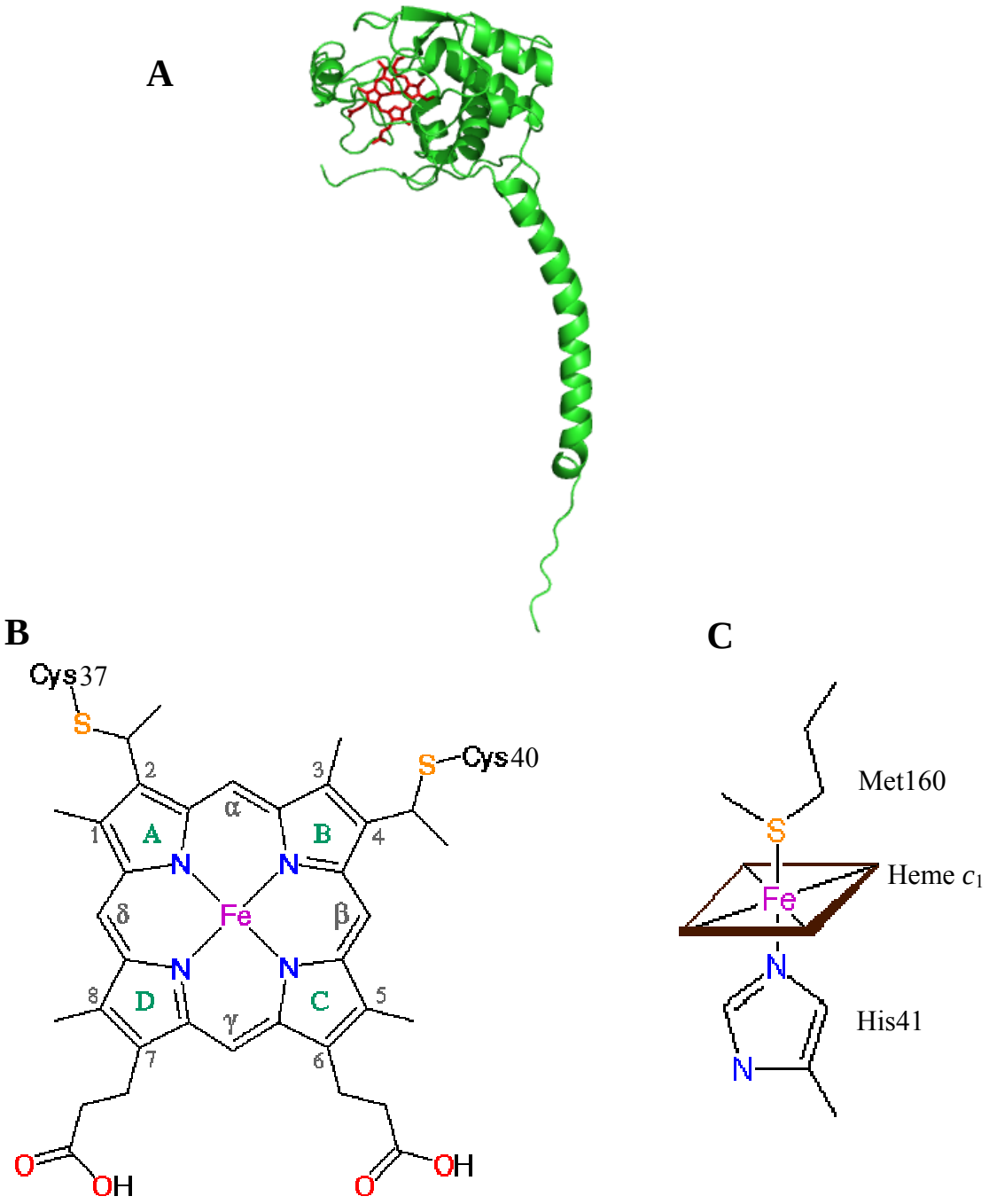

Figure I-5: Structure of cytochrome c_1. (A) The overall structure of cytochrome c_1; (B) Structure of heme c_1; (C) The ligands for heme c_1. Heme c_1 in Panel A is shown as stick mode in red.

side. The docking site for subunits is formed by Loop α_3-β_1 and the N-terminal extension before α1. In the crystal $P6_522$ form, the docking site for ISP is formed by the Loop α_1''-α_2 and β_2.

III: Inhibitors of Cytochrome bc_1

Cytochrome bc_1 inhibitors are usually grouped into two major classes based on their binding sites. Inhibitors binding to the Qp pocket belong to class I, also called class P, and those binding to the Q_N pocket belong to class II, also called class N (46-48). Based on chemical characteristics of the inhibitors, and the iron-sulfur cluster of ISP upon binding of inhibitors, class I inhibitors can be further classified into three sub-classes (Ia, Ib and Ic). In the structures of class Ia inhibitors, a β-methoxyacrylate (MOA) group is typically present as a characteristic structural element. The binding of class Ia inhibitors to cytochrome *b* can cause a red-shift in the α and β-bands of the reduced heme b_L spectrum. Class Ib inhibitors contain a chromone ring system. The binding of these inhibitors can lead to a significant increment in the middle potential of ISP. Likewise, they also can cause a red-shift of the reduced heme b_L spectrum. Class Ic inhibitors are 2-hydroxy quinone analogues. They can cause a smaller positive redox potential shift of ISP other than effect on the spectrum of the heme b_L. Figure I-6 and Table I-5 show the common inhibitors of cytochrome bc_1 and their classification, respectively.

Based on specific binding interactions and conformational changes observed in both cytochrome *b* and ISP, class P inhibitors can be divided into two subgroups: Pm (for mobile ISP) and Pf (for fixed ISP) (49). P_m inhibitors contain a common motif β-methoxyacrylate which occupies the identical position of the Qp pocket . The binding of

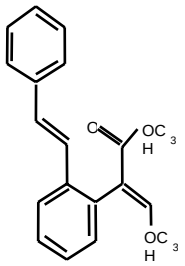

MOA-stilbene

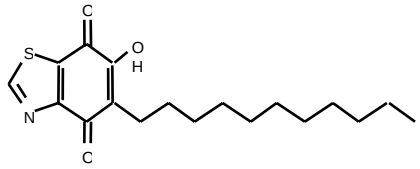

UHDBT

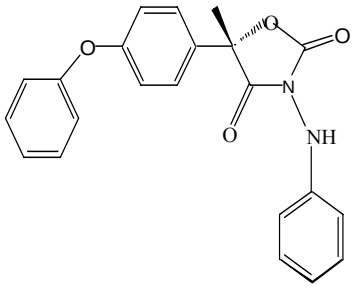

Famoxadone

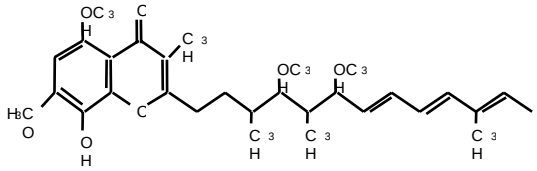

Stigmatellin

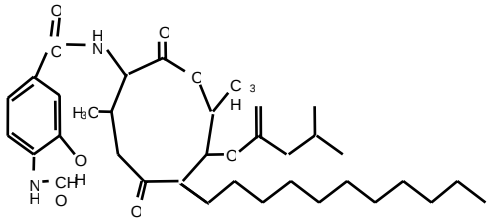

Antimycin A

Figure I-6: Chemical structure of some cytochrome bc_1 inhibitors

Table I-5: Categorization of cytochrome bc_1's inhibitors (46-48)

Class		Inhibitors
I	a	Myxothiazol, MOAs
	b	Stigmatellin
	c	UHDBT
II		Antimcyin

P_m inhibitors will push the cd1 helix of cytochrome *b* to make the Qp pocket more open. In X-ray crystallographic structures, the binding of Pm inhibitor to cytochrome bc_1 always make the anomalous signal of ISP disordered (<0.35). On the contrary, the binding of P_f inhibitors always fixes the ISP at the *b*-position. In addition, the binding of P_f inhibitors can increase redox potential of ISP subunit in cytochrome bc_1 (50). In general, P_f inhibitors consist of stigmatellin, famoxadone and UHDBT. Inhibitors myxothiazol, MOAs, and azoxustrobin belong to P_m subgroup.

IV. Catalytic Mechanism of Cytochrome bc_1

1. The Q-cycle Hypothesis:

Cytochrome bc_1 complex catalyzes the electron transfer from ubiquinol to cytochrome c with concomitant proton translocation across mitochondrial intermembrane. Its catalysis mechanism has drawn a lot of scientists' attention. Through decades of efforts, scientists now have pretty clear views on cytochrome bc_1's catalysis mechanism. In 1972, the oxidant-induced reduction of cytochrome *b* in cytochrome bc_1 complexes led Wikström and Berden to hypothesize a bifurcated pathway for QH2 oxidation (51). Later, in 1975, combining this idea with the Q-loop concept (38,52), Peter Mitchell proposed a protonmotive Q-cycle to elucidate bc_1 complex's catalysis (38,52). In this protonmotive Q-cycle, Q_P and Q_N pockets were first postulated for the oxidation of QH_2 on the positive side of the membrane and the reduction of ubiquinone on the negative side of the membrane (53). However, in this hypothesis, Mitchell didn't specify the primary oxidant of ubiquinol. Trumpower's contribution solved this problem by having demonstrated that the iron-sulfur cluster in the Rieske protein of cytochrome bc_1 is the primary oxidant of

ubiquinone instead of heme b_L in cytochrome *b* (54,55). With more efforts from different groups, protonmotive Q-cycle has been supported by more and more experiments (56-61) and become more explicit. Now, the modified Q-cycle (62-66) has been generally accepted. Figure I-7 shows the modified "Q-cycle". The reaction catalyzed by bc_1 is a bifurcated reaction. In general, reduced Q binds the Qp pocket and, in there, two electrons from reduced Q will be passed to two different chains: the high potential chain and the low potential chain. The high potential chain consists of iron-sulfur cluster of ISP, heme c_1 in cytochrome c_1 and mobile electron carrier cytochrome *c*. The low potential chain is composed of heme b_L and heme b_H in cytochrome *b* and Q/QH in the Q_N pocket. During the bc_1 catalysis, proton pumping from mitochondrial matrix to intermembrane space is coupled to electron transfer. The Qp pocket is close to intermembrane space side and Q_N close to the matrix side. In the Qp pocket , two protons are translocated into the intermenbrane space from QH_2 while QH_2 is oxidized by ISP and heme b_L, then oxidized Q in the Q_N pocket will accept two electrons from heme b_H during catalysis. Meanwhile, this re-reduced Q will take two protons from mitochondrial matrix and diffuse into the Qp pocket for next catalysis cycle. Therefore, the overall reaction catalyzed by bc_1 should be the equation (a) below:

$$QH_2 + 2\ \text{cyt.}\ c^+ + 2H_N^+ \longleftrightarrow Q + 2\text{cyt.}\ c + 4H_P^+ \quad \text{(a)}$$

From the equation (a) we can see that, in each catalysis cycle, two electrons will be transferred and 4 protons will be pumped into the intermembrane space, two from QH_2 and the other two from the mitochondrial matrix.

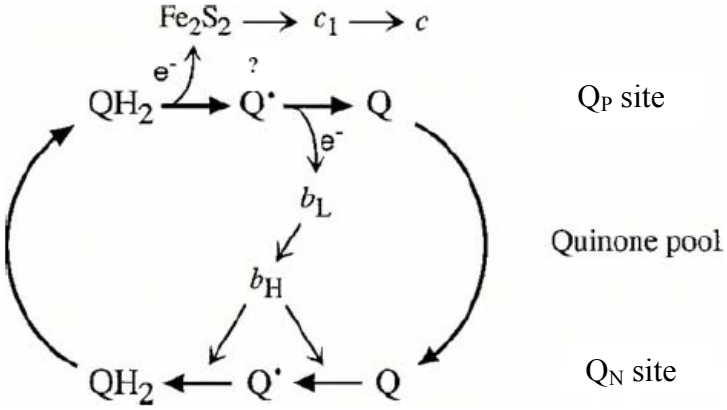

Figure I-7**: Schematic diagram of the Q-cycle mechanism of cytochrome *bc*$_1$**. Arrows denote substrate transformation or movement.

2. The oxidation of QH_2 at the Qp pocket

The oxidation of QH_2 at the Qp pocket is a bifurcated reaction: one electron goes to ISP and the other one goes to heme b_L. Electron transfer from ubiquinol to the iron-sulfur cluster is significantly exergonic whereas electron transfer from ubiquinol to heme b_L is usually somewhat less endergonic. The overall reaction is an exergonic reaction and its reaction is shown below (Calculated for bovine enzyme using Em7 of +70, +290, +250 and -20 mv for QH_2/Q, Fe_2S_2, cyt c_1 and cyt b_L) (14,67).

$$QH_2 + Fe_2S_2^{ox} + \text{cyt } b_L^{ox} \rightarrow Q + Fe_2S_2^{red} + \text{cyt } b_L^{red} + 2H^+ , \Delta G^{o\prime} \approx -13 \text{ kJ/mol} \quad (b)$$

The activation barrier for QH_2 oxidation at the Qp pocket is between 30-40 kJ/mol (63,68). Crofts and Wang (63,68) thought this barrier represented the formation of a highly unstable semiquinone anion at the Q_P pocket. Rather, Brandt (69) thought the first deprotonation of ubiquinone is the endergonic step so that the activation barrier energy is required for this deprotonation, which is supported by the strict pH dependence of the activation barrier (69) . However, Crofts argued that the experimental data from his lab doesn't show any pH dependence of the activation barrier (63,70). Consistent with the pH dependence of activation barrier, the steady-state rate of QH_2 oxidation in mitochondrial complexes showed pH dependence over the range 5.5-9.5 (68,71). This pH dependence of the rate is attributed to two controlling groups, one with a pK_a at 6.5, and a second at 9.5, which has to be protonated. For a rapid electron transfer, the one with a pK_a at 6.5 has to be at a dissociate state while the one at 9.5 has to been protonated. Brandt excluded the involvement of Histidine groups ligated with the iron-sulfur cluster of ISP since histidine pK_1 is at 7.6 (69). According to Brandt hypothesis, the limiting-step of QH_2 oxidation at is the deprotonation of QH_2, which is responsible for most of the

activation barrier. An argument arose from Crofts (72) who thought the limiting step is the first electron transfer from QH_2 to ISP_{ox}, and the formation of ISP-QH_2 complex consumes most of the activation energy. He suggested that the ES-complex was formed through two H-bonds: one is between the ring-OH of the quinol and the N_ε of ISP-161, and the other one is the other –OH of quinol and the carboxylate group of Glu-272. In line with his thought, the electron transfer from ISP to cyt c_1, from b_L to b_H and the oxidation of bound QH_2 takes less than 10 μs, less than 100 μs and around 750 μs, respectively (66). Our group found that the rate-limiting step is the electron transfer from reduced ISP to cyt. c_1, since reduction of heme b_H is faster than that of cytochrome c_1 during catalysis (73). This hypothesis is supported by Hansen et al's work (74).

An alternative reaction for QH_2 oxidation at the Qp pocket is thermodynamically much more favorable than the reaction above (Equation b).

$$QH_2 + 2Fe_2S_2^{ox} + \text{cyt } c_1{}^{ox} \rightarrow Q + Fe_2S_2^{red} + \text{cyt } c_1{}^{red} + 2H^+, \Delta G^{o'} \approx -39 \text{ kJ/mol} \quad (c)$$

However, this reaction is never observed, even in the so called oxidant-induced reduction experiment. What prevents this thermodynacially favorable reaction occurring? What is the mechanism for this obligatory bifurcated oxidation? Several models have been proposed to answer these questions.

Based on the existence of semiquinone at the Q_P pocket, all of these mechanisms can be classified into two major categories (Figure I-8): the sequential mechanism (75,76) and the concerted mechanism (77,78). In the sequential mechanism, QH_2 transfers one electron to the oxidized iron-sulfur cluster of ISP and then become semiquinone. Semiquinone has lower mid-point potential (from -300 mv to -400mv) (79) than heme b_L so that it can transfer an electron to heme b_L. Therefore, according to the sequential

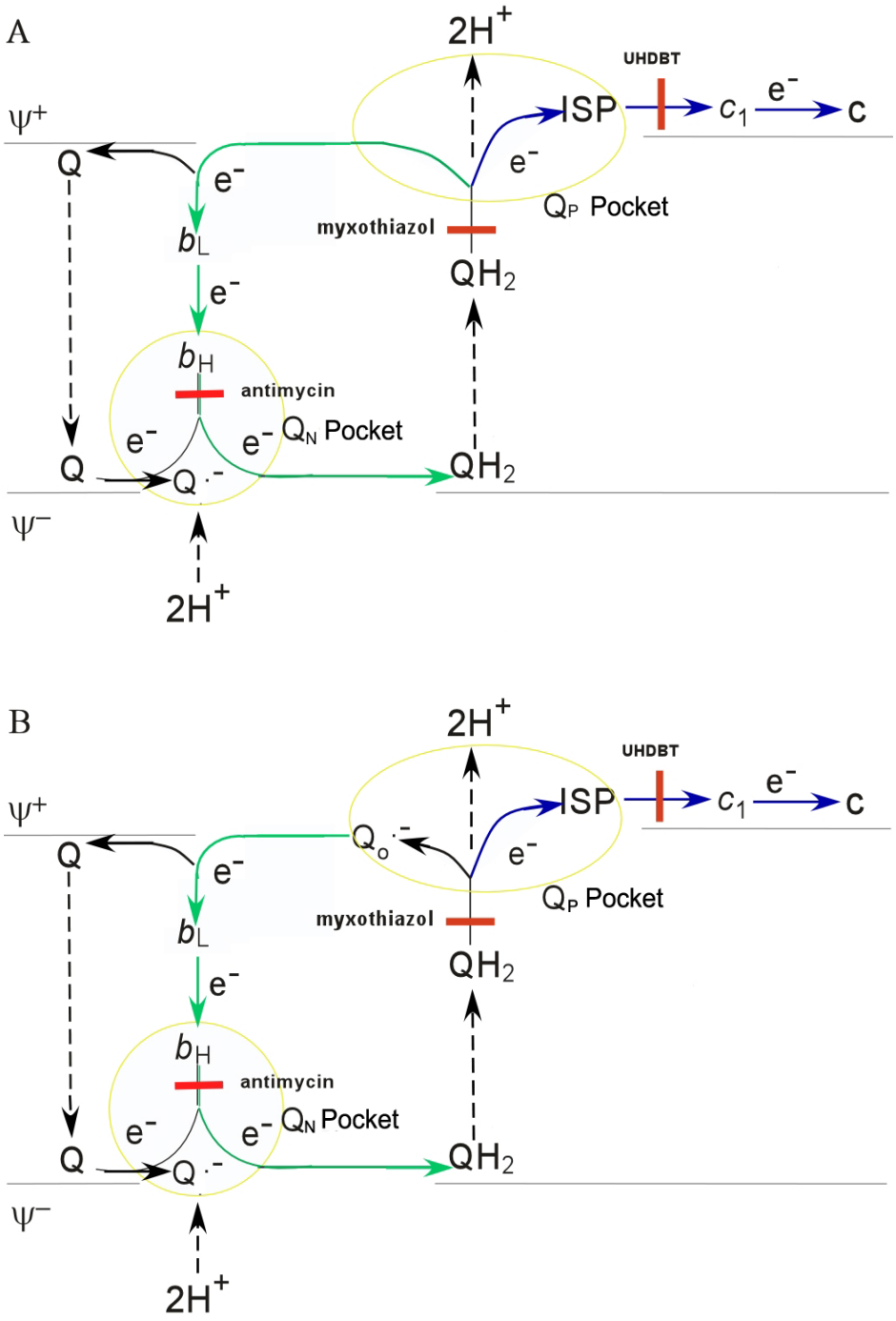

Figure I-8: Diagrams showing the concerted mechanism and the sequential mechanism of QH_2 oxidation at Q_P Pocket. Panel A shows the concerted mechanism; Panel B shows the sequential mechanism. The big difference between these two mechanism is the existence of semiquinone at Q_P pocket. Red bars indicate action sites of some inhibitors.

mechanism, a distinct ubisemiquinone intermediate should exist at Q_P pocket. On the contrary, in concerted mechanism, the reductions of ISP and heme b_L by QH_2 occur at the same time, so that no ubisemiquione is present at the Q_P pocket.

Based on the way in which the reduction of ISP and the reduction of Heme b_L link together, some hypotheses were proposed in the sequential mechanism: "Catalytic switch model"(80,81) was proposed first. In this model, bc_1 conformational change is required for QH_2 bifurcated oxidation, in which the active reductant bound in the Qp pocket alternatively contacts the iron-sulfur center and the heme b_L. This switch was thought first to be controlled by the redox state of the iron-sulfur cluster, but the electron transfer from heme b_L to heme b_H was also suggested. In "the proton-gated affinity change" mechanism (75), the ubisemiquione caused by ISP reduction is stabilized by anti-ferromagnetic coupling to the reduced iron-sulfur protein. This stabilization will raise the potential of the iron-sulfur cluster such that the cluster cannot be oxidized by cytochrome c_1 until the semiquinone is oxidized by heme b_L (75). In this mechanism, a stable semiquione will be present at Q_P pocket. The failure to detect semiquione at the Qp pocket by EPR is that the semiquione is magnetically coupled to the reduced iron-sulfur cluster (75). In another sequential coupled mechanism-"proton-gated charge-transfer mechanism" (14), two ubiquinone binding sites exist in the Q_P pocket. One is QP_s (s stands for strong binding) and the other one is QP_w (w stands for weak binding). Ubiquione bound at the Q_{Ps} site acts as a prosthetic group and is not exchanged during turnover (79). Substrate ubihydroquione will bind to the Q_{Pw} site. Once substrate ubihydroquinone binds to Q_{Pw} site, it will give one proton away and become QH^-. Electron transfer from QH^- onto Q_{Ps} will stabilize the formed Q_{Ps}-semiquinone by decreasing potential of the ISP cluster. This

double-semiquinone intermediate allows rapid reduction of the two redox centers, thereby completing the substrate oxidation.

For the sequential mechanism, the detectable semiquinone at the Qp pocket is the key point. The failure to detect this semiquinone at the Qp pocket makes this mechanism relatively vulnerable. De Vries had reported an EPR-detectable semiquione at the Qp pocket (82), but other groups showed that this EPR signal assigned to semiquione at the Qp pocket does not arise from a semiquinoe species (76). Recently, using a mutant lacking heme b_H, some groups found a semiquinone signal at Q_P pocket (83). This semiquinone signal was sensitive to stigmatellin binding. However, even the authors are not sure if this semiquione is a genuine intermediate in normal Q_P pocket action (83). Under anaerobic condition, Jonathan L. Cape *etal* reported that a semiquione radical was observed at Q_P pocket, using continuous wave and pulsed EPR spectroscopy. This observation is also questioned that the semiquinone signal is more likely semiquinone produced in an abnormal pathway leading to the ROS production.

In the concerted mechanism (78,84), semiquinone is not present as an intermediate during the QH_2 oxidation. Ubiquinol form a ubiquinol-imidazolate complex with His-161 of the redox active iron of the iron-sulfur cluster. This complex is the electron donor for the iron-sulfur cluster and the heme b_L. It will form a hydrogen bond to Glu-272 of cytochrome *b*, docked within electron transfer distance of the heme b_L. Once the hydrogen bond to Glu-272 is formed, the ubiquinol-imidazolate complex will simultaneously transfer electrons to the iron-sulfur cluster and heme b_L. Since there is no semiquione formed during the QH_2 oxidation, observing it with EPR is not expected.

All of these mechanisms can account for certain experimental results. Unfortunately, so far none of them have received any strong experimental evidence to support their key presumption in their proposals. For the sequential mechanism, to this date, no any strong evidence shows the existence of semiquinone. For the concerted mechanism, it does not need to explain the failure to detect semiquinone at the Qp pocket. The impediment of bound antimycin at the Q_N pocket to the electron transfer from ISP to cyt c_1 during the oxidation of second QH_2 is adopted by authors as an evidence for the concerted mechanism (84). However, this observation is more likely that low potential chain controls the movement of ISP instead of the reduction of ISP by QH_2 at Qp site. Another piece of evidence(78) for this concerted mechanism provided by authors is that only one monomer of bc_1 complexes functions in the low QH_2 concentration, which was speculated according to anti-cooperative binding behavior of stigmatellin at Q_P pocket. Only one active monomer in bc_1 dimeric complexes is also implied from the X-ray co-crystallographic structure of bc_1 complexes with bound cytochrome *c* (31). A direct piece of evidence for the concerted mechanism from Dr. Yu's group shows that ISP and heme b_L are reduced simultaneously(85). However, we still don't know if their reductions are dependent on each other or not, and the time resolution leaves room for further experimentation.

3. Movement of ISP head domain

The finding of the function-required movement of ISP head domain during bc_1 catalysis enriched "Q-cycle" mechanism (29,35,37,41,42). This new finding has been integrated into some new mechanisms for the QH_2 oxidaiton at the Q_P pocket. In 1998, considering this functional movement of ISP, Ulrich Brandt slightly modified the

"catalytic switch" model (67). In this modified version, the ISP head domain is this catalytic switch. It stays at "*b*-position" as the iron-sulfur cluster and heme b_L are oxidized, which will ensure QH_2 is only oxidized at the Qp pocket when a bifurcation of electron flow is possible. QH_2 at the Qp pocket transfers the first electron to the iron-sulfur cluster, which triggers switch to "c_1-position", at which the iron-sulfur cluster is oxidized by heme c_1 and heme b_L is reduced by semiquinone simultaneously. Reduced heme b_L will transfer electrons to heme b_H, which will trigger a switch to "*b*-position". Then reduced c_1 and heme b_H will be oxidized by electron carrier cytochrome *c* and Q/QH at the Q_N pocket respectively.

The movement of the head domain of ISP sounds reasonable as a switch which contributes to the obligatory of bifurcated oxidation. However, what leads to this movement still remains unclear. Apparently, this movement is dependent on the electron transfer in the low potential chain. More efforts are needed to find strong evidence for it.

V. Study System

Since our research goals need us to construct mutant protein for our study, we have to choose a good research system which perfectly fit our requirement. Considering all aspects of our research project, we choose the cytochrome bc_1 complexes from *Rhodobacter spaeroides* as our research system.

R. sphaeroides is an anoxygenic, non-sulfur, purple facultative photosynthetic bacterium, belonging to the α-subdivision of the proteobacteria which can grow in a wide variety of growth conditions. *R. sphaeroides* has an extensive range of energy acquiring mechanisms, such as photosynthesis, lithotrophy, aerobic and anaerobic respiration (86).

In *R. sphaeroides*, Cytochrome bc_1 complex is not only in aerobic and anaerobic respiration electron transfer chains, but also in the photosynthetic electron transfer chain. It catalyzes the electron transfer from QH_2 to oxidized cytochrome c_2 instead of equivalent cytochrome *c* in mitochondrial cytochrome bc_1 catalysis. Different from plants and algae, which carry out photosynthesis in an aerobic environment with oxygen production, the synthesis of some photosynthetic pigment in *R. sphaeroides* is repressed by oxygen. In *R. sphaeroides* photosynthesis, the electron carrier cytochrome c_2 is oxidized by the reaction center instead of cytochrome c_2 oxidase. Figure I-9 shows a demonstration of these three bc_1 anticipated energy-producing processes (86).
From Figure I-9, we can see that the cytochrome bc_1 complex is not essential for its aerobic growth, in which quinol can be oxidized by quinol oxidase as an alternative pathway. In addition to the cytoplasmic membrane (CM), *R. sphaeroides* has an intracytoplasmic membrane (ICM) system, which is derived from and is contiguous with CM. In most cases, the photosynthetic apparatus of *R. sphaeroides* are located in the ICM. The low oxygen tension can induce the ICM formation and most extensive ICM is developed during anaerobic growth [reviewed in (87)]. Thus, for bc_1 complexes with fatal mutation, *R. sphaeroides* are grown under "semi-aerobic" conditions. In this case, limited oxygen will induce the development of ICM and the expression of cytochrome bc_1 complexes.

R. sphaeroides cytochrome bc_1 complex contains four subunits: three common subunits (cytochrome *b*, cytochrome c_1 and ISP) and one supernumerary subunit (called subunit IV) (88-91). These three common subunits share a high sequence similarity with those from other species, except for several extra fragments in them. Compared to

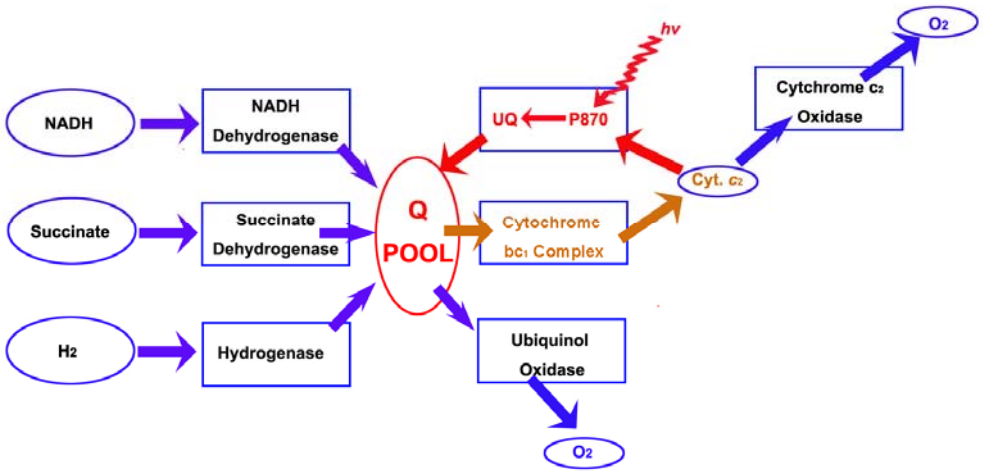

Figure I-9: The schematic diagram of the photosynthetic and respiratory electron transport system of *R. sphaeroides*

mitochondrial bc_1 complexes, *R. sphaeroides* cytochrome bc_1 complexes have lower activity, only 10% of bovine mitochondrial bc_1's activity. As a research system, *R. sphaeroides* cytochrome bc_1 complex has a much simpler subunit composition than other mitochondrial cytochrome bc_1 complexes, which makes it more suitable for studying cytochrome bc_1 catalysis involving only three common subunits.

As we know, the gene sequence of *R. sphaeroides* cytochrome bc_1 complex is only around 3.3 kb, much shorter than mitochondrial cytochrome bc_1. This DNA length can be inserted into a plasmid for protein expression, which will facilitate our gene manipulation on cytochrome bc_1 complexes. In addition, efficient molecular engineering procedures for *R. sphaeroides* are well established (92,93),

Based on all of these advantages described above, our lab chose *R. sphaeroides* cytochrome bc_1 complex as our research model and have established a good system and an efficient engineering procedure for *R . sphaeroides* cytochrome bc_1 complex.

VI. Research Interests and Achievement

Current Q-cycle theory can elucidate the catalytic mechanism of bc_1 complexes very well. However, just as what we discussed above, the mechanism of the obligatory oxidation of QH_2 at the Q_P pocket still remains unclear. The proposed mechanisms are controversial. There is no strong evidence to support either of them yet. In this dissertation, two mutants, one lacking heme b_L and the other one lacking heme b_H, were constructed and used to investigate the mechanism of QH_2 oxidation at the Q_P pocket. Investigation with these two mutants also indicates that the ISP movement occurs after reduced heme b_L gets reoxidized by heme b_H. These results are described in Chapter II. In

Chapter II, the results also indicate that superoxide production in bc_1 doesn't require electron transfer but a hydrophobic environment, which is described in details in Chapter III.

As we mentioned before, there is no crystallographic structures available with QH_2 at the Q_P pocket. Likewise, no crystallographic structure with ISP fixed at c_1-position has been reported. In Chapter IV, we constructed a mutant S141C (ISP)/G180C (cyt.c_1) in which ISP is fixed at c_1-position by a pair of engineered inter-subunit disulfide bond. This mutant protein has less than 10% of specific activity of wild type bc_1 complex. However, after treatment with β-mecaptoethanol, the specific activity will increase to 80% of that of wild type bc_1. The electron transfer rate in this mutant is 100 times faster than that in wild type cytochrome bc_1, indicating ISP is fixed at c_1-position in this mutant. Since ISP is fixed at c_1-position in mutant S141C/G180C, QH_2 cannot be oxidized by ISP and will stay at the Qp pocket much longer than that in wild type bc_1. Collaborating with Dr. Di Xia, we put hope on this mutant protein for crystallographic structures with QH_2 at the Q_P pocket. In Chapter IV, a series of mutants in the ef loop of the cytochrome *b* subunit were constructed, trying to identify some residues which are important for cytochrome bc_1's activities. Alanine-scanning shows that mutations I292A and L286A can significantly affect the catalytic activities. Further investigation indicates that the bulky side chains on these two positions are important for the catalytic activities. The bigger the side chain, the higher the activities. Other residues in the ef loop don't show similar results, indicating these two residues probably play roles during the release and capture of ISP head domain.

REFERENCE

1. Schagger, H., and Pfeiffer, K. (2001) *J. Biol. Chem.* **276**, 37861-37867
2. Fearnley, I. M., and Walker, J. E. (1992) *Biochimica et Biophysica Acta (BBA) - Bioenergetics* **1140**, 105-134
3. Yu, L., Xu, J. X., Haley, P. E., and Yu, C. A. (1987) *J. Biol. Chem.* **262**, 1137-1143
4. Ohnishi, T., and Salerno, J. C. (1976) *J. Biol. Chem.* **251**, 2094-2104
5. Ackrell, B. A., Kearney, E. B., Mims, W. B., Peisach, J., and Beinert, H. (1984) *J. Biol. Chem.* **259**, 4015-4018
6. Rich, P. R. (1986) *Journal of Bioenergetics and Biomembranes* **18**, 145-156
7. Tsukihara, T., Aoyama, H., Yamashita, E., Tomizaki, T., Yamaguchi, H., Shinzawa-Itoh, K., Nakashima, R., Yaono, R., and Yoshikawa, S. (1996) *Science* **272**, 1136-1144
8. Schultz, B. E., and Chan, S. I. (2001) *Annual Review of Biophysics and Biomolecular Structure* **30**, 23-65
9. Berry, E. A., Guergova-Kuras, M., Huang, L.-s., and Crofts, A. R. (2000) *Annual Review of Biochemistry* **69**, 1005-1075
10. Sun, J., and Trumpower, B. L. (2003) *Arch. Biochem. Biophys* **419**, 198-206
11. T'Sai, A.-L., and Palmer, G. (1983) *Biochimica et Biophysica Acta (BBA) - Bioenergetics* **722**, 349-363
12. Chance, B. (1972) *FEBS Letters* **23**, 1-20

13. Yu, C.-A., Yu, L., and King, T. E. (1979) *Archives of Biochemistry and Biophysics* **198**, 314-322

14. Brandt, U. (1996) *FEBS Letters* **387**, 1-6

15. von Jagow, G., and Ohnishi, T. (1985) *FEBS Letters* **185**, 311-315

16. Bowyer, J. R., Dutton, P. L., Prince, R. C., and Crofts, A. R. (1980) *Biochimica et Biophysica Acta (BBA) - Bioenergetics* **592**, 445-460

17. von Jagow, G., Ljungdahl, P. O., Graf, P., Ohnishi, T., and Trumpower, B. L. (1984) *J. Biol. Chem.* **259**, 6318-6326

18. Bowyer, J. R., Edwards, C. A., Ohnishi, T., and Trumpower, B. L. (1982) An analogue of ubiquinone which inhibits respiration by binding to the iron-sulfur protein of the cytochrome b-c1 segment of the mitochondrial respiratory chain.

19. Zhang, L., Tai, C.-H., Yu, L., and Yu, C.-A. (2000) *J. Biol. Chem.* **275**, 7656-7661

20. Liu, X., Yu, C.-A., and Yu, L. (2004) *J. Biol. Chem.* **279**, 47363-47371

21. Yun, C. H., Crofts, A. R., and Gennis, R. B. (1991) *Biochemistry* **30**, 6747-6754

22. Ugulava, N. B., and Crofts, A. R. (1998) *FEBS Letters* **440**, 409-413

23. Yu, L., Dong, J.-H., and Yu, C.-A. (1986) *Biochimica et Biophysica Acta (BBA) - Bioenergetics* **852**, 203-211

24. Wood, P. M. (1980) *Biochem. J.* **189**, 385-391

25. Motokawa, Y., and Kikuchi, G. (1966) *biochem. Biophys. Acta* **120**, 174-181

26. Ljungdahl, P. O., Pennoyer, J. D., Robertson, D. E., and Trumpower, B. L. (1987) *Biochim. Biophys. Acta - Bioenergetics* **891**, 227

27. Tso, S.-C., Shenoy, S. K., Quinn, B. N., and Yu, L. (2000) *J. Biol. Chem.* **275**, 15287-15294

28. Yue, W.-h., Zou, Y.-p., Yu, L., and Yu, C.-a. (1991) *Biochemistry* **30**, 2303-2306

29. Xia, D., Yu, C.-A., Kim, H., Xia, J.-Z., Kachurin, A. M., Zhang, L., Yu, L., and Deisenhofer, J. (1997) *Science* **277**, 60-66

30. Iwata, S., Lee, J. W., Okada, K., Lee, J. K., Iwata, M., Rasmussen, B., Link, T. A., Ramaswamy, S., and Jap, B. K. (1998) *Science* **281**, 64-71

31. Lange, C., and Hunte, C. (1999) *Proc. Natl. Acad. Sci. U.S.A* **99**, 2800-2805

32. Hunte, C. (2001) *FEBS Letters* **504**, 126

33. Esser, L., Elberry, M., Zhou, F., Yu, C.-A., Yu, L., and Xia, D. (2008) *J. Biol. Chem.* **283**, 2846-2857

34. Leonard K, W. P., Arad T, Weiss H. (1981) *J Mol Biol* **149**, 259-274

35. Kim, H., Xia, D., Yu, C.-A., Xia, J.-Z., Kachurin, A. M., Zhang, L., Yu, L., and Deisenhofer, J. (1998) *Proc. Natl. Acad. Sci. U.S.A* **95**, 8026-8033

36. Gao, X., Wen, X., Yu, C.-A., Esser, L., Tsao, S., Quinn, B., Zhang, L., Yu, L., and Xia, D. (2002) *Biochemistry* **41**, 11692-11702

37. Zhang, Z., Huang, L., Shulmeister, V. M., Chi, Y.-I., Kim, K. K., Hung, L.-W., Crofts, A. R., Berry, E. A., and Kim, S.-H. (1998) *Nature* **392**, 677-684

38. Mitchell, P. (1976) *J. Theor.Biol.* **62**, 327

39. Gao, X., Wen, X., Esser, L., Quinn, B., Yu, L., Yu, C., and Xia, D. (2003) *Biochemistry* **42**, 9067-9080

40. Link, T. A., and Iwata, S. (1996) *Biochim. Biophys. Acta - Bioenergetics* **1275**, 54-60

41. Xiao, K., Yu, L., and Yu, C.-A. (2000) *J. Biol. Chem.* **275**, 38597-38604

42. Tian, H., Yu, L., Mather, M. W., and Yu, C.-A. (1998) *J. Biol. Chem.* **273**, 27953-27959

43. Kunhong xiao, L. Y., Chang-An Yu. (2000) *Journal of biological chemistry* **275**, 38597 - 38604

44. Tian, H., White, S., Yu, L., and Yu, C.-A. (1999) *J. Biol. Chem.* **274**, 7146-7152

45. Stonehuerner, J., O'Brien, P., Geren, L., Millett, F., Steidl, J., Yu, L., and Yu, C. A. (1985) *J. Biol. Chem.* **260**, 5392-5398

46. von Jagow, G. a. L., T.A. (1986) *Methods in Enzymology* **126**, 253-271

47. Link, T. A., Haase, U., Brandt, U., and Jagow, G. (1993) *Journal of Bioenergetics and Biomembranes* **V25**, 221-232

48. Geier, B. M., Haase, U., and Von Jagow, G. (1993) *biol. Soc. Trans* **22**, 203-209

49. Esser, L., Quinn, B., Li, Y.-F., Zhang, M., Elberry, M., Yu, L., Yu, C.-A., and Xia, D. (2004) *Journal of Molecular Biology* **341**, 281

50. Ohnishi, T., Brandt, U., and von Jagow, G. (1988) *Eur J Biochem* **176**, 385-389

51. Wikstrom, M. K. F., and Berden, J. A. (1972) *Biochim. Biophys. Acta - Bioenergetics* **283**, 403-420

52. Mitchell, P. (1961) *Nature* **191**, 144-148

53. Mitchell, P. (1975) *FEBS Letters* **59**, 137-139

54. Trumpower, B. L. (1976) *Biochemical and Biophysical Research Communications* **70**, 73-80

55. Trumpower, B. L., and Edwards, C. A. (1979) *J. Biol. Chem.* **254**, 8697-8706

56. Crofts, A. R., and Wraight, C. A. (1983) *Biochim. Biophys. Acta - Reviews on Bioenergetics* **726**, 149-185

57. Rich, P. R. (1984) *Biochim. Biophys. Acta - Reviews on Bioenergetics* **768**, 53-79

58. Robertson, D. E., and Dutton, P. L. (1988) *Biochimica et Biophysica Acta (BBA) - Bioenergetics* **935**, 273-291

59. Crofts, A. R., and Wang, Z. (1989) *Photosynthesis Research* **22**, 69-87

60. Gennis, R. B., Barquera, B., Hacker, B., Doren, S. R., Arnaud, S., Crofts, A. R., Davidson, E., Gray, K. A., and Daldal, F. (1993) *Journal of Bioenergetics and Biomembranes* **25**, 195-209

61. Crofts, A. (2004) *Photosynthesis Research* **80**, 223-243

62. Crofts, A. R. (1985) *The Enzymes of Bioclogical Memebranes* **4**, 347-382

63. Crofts, A. R., and Z., W. (1989) *Photosynthesis Research* **22**, 69-87

64. Brandt, U., and Trumpower, B. (1994) *Crit Rev Biochem Mol Biol* **29**, 165-197

65. Crofts, A. R., Shinkarev, V. P., Kolling, D. R. J., and Hong, S. (2003) *J. Biol. Chem.* **278**, 36191-36201

66. Crofts, A. R. (2004) *Photosynthesis Research* **80**, 223

67. Brandt, U. (1998) *Biochim. Biophys. Acta - Bioenergetics* **1365**, 261-268

68. Brandt, U., and Okun, J. G. (1997) *Biochemistry* **36**, 11234-11240

69. Brandt, U. (1996) *Biochim. Biophys. Acta* **1275**, 41-46

70. Hong, S., Ugulava, N., Guergova-Kuras, M., and Crofts, A. R. (1999) *J. Biol. Chem.* **274**, 33931-33944

71. Link, T. A., and von Jagow, G. (1995) *J. Biol. Chem.* **270**, 25001-25006

72. Crofts, A. R. (2004) *Annual Review of Physiology* **66**, 689-733

73. Yu, C.-A., Wen, X., Xiao, K., Xia, D., and Yu, L. (2002) *Biochim. Biophys. Acta - Bioenergetics* **1555**, 65-70

74. Kirk C. Hansen, Brian E. Schultz, Guangyang Wang, and Chan, S. I. (2000) *Biochim. Biophys. Acta* **1456**, 121

75. Link, T. A. (1997) *FEBS Letters* **412**, 257-264

76. Junemann, S., Heathcote, P., and Rich, P. R. (1998) *J. Biol. Chem.* **273**, 21603-21607

77. Snyder, C. H., Gutierrez-Cirlos, E. B., and Trumpower, B. L. (2000) *J. Biol. Chem.* **275**, 13535-13541

78. Trumpower, B. L. (2002) *Biochim. Biophys. Acta - Bioenergetics* **1555**, 166

79. Huangen Ding, C. C. M., Dan E. Robertson, Mariko K. Tokito, Fevzi Daldal, P. Leslie Dutton;. (1995) *biochemistry* **34**, 15979-15996

80. Brandt, U., Haase, U., Schagger, H., and von Jagow, G. (1991) *J. Biol. Chem.* **266**, 19958-19964

81. Brandt, U., and von Jagow, G. (1991) *Eur J Biochem* **195**, 163-170

82. De Vries, S., Albracht, S. P., Berden, J. A., and Slater, E. C. (1981) *J. Biol. Chem.* **256**, 11996-11998

83. Zhang, H., Osyczka, A., Dutton, P. L., and Moser, C. C. (2007) *Biochim. Biophys. Acta - Bioenergetics* **1767**, 883-887

84. Christopher H. Snyder, E. B. G.-C., and Bernard L. Trumpower. (2000) *Journal of biological chemistry* **275**, 13535 - 13541

85. Zhu, J., Egawa, T., Yeh, S.-R., Yu, L., and Yu, C.-A. (2007) *Proc. Natl. Acad. Sci. U.S.A* **104**, 4864-4869

86. Ferguson, S. J., Jackson, J. B., and McEwan, A. G. (1987) *FEMS Microbiology Letters* **46**, 117-143

87. Yurkov, V. V., and Beatty, J. T. (1998) *Microbiol. Mol. Biol. Rev.* **62**, 695-724

88. Yu, L., Mei, Q. C., and Yu, C. A. (1984) *J. Biol. Chem.* **259**, 5752-5760

89. Ljungdahl, P. O., Pennoyer, J. D., Robertson, D. E., and Trumpower, B. L. (1987) *Biochimica et Biophysica Acta (BBA) - Bioenergetics* **891**, 227-241

90. Katherine M. Andrews, A. R. C., Robert B. Gennis. (1990) *Biochemistry* **29**, 2645-2651

91. Purvis, D. J., Theiler, R., and Niederman, R. A. (1990) *J. Biol. Chem.* **265**, 1208-1215

92. Yun, C. H., Beci, R., Crofts, A. R., Kaplan, S., and Gennis, R. B. (1990) *Eur J Biochem* **194**, 399-411

93. Usui, S., and Yu, L. (1991) *J. Biol. Chem.* **266**, 15644-15649

CHAPTER II

ON THE MECHANISM OF QUINOL OXIDATION AT Q_P SITE IN CYTOCHROME BC_1 COMPLEX: STUDIED BY MUTANTS WITHOUT CYTOCHROME B_L OR B_H

Abstract

To elucidate the mechanism of bifurcated oxidation of quinol in the cytochrome bc_1 complex, *Rhodobacter sphaeroides* mutants, H198N and H111N, lacking heme b_L and heme b_H, respectively, were constructed and characterized. Purified mutant complexes have the same subunit composition as that of the wild-type complex, but have only 9-11% of the electron transfer activity, which is sensitive to stigmatellin or myxothiazol. The E_ms for hemes b_L and b_H in the H111N and the H198N complexes are -95 mV and -35 mV, respectively. The pseudo first order reduction rate constants for hemes b_L and b_H in the H111N and the H198N, by ubiquiniol, are 16.3 and 12.4 s^{-1}, respectively. These indicate that the Q_p site in the H111N mutant complex is similar to that in the wild-type complex. Pre-steady state reduction rates of heme c_1 by these two mutant complexes decreases to a similar extent of their activity, suggesting that the decrease in electron transfer activity is due to impairment of movement of the head domain of reduced ISP, caused by disruption

of electron transfer from heme b_L to heme b_H. Both mutant complexes produce as much superoxide as does antimycin A treated or proteinase k digested wild type complex. The fact that superoxide generating activities of wild type and mutant complexes are not affected by proteinase treatment suggests that a protein component of the complexes is not essential for superoxide production. Ascorbate eliminates all superoxide generating activity in the intact, antimycin inhibited, or proteinase treated wild type or mutant complexes.

Introduction

The cytochrome bc_1 complex, also known as complex III or ubiquinol-cytochrome *c* oxidoreductase, is an essential segment of the electron transfer chain in mitochondria and photosynthetic bacteria (1). The complex catalyzes electron transfer from quinol to cytochrome *c* (c_2 in some bacteria) with concomitant translocation of protons across the inner membrane of mitochondria or cytoplasmic membrane of bacteria. Intensive biochemical and biophysical studies on this complex (2-4) have led to the formulation of the "protonmotive Q-cycle" mechanism for electron and proton transfer in this complex (5-7). The key step of the Q-cycle mechanism is the bifurcated oxidation of quinol at the quinol oxidation site (Q_P). In the Q-cycle mechanism, it was postulated that the first electron of quinol is transferred to the "high-potential chain", consisting of iron-sulfur protein (ISP) and cytochrome c_1. Then the second electron of quinol, via a transient semiquinone, is passed through the "low-potential chain" consisting of cytochromes b_L and b_H, to reduce ubiquinone or ubisemiquinone bound at the quinol reduction site (Q_N). One drawback of this sequential scheme is the lack of a "functional" semiquinone at the Q_P site (8-10), even though some radicals have been reported under abnormal conditions (11,12). Recently, pre-steady state kinetic analysis of the reduction of cytochrome b_L and ISP in a same sample using fast quenching coupled with EPR (13) indicates that both iron-sulfur cluster (ISC) and heme b_L are reduced by quinol at the same rate, suggesting a concerted scheme for the bifurcated oxidation of quinol at the Q_P site (13,14).

Although the concerted mechanism explains why the proposed semiquinone at the Q_P site is not detected (13), the proponents of sequential mechanism argue that the similar reduction rates observed in heme b_L and ISC is due to the low (60 μs) time resolution of the instrument used. They attribute the missing of semiquinone to its low stability and the fast electron transfer to heme b_L (15). One way to confirm the existence of semiquinone at Q_P site is using a mutant complex lacking heme b_L. If the sequential mechanism exists, one should expect to see some Q_p site semiquinone in this mutant complex, due to the lack of its electron acceptor, heme b_L.

The first cytochrome bc_1 complex crystallographic structure from bovine heart mitochondria was reported in 1997 (16). Since then, more X-ray crystallographic structures of bc_1 complexes from different species have become available (17-20). Based on the poor electron density of ISP and the larger than expected distance between ISC and heme c_1 in the first crystallographic structure, a need for head domain movement and flexibility of the neck region of ISP were proposed (16-18) and confirmed experimentally (21-27). The head domain of ISP is considered to have two docking positions: "*b*" position and "c_1" position (17). Reduction of ISP by quinol takes place when the head domain of ISP is located at the *b*-position. It then moves to the c_1-position to reduce cytochrome c_1. Although few investigators question the requirement for movement of the ISP head domain during bc_1 catalysis (17,21-27), there is no consensus for what the driving force for this movement is (8,13,28-31).

One proposed mechanism suggests that movement of reduced ISP head domain from *b*-position to c_1 position is regulated by protein conformational changes induced by electron transfer from heme b_L to heme b_H (13,31). Recent results (32,33) of analyses of the binding affinity and inhibitory efficacies of P_m and P_f inhibitors, at different redox states of cytochrome bc_1 complex, are consistent with this proposal. One way to further substantiate this proposal is to determine the electron transfer activity and pre-steady state reduction rates of hemes c_1, b_L and b_H, by quinol, in the presence and absence of inhibitors, in mutant complexes lacking heme b_L or heme b_H and compare with those obtained from the wild-type complex. If this proposal is correct, one would expect to see a decrease in electron transfer activity and the rate of heme c_1 reduction in b_H and b_L knock-out mutant complexes.

Formation of superoxide anion is a well established side reaction during the oxidation of quinol by cytochrome bc_1 complex. Addition of antimycin to the intact bc_1 complex increases superoxide production (34-36). The electron leakage (or superoxide production) site can be at semiquinone (37) of the Q_p site or reduced heme b_L (34,38), depending on the mechanism by which bifurcation of ubiquinol proceeds. If bifurcation of quinol at the Q_p site proceeds by the sequential mechanism, semiquinone formed at the Q_P site and reduced heme b_L would both be the electron leakage sites during bc_1 catalysis. Thus, one would expect to see at least some increase in superoxide production in the mutant complex lacking heme b_L, due to the possible increase of semiquinone. If

bifurcation of ubiquinol at the Q_p site proceeds by the concerted mechanism, reduced heme b_L would be the only electron leakage site, since there will be no semiquinone at the Q_P site during bc_1 catalysis.

The mechanism for superoxide production by the bc_1 complex is unclear. Although it is generally believed that the protein components of the bc_1 complex are essential for superoxide production, perhaps a hydrophobic environment provided by the complex, during quinol oxidation, leads to superoxide formation. To test this possibility, the wild-type complex was subjected to proteinase K digestion at room temperature and the electron transfer activity and superoxide production were monitored during the digestion course. It was a surprise to see that electron transfer activity decrease correlates with superoxide production increase, suggesting that protein components of the complex play little role in superoxide generation during oxidation of quinol. Comparing superoxide production by wild-type and by mutant complexes lacking either heme b_L or heme b_H, under various conditions, should provide insight into the superoxide production mechanism.

Herein we report detailed procedures for generating *R. sphaeroides* mutants expressing cytochrome bc_1 complex lacking either heme b_L (H198N) or heme b_H (H111N), purifying cytochrome bc_1 complexes from intra-cytoplasmic membranes (ICM) of both mutants, and characterizing the purified mutant complexes in subunit composition, electron transfer activity, absorption spectral properties, redox protential, presteady state

reduction kinetics of hemes (b_L, b_H, and c_1) and superoxide production of purified and proteinase treated complexes. Based on the observation that proteinase K digested wild-type complex produces the same amount of superoxide as does antimycin-treated complex, it is speculated that protein components of the bc_1 complex have small role in superoxide formation during quinol oxidation.

Experimental Procedures

Materials- Cytochrome *c* (horse heart, type III), stigmatellin, myxothiazol, antimycin A and xanthine oxidase were purchased from Sigma. *n*-Dodecyl-β-D-maltopyranoside (DM) and *n*-Octyl-β-D-gluocopyranoside (OG) were from Anatrace. Proteinase K was purchased from Invitrogen. Nickel nitrilotriacetic acid gel and a Qiaprep spin Miniprep kit were from Qiagen. 2-Methyl-6-(4-methoxyphenyl) -3,7-dihydroimidazol[1, 2-α] pyrazin-3-one, hydrochloride (MCLA) was from Molecular Probes, Inc. 2,3-Dimethoxy-5-methyl-6-(10-bromodecyl)-1,4-benzoquinol($Q_0C_{10}BrH_2$) was prepared as previously reported (39). All other chemicals were of the highest purity commercially available.

Generation of R. sphaeroides cytochrome bc_1 mutants- Mutations were constructed by the QuickChange site-directed mutagenesis kit from Stratagene using a supercoiled double-stranded pGEM7Zf(+)-*fbc*B as template. Forward and reverse primers were used for PCR amplification (Table I). The pGEM7Zf(+)-*fbc*B plasmid (40) was constructed by

Table I: Oligonucleotides used for site-directed mutagenesis

H198N(F)*	CGGTTCTTCTCGCTGAAC#TACCTGCTGCCCTTCG
H198N(R)	CGAAGGGCAGCAGGTAGTTCAGCGAGAAGAACCG
H111N(F)	CGCGGTCTATCTGAACATCTTCCGCGGCCTC
H111N(R)	GAGGCCGCGGAAGATGTTCAGATAGACCGCG

* F and R in the parentheses denote forward and reverse primers, respectively.

The underlined bases correspond to the genetic codes for the amino acid(s) to be mutated.

ligating the *Nsi*I-*Xba*I fragment from pRKDfbcFBC$_{6H}$Q into *Nsi*I and *Xba*I sites of the pGEM7Zf(+) plasmid. The *Nsi*I-*Xba*I fragment from the pGEM7Zf(+)-*fbc*B$_m$ plasmid was ligated into the *Nsi*I and *Xba*I sites of the pRKD418-fbcFB$_{Km}$C$_{6H}$Q plasmid to generate the pRKD418-*fbc*FB$_m$C$_{6H}$Q plasmid. A plate-mating procedure (41) was used to mobilize the pRKD418-*fbc*FB$_m$C$_{6H}$Q plasmid in *E. coli* S17 cells into *Rhodobacter sphaeroides* BC17 cells. The presence of engineered mutations was confirmed by DNA sequencing of the NsiI-XbaI fragment as previously reported (41). DNA primers were purchased from Invitrogen Company. DNA sequencing was performed by the Recombinant DNA/Protein Core Facility at Oklahoma State University.

Enzyme Preparations and Activity Assays- Chromatophores, intracytoplasmic membrane and the His$_6$-tagged cytochrome bc_1 complexes were prepared as previously reported (21). To assay cytochrome bc_1 complex activity, chromatophores or purified cytochrome bc_1 complexes were diluted with 50 mM Tris-Cl, pH 8.0, containing 200 mM NaCl and 0.01% DM to a final concentration of cytochrome c_1 of 1 μM. Appropriate amounts of the diluted samples were added to 1 ml of assay mixture containing 100 mM Na^+/K^+ phosphate buffer, pH 7.4, 300 μM EDTA, 100 μM cytochrome *c*, and 25 μM $Q_0C_{10}BrH_2$. Activities were determined by measuring the reduction of cytochrome *c* (the increase of absorbance at 550 nm) in a Shimadzu UV 2401 PC spectrophotometer at 23 °C, using a millimolar extinction coefficient of 18.5 for calculation. The non-enzymatic

oxidation of $Q_0C_{10}BrH_2$, determined under the same conditions in the absence of enzyme, was subtracted from the assay.

Determination of heme content in bc_1 complexes- To determine the concentrations of hemes c_1 and b in wild-type and mutant complexes of H111N and H198N, purified cytochrome bc_1 samples were diluted to a concentration of 5μM of cytochrome c_1 in 1.0 ml aqueous solution containing 200 mM NaOH and 40% pyridine. An appropriate amount of $K_3Fe(CN)_6$ was added to assure bc_1 complexes were fully oxidized. Spectra of oxidized bc_1 samples were recorded in a Shimadzu UV-2401 P C spectrophotometer at 23 ^oC. Solid sodium dithionite (a few grains) was then added, and several successive spectra of the reduced pyridine hemochromes were recorded (every 20 seconds) until there were no significant differences between two consecutive spectra. Table II lists the extinction coefficients (42) of pyridine hemochromes used to calculate the concentration of hemes b and c_1. To calculate the concentration of hemes b and c_1 in a bc_1 sample, the equation pair below was employed. In these equations ε stands for the extinction coefficient. The subscript numbers of ε indicate the corresponding wavelengths. C stands for concentration.

$$C_{c1} \times \varepsilon^{c1}_{549-540} + C_b \times \varepsilon^{b}_{549-540} = OD_{549-540}$$

$$C_{c1} \times \varepsilon^{c1}_{558-580} + C_b \times \varepsilon^{b}_{558-580} = OD_{558-580}$$

Potentiometric Titrations of the Cytochrome b of Mutant Cytochrome bc_1 Complexes- Redox titrations of cytochromes b in wild type and mutant bc_1 complexes were essentially according to the published method (43,44). 3-ml aliquots of the bc_1 complex (2

Table II: Difference millimolar extinction coefficients of reduced pyridine hemochromogen of hemes *b* and c_1 at the selected wavelengths

Hemochromogen	$\varepsilon^{\mathrm{mM}}_{549-540\,\mathrm{nm}}$	$\varepsilon^{\mathrm{mM}}_{558-580\,\mathrm{nm}}$
Heme c_1	21.13	4.28
Heme *b*	9.98	32.86

μM cytochrome *b*) in 0.1 M Na^+/K^+ phosphate buffer, pH 7.0, containing 25 μM of 1,4-benzoquinone (E_m, 293mV), 2,3,5,6 -tetramethyl-p-phenylenediamine (E_m, 260 mV), 1,2-naphthoquinone (E_m, 143 mV), phenazine methosulfate (E_m, 80 mV), phenazine ethosulfate (E_m, 55 mV), 1,4-naphthoquinone (E_m, 36 mV), duroquinone (E_m, 5 mV), pyocyanine (E_m, -34 mV), indigo carmine (E_m, -125 mV), and anthraquinone-2-sulfonic acid (E_m, -225 mV), were used. Reductive titrations were carried out by addition of sodium dithionite solution to the ferricyanide-oxidized samples and oxidative titrations by addition of ferricyanide solution to the dithionite-reduced samples. At indicated E_h values during the redox titration, absorption spectra from 600 to 500 nm were taken. The optical absorbance at 560 nm, minus that at 580 nm, was used for determination of cytochrome *b* reduction. Midpoint potentials of cytochrome b_L and b_H were calculated by fitting the redox titration data, using the Nernst equation for a one-electron carrier (n = 1), by Kaleidagraph (44).

Fast-Kinetics Study- To determine electron transfer rates between the quinol and heme *b* or heme c_1, the cytochrome bc_1 complex was mixed with ubiquinol ($Q_0C_{10}BrH_2$) in equal volume at room temperature in an Applied Photophysics stopped-flow reaction analyzer SX.18MV (Leatherhead, England). The concentration of bc_1 complex was 12 μM (based on cytochrome c_1) in 50 mM of Tris-Cl, pH 8.0 at 4˚C, containing 200 mM NaCl and 0.01% DM. For use in the stopped-flow, $Q_0C_{10}BrH_2$ in ethanol was diluted to 240 μM in the same buffer. Reductions of cytochrome *b* and cytochrome c_1 in wild type were

monitored by the increase of absorption difference of $OD_{560\text{-}580}$ and $OD_{551\text{-}539}$, respectively with a photodiode array scan between 600-500 nm. Reductions of cytochrome b_L in H111N and b_H in H198N were determined from the increase in $OD_{565\text{-}580}$ and $OD_{560\text{-}580}$. When an inhibitor was used, the cytochrome bc_1 complex was treated with 5-fold molar excess of inhibitor over heme c_1, for 5 minutes at 4°C, prior to the experiment. Since the concentration of ubiquinol used was 20 times higher than that of cytochrome bc_1 complex, the reactions between bc_1 and quinol were treated as pseudo first order reactions. Time traces of the reaction were fitted with first-order rate equation to obtain the pseudo first rate constants k_1 by kaleidagraph.

Detection of Q radical at the Q_P site with EPR- 300 µl of 150 µM purified cytochrome bc_1 complexes was treated with 10-fold excess of ubiquinol to fully reduce cytochrome c_1 in 10 seconds and frozen in liquid nitrogen. EPR spectra were recorded at -170 ºC with the following instrument settings: microwave frequency, 9.4 GHz; microwave power, 2.2 milliwatts; modulation amplitudes, 6.3 G; modulation frequency, 100 kHz; time constant, 655.4 ms; sweep time: 167.8 s; conversion time, 163.8 ms.

Determination of Superoxide Production- Superoxide anion generation was determined by measuring the chemiluminescence of MCLA-$O^{\cdot-}$ adduct (45), in an Applied Photophysics stopped-flow reaction analyzer SX.18MV (Leatherhead, England), by leaving the excitation light off and registering light emission (46,47). Reactions were carried out at 23 °C by mixing 1:1 solutions A and B. Solution A contains 100 mM Na^+/K^+

phosphate buffer, pH 7.4, 1 mM EDTA, 1 mM KCN, 1 mM NaN_3, 0.1% bovine serum albumin, 0.01% DM, and 5.0 μM of wild-type or mutant bc_1 complex. Solution B was the same as A with bc_1 complex being replaced with 125 μM $Q_0C_{10}BrH_2$ and 4 μM MCLA. Once the reaction starts, the produced chemiluminescence in voltage was consecutively monitored for 2 seconds.

Proteolytic cleavage of protein subunits of the cytochrome bc_1 complex- To digest subunits of the cytochrome bc_1 complex, the wild-type complex was diluted with 50mM Trish-HCl buffer, pH 7.4, containing 200 mM NaCl and 0.01% DM, to a protein concentration of 20 mg/mL and incubated with 0.4 mg/mL of proteinase K at room temperature. The electron transfer activity and superoxide generation activity were followed during the course of incubation. When electron transfer activity is completely lost, the incubated mixture was subjected to SDS-PAGE to confirm the protein digestion.

Results and Discussion

Characterization of mutants lacking either heme b_L (H198N) or heme b_H (H111N)- In the cytochrome *b* subunit of cytochrome bc_1 complex from *Rhodobacter sphaeroides*, His97 and His198 are the ligands of heme b_L while His111 and His212 are the ligands of heme b_H. Two mutants, H198N and H111N, in which histidine-198 and histidine-111 of cytochrome *b* were respectively substituted with Asn were constructed and selected for the present study. The H198N mutant knocks out heme b_L, while the H111N mutant knocks out heme b_H. Since the cytochrome bc_1 complex is absolutely required for photosynthetic

growth of this bacterium, and hemes b_L and b_H constitute the low potential electron transfer chain in the proposed Q-cycle mechanism, it is important to see whether or not these two mutants can support photosynthetic growth. Cultures of wild-type and mutants were placed in a light tank after four hours of dark grow. Photosynthetic growth was followed by the increase of cell intensity. None of the mutants show any evidence of growth in 6-8 days. In order to grow cells for the preparation of mutated bc_1 complexes, H198N and H111N were grown semi-aerobically. These two mutants can grow semiaeroically at a rate comparable to that of the wild-type cells. ICM were prepared from semiaerobically grown cells and used for preparation of corresponding mutant complexes.

ICMs prepared from mutants H198N and H111N contain subunits cytochrome *b*, cytochrome c_1, ISP and subunit IV in the same concentrations as those detected in the wild-type ICM, determined by Western blot using antibodies against these four individual proteins. This result indicates that lacking heme b_L in the H198N mutant and lacking heme b_H in the H111N mutant does not impair the complex assembly into the ICM membrane. This finding is contradictory to the previous report (53) that ICMs from mutants lacking heme b_H (H111N, H111D and H212D) have subunits of cytochromes *b* and c_1, while no such subunits were detected in ICMs from mutants lacking heme b_L (H97N, H97D, H198N, H198Y). While constructing mutants lacking heme b_L or heme b_H we observed that some heme b_L knocked out mutants, such as H97F and H97N, are unstable, purification attempts were not successful. The structural stability of H198N and

H111N mutant complexes in their ICMs enables us to purify and characterize these two mutant complexes with methods similar to those used for the wild-type complex.

Figure II-1 compares SDS-PAGE patterns of purified complexes, wild-type and mutants and their proteinase K-treated products. The purification procedure involves DM solubilization followed by Ni-affinity gel column chromatography (21). The yields and subunit compositions of purified mutant complexes are comparable to those of the wild-type.

Figure II-2 shows absorption spectra of purified wild-type (A) and mutant complexes of H198N (B) and H111N (C). The presence of cytochromes b_H and b_L in the wild-type complex, is revealed by a difference spectrum of dithionite-partially reduced minus ascorbate reduced and a difference spectrum of dithionite-fully reduced minus dithionite-partially reduced, respectively (48). If a catalytic amount of succinate-Q reductase is added to a purified wild-type complex, b_H is observed from a difference spectrum of succinate-reduced minus ascorbate-reduced and b_L from a difference spectrum of dithionite-reduced minus succinate-reduced (49). Ascorbate reduces cytochrome c_1; succinate reduces cytochromes c_1 and b_H; dithionite reduces cytochromes c_1, b_H and b_L. Cytochrome b_H has an alpha absorption peak at 560 nm, whereas cytochrome b_L has a double-alpha peak with absorption at 565 nm and a shoulder at 558 nm (see Figure II-2A). The alpha absorption peak of cytochrome *b* in the H198N mutant complex (Figure II-2B), which is obtained from a difference spectrum of dithionite-reduced minus

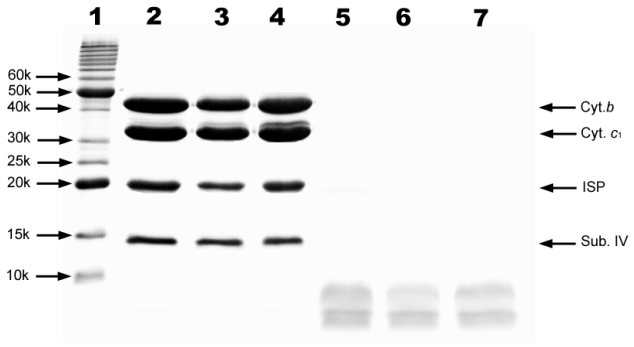

Figure II-1. SDS-PAGE of purified cytochrome bc_1 complexes from wild type and mutants H198N and H111N. Lanes 1-7 are for polypeptide standard, wild type, mutant H198N, mutant H111N and proteinase K-treated wild type, H198N, H111N, respectively. Aliquots of purified bc_1 complexes were incubated with 1% SDS with 0.4% β-ME at 37 °C for 20 minutes. Digested samples containing about 200 pmol of cytochrome c_1 were subjected to electrophoresis. The molecular weights of standard polypeptides are: 10, 15, 20, 25, 30, 40, 50 and 60 kDa.

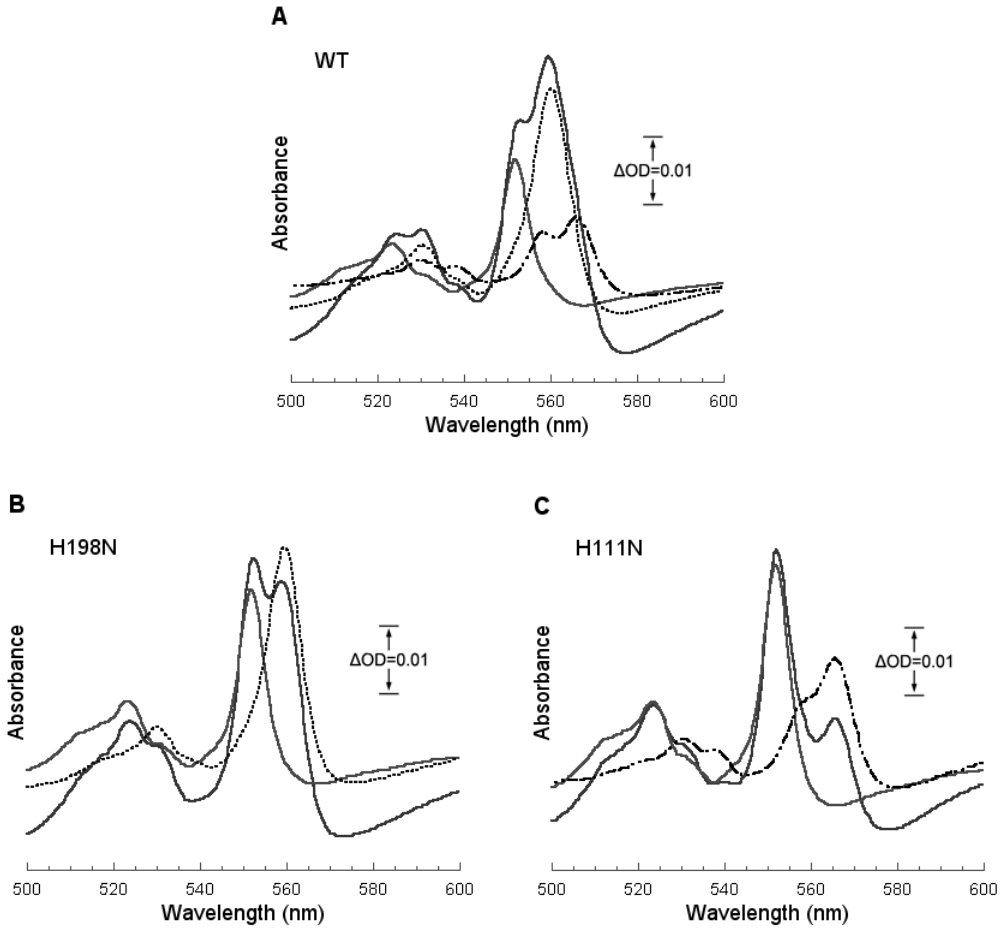

Figure II-2. Absorption spectra of wild-type and mutant bc_1 complexes. A, B and C are for the wild type, mutants H198N and H111N complexes, respectively. The cytochrome c_1 concentration of complexes used was 1μM for A, 1.5 μM for B and C. The gray spectrum stands for ascorbated-reduced sample; and black solid spectrum for the dithionite-fully reduced sample. The black dotted and black dot-dash spectra in B and C, respectively, are difference spectra of the dithionite fully reduced minus ascorbate reduced samples. Black dotted and black dot-dash spectra in A are the difference spectra of the dithionite partially reduced (~ -50 mV) minus ascorbate reduced and of the dithionite fully reduced minus the dithionite partially reduced, respectively.

ascorbate-reduced, is at 560 nm, indicating that only cytochrome b_H is present in this mutant complex. The alpha peak of cytochrome *b* in the H111N mutant complex is at 565 nm with a shoulder at 558 nm (Figure II-2C), indicating that only cytochrome b_L is present in this mutant complex.

To detect the presence of trace amounts of other cytochrome *b* in a given mutant, the complex was titrated with dithionite solution to reduce cytochromes *b* gradually (data not shown). In the mutant H198N complex, the last reduced heme *b* showed a heme b_H absorption spectrum, the same as that of the very first reduced one, suggesting that the H198N mutant complex contains only heme b_H. If there is some heme b_L in this mutant complex, the difference spectrum of the last dithionite reduced minus the second to last dithionite reduced should differ from that of the first dithionite reduced minus ascorbate reduced, because heme b_L is expected to be reduced last due to its low redox potential. In the H111N mutant complex, the difference spectrum of the first dithionite reduced minus ascorbate reduced is the same as the difference spectrum obtained from the last dithionite reduced minus the second to the last dithionite reduced. These two difference absorption spectra are identical to those of heme b_L in the wild type complex, suggesting that the H111N mutant complex contains only heme b_L.

In general, for bc_1 complexes, hemes *b*, including heme b_L and b_H, are calculated from the difference extinction coefficient of 28.5/mM·cm between 560 nm and 580 nm in the difference spectrum of dithionite reduced minus ascorbate reduced samples. The

heme c_1 is calculated from a difference spectrum of ascorbate reduced minus ferricyanide oxidized complex using a difference extinction coefficient of 17.5/mM·cm between 551 and 539 nm. Since the extinction coefficient of individual heme b_L and heme b_H is not firmly established, we used the alkaline pyridine hemochromogen spectrum to determine the concentrations of hemes *b* and c_1 in mutant complexes of H198N and H111N. The equations used for calculation are listed in the "Experimental Procedure" section. In wild type bc_1 complex the b/c_1 molar ratio is about 1.65. In mutant complexes of H198N and H111N, b/c_1 molar ratios are close to 1.0 (see Table III). Based on the heme *b* contents determined by pyridine hemochrome and the difference absorption spectra of dithionite reduced minus ascorbate reduced mutant complexes, the difference extinction coefficients for hemes b_L and b_H were calculated to be 12.0/mM·cm between 565 nm and 580 nm and 24.5/mM·cm between 560 nm and 580nm, respectively. The lower than expected b/c_1 ratio in the wild type complex is probably due to the presence of excess cytochrome c_1 in the complex, as the His-tag is located at the C-terminus of cytochrome c_1 protein. The presence of excess cytochrome c_1 in the wild type complex was confirmed by the protein crystallization (50,51). In crystalline bc_1 complex, b/c_1 molar ratio is 2. The excess cytochrome c_1 is found in the mother liquid after crystallization.

Effect of mutations on the electron transfer activity and the redox potential of b hemes- Specific activities of purified mutant complexes were determined and compared to the wild-type complex. Mutant complexes of H198N and H111N have low bc_1 activities,

Table III: Characterization of mutant H198N and H111N bc_1 complexes

	WT	H198N	H111N
Photosynthetic growth	Yes	No	No
Cyt.*b*/Cyt.c_1 ratio	1.65	1.0	0.98
Specific activity*	3.5	0.4	0.32
Antimycin sensitivity	Yes	36.4%#	No
Stigmatellin sensitivity	Yes	Yes	Yes
Myxothiazol sensitivity	Yes	Yes	Yes

*The unit of specific activity is μmoles cytochrome *c* reduced/min/nmole cytochrome c_1

The 36.4% means the loss of 36.4% of its bc_1 activity upon antimycin treatment.

about 9-11% of that in the wild type complex (Table III). The bc_1 activity detected in these two mutant complexes is inhibited by stigmatellin and myxothiazol, indicating ubiquinol can bind and be oxidized at the Q_P site in both complexes. As expected, the H111N mutant complex is completely resistant to antimycin. However, it is somewhat surprising that H198N is partially sensitive to antimycin.

To see if these substitutions have any effect on the E_m of heme b_L or heme b_H, Ems of heme b_L and b_H in mutants H111N and H198N were determined, respectively. As shown in Figure II-3, heme b_H in the H198N mutant complex has an Em of -35 mV, significantly lower than the Em of heme b_H in the wild type complex (50 mV). The Em of heme b_L in the H111N mutant complex is -95 mV, comparable to that of in the wild type complex (-93 mV). However, this value is lower than that reported by others (52) using ICM of the same mutant. Thus the substitution in mutant H198N has some effect on the Em of heme b_H whereas the substitution in mutant H111N has little effect on the Em of heme b_L. These results seem contradictory to the columbic interaction between hemes b_L and b_H reported in the literature (15,52).

Effect of mutations on the rate of heme c_1 reduction by quinol- The loss of heme b_L and heme b_H in the mutant complexes of H198N and H111N, respectively, provides us an opportunity to study the effect of the low potential chain on c_1 reduction and movement of the ISP head domain. The fast-kinetics study is carried out on the Stop-flow instrument of Applied photophysics Ltd. Figure II-4 shows the time traces of heme c_1 reduction, for 1.2

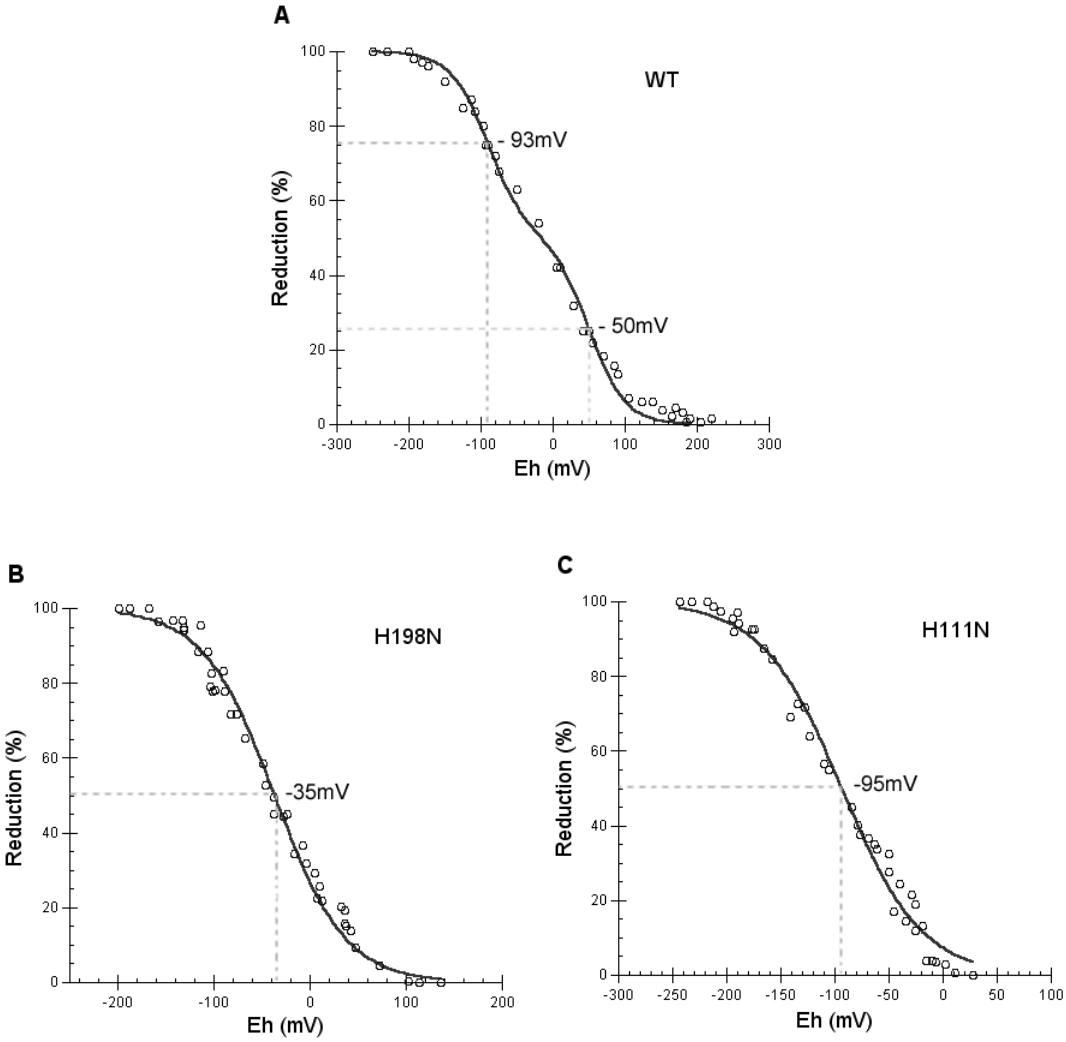

Figure II-3. Redox potential titration of heme *b* in wild type (A), H198N (B) and H111N (C) mutants cytochrome bc_1 complexes. Oxidative and reductive titrations were performed using potassium ferricyanide and sodium dithionite respectively, as described in "Experimental Procedures".

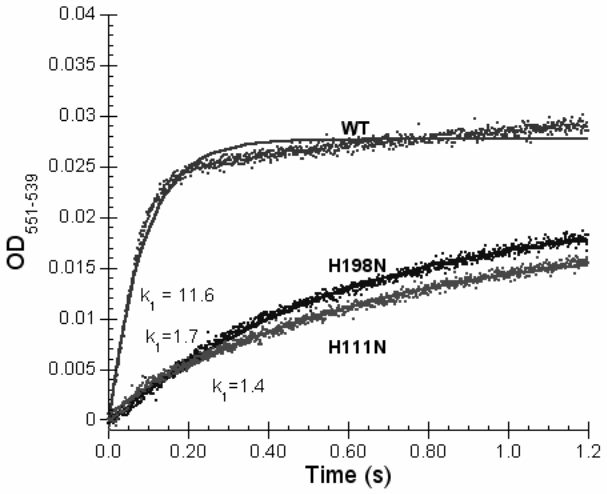

Figure II-4. Time trace of heme c_1 reduction by $Q_0C_{10}BrH_2$ in wild-type and mutant complexes. Experiments were performed with The Applied Photophysics stopped-flow reaction analyzer SX 18MV. Reactions and measurements were performed as described in "Experimental Procedures". The final concentrations of complexes and $Q_0C_{10}BrH_2$ were 6 and 120 μM, respectively. Solid lines represent fitted curves.

seconds, in wild-type and mutant complexes of H198N and H111N. Heme c_1 reduction rates in the two mutant complexes are much lower than that in the wild type complex. Assuming heme c_1 reduction is a pseudo first order reaction, the k_1s are determined to be 11.6, 1.7, and 1.4 s^{-1} for the wild-type and mutant complexes of H198N and H111N, respectively. The heme c_1 reduction rates in the H198N and H111N mutant complexes are only about 15-12% of that in the wild type complex. Despite of low reduction rates of heme c_1 in the two mutant complexes, maximum levels of heme c_1 reduction are the same as that of the wild type complex. 50 % of the total heme c_1 is reduced by ubiquinol as reported (53). Since the Q_P sites in the H198N and H111 mutant complexes are similar to that in the wild-type complex, as both mutant complexes are sensitive to stigmatellin and myxothiazol (the Q_P site inhibitor), the decrease in rate of heme c_1 reduction is not due to the initial bifurcated oxidation of quinol. Likely, this decrease results from impairment of movement of the head domain of reduced ISP, from the *b*-position to c_1 position, caused by disruption of electron transfer from heme b_L to heme b_H in these mutant complexes.

Figure II-5 shows the effect of antimycin A and stigmatellin on the reduction rates of heme c_1 in the wild-type and mutant complexes. Antimycin A is a Q_N site inhibitor and stigmatellin is a Q_P site inhibitor. In the wild type complex antimycin A decreases heme c_1 reduction pseudo first order rate constant from 11.6 to 4.7 s^{-1} (Figure II-5A). This is consistent with the previous report (14) that antimycin A has a significant effect on the reduction rate of heme c_1 in cytochrome bc_1 complexes. In the H198N mutant complex,

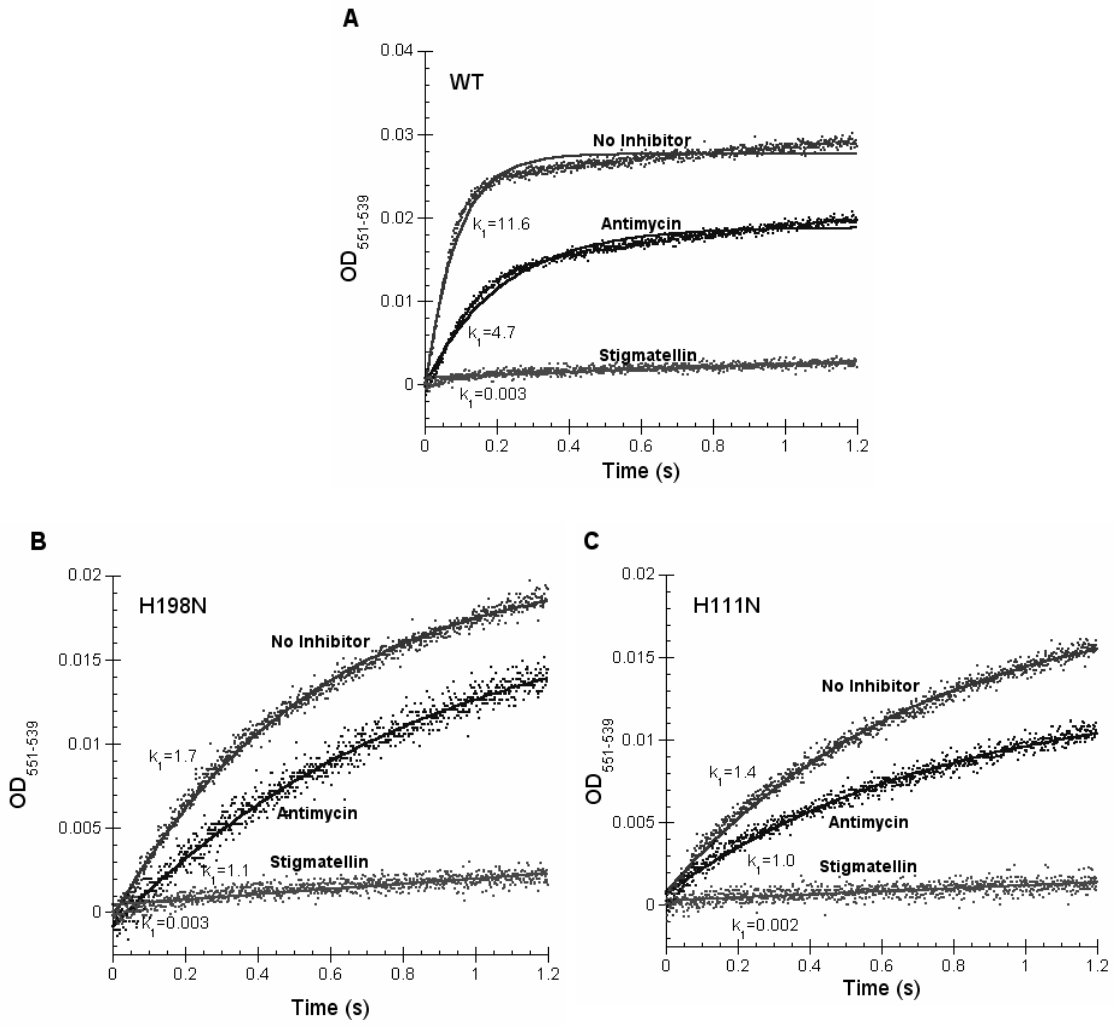

Figure II-5. Time trace of cytochrome c_1 reduction by $Q_0C_{10}BrH_2$ in the wild-type (A) and mutants, H198N (B) and H111N (C), complexes in the presence of inhibitors. Experiment conditions were the same as that in Figure 4 except the presence of inhibitors. Solid lines represent fitted curves.

the rate constant decreases from 1.7 to 1.1 s^{-1}. In the H111N mutant complex, the rate constant decreases from 1.4 to 1.0 s^{-1}. Since both mutant complexes, in which no intact low potential chain is available, also show a decreased rate of heme c_1 reduction in the presence of antimycin A, similar to that observed in the wild-type complex, this inhibitor effect cannot due to blocking of electron transfer in the low potential chain. It probably due to the long range effect of antimycin on Q_p site binding to the Q_N site. In other words, the effect of antimycin A on heme c_1 reduction rate is not through the low potential redox component but through the cytochrome *b* protein subunit.

Addition of stigmatellin to the wild-type and mutant complexes abolishes heme c_1 reduction. These results further confirm that the Q_P site in these two mutant complexes is functional.

Effect of mutations on the rates of heme b_L and heme b_H reductions by quinol- Figure II-6 shows hemes *b* reduction by quinol, in the presence and absence of antimycin and stigmatellin, in wild type and mutant bc_1 complexes. In the H198N mutant complex (Figure II-6B), a small portion of heme b_H is reduced by quinol, in the absence of inhibitors, and the reduction is biphasic. The rate constants for the fast and slow reduction phases are 12.4 and 0.86 s^{-1}, respectively. Fast phase reduction is abolished when antimycin is present. As expected, the presence of stigmatellin has little effect because heme b_H is reduced by quinol through the Q_N site, not the Q_P site.

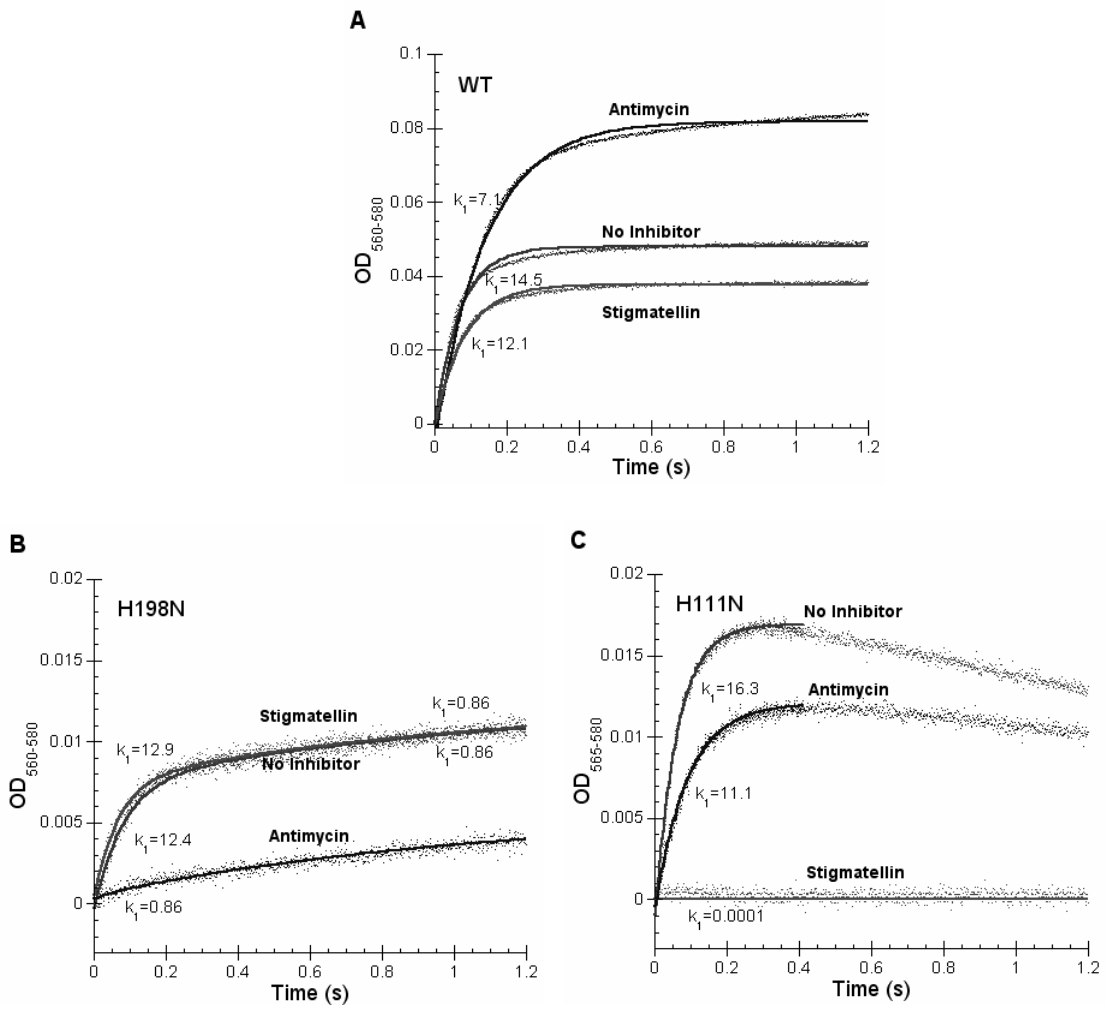

Figure II-6. Time trace of cytochrome *b* reduction by $Q_0C_{10}BrH_2$ in wild-type (A) and H198N (B) and H111N (C) mutant complexes. Reactions and measurements were performed as described in "Experimental Procedures". The reaction was monitored by photodiode array scanning for 1.26 seconds. Reductions of cytochromes b_L and b_H, were determined from the increase in $OD_{565-580}$ and $OD_{560-580}$. Cytochrome *b* (including b_L and b_H) was determined from the increase in $OD_{560-580}$.

In the H111N mutant complex (Figure II-6C), a small portion of heme b_L is rapidly reduced by quinol, in the absence of inhibitors, with a reduction rate constant of about 16.3 s^{-1}, followed by a slow reoxidation. It is likely that the reoxidation of heme b_L will lead to superoxide formation. The slower decay rate of superoxide formed in the H111N complex as compared to that formed in the H198N complex, as will be described in Figure II-8B and C, supports this speculation. Addition of stigmatellin abolishes this reduction. Addition of antimycin affects the rate and extent of heme b_L reduction: the rate constant decreases from 16.3 to 11.1 s^{-1} and the extent of b_L reduction decreases by 30%. In the wild-type complex antimycin also affects both the rate and the extent of heme *b* reduction by quinol (see Figure II-6A): it decreases the rate but increases the extent (14,54-58). It should be noted that heme *b* reduction observed in the wild type complex, in the absence of inhibitor, is mostly heme b_H. The input of electron for reduction could come from the Q_p site via heme b_L, and less likely, directly from quinol at the Q_N site, since the reduction rate of heme b_L (k_1=16.3 s^{-1}) is larger than that of heme b_H (k_1=12.4 s^{-1}) (Figure II-6B and 6C). These results seem contradictory to a report indicating that the rate of heme b_H reduction is larger than that of heme b_L in the yeast cytochrome bc_1 complex (59). The observation that the reduction rate of heme b_L in the H111N mutant complex is similar to, albeit higher than, that of the wild type complex (see Figure II-6A), indicates that the Q_P site in this mutant complex is functional. This finding further supports the idea that antimycin has long range effect on the Q_p site to decrease the rates of heme c_1 and heme b_L reduction.

Attempt to detect Q radical at the Q_P site with mutant H198N- Since H198N has no heme b_L, and thus no electron acceptor for semiquinone, more semiquinone radical would have increased if the sequential mechanism for bifurcated quinol oxidation is functioning. Figure II-7 shows EPR spectra from wild type and mutant bc_1 complexes. In the absence of antimycin a strong signal at g=2.00 is observed in the quinol reduced cytochrome bc_1 complexes from wild-type (Figure II-7A, curve 1) and mutant H198N (Figure II-7B, curve 1). This signal decreases significantly when antimycin is added (Figures 7A and B, curve 2). Apparently the portion of signal that disappears (Figures 7A and B, curve 4) is the signal of semiquinone radical at the Q_N site. However, the signal portion that is insensitive to antimycin is not the long missing semiquinone at the Q_P site, because it is also present in fully oxidized complexes of wild type and mutant H198N (Figures 7A and B, curve 3). It should be noted that this free radical, of unknown origin, is much more concentrated in the H198N complex than in the wild type complex. Its origin is currently under investigation.

The EPR spectra for mutant H111N bc_1 complex (Figure II-7C) were also determined. Oxidized H111N has an unusual EPR spectrum which is not due to contamination. This spectrum appears to be a characteristic of mutants lacking heme b_H, because another heme b_H deficient mutant, H212N, has a similar EPR spectrum (data not shown). The concentrations of ISP in all three complexes were about the same, as indicated by the g=1.89 signal. The g=1.89 signal in Figure II-7C looks smaller because the

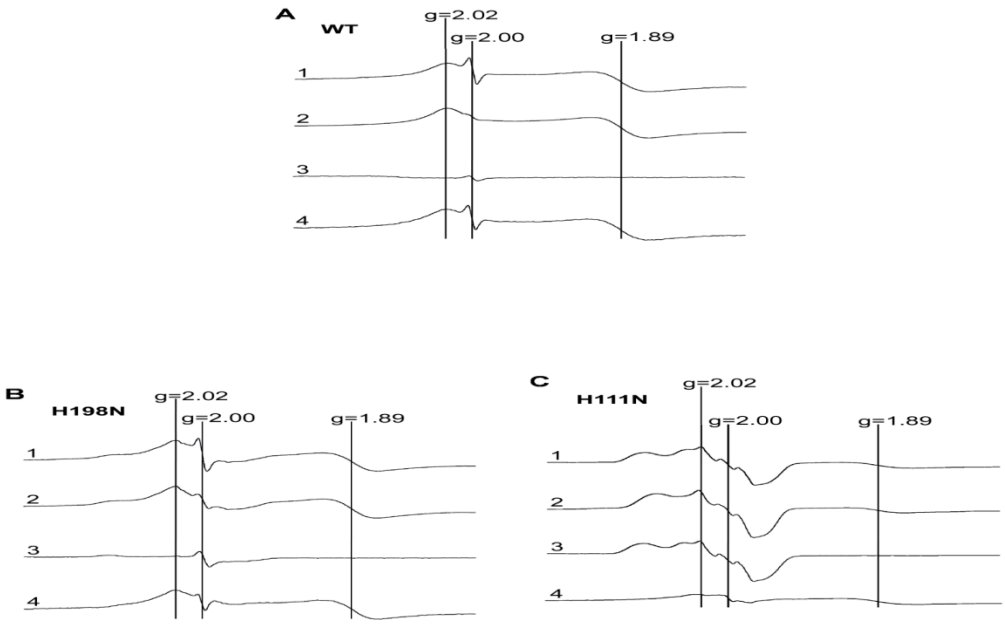

Figure II-7. EPR spectra of ISP and free radical (semiquinone) under different conditions. Purified wild-type (A), H198N (B), and H111N(C) bc_1 complexes were treated with 10-fold excess of $Q_0C_{10}BrH_2$ solution, to fully reduce cytochrome c_1, and frozen in liquid nitrogen. EPR spectra were recorded at -170ºC with the following instrument settings: microwave frequency, 9.4GHz; microwave power, 2.2 milliwatts; modulation amplitudes, 6.3 G; modulation frequency, 100 kHz; time constant, 655.4 ms; sweep time: 167.8 s; conversion time, 163.8 ms. Curve 1 is the spectrum for cytochrome bc_1 complexes reduced by $Q_0C_{10}BrH_2$; Curve 2 for those reduced by $Q_0C_{10}BrH_2$ in the presence of antimycin; Curve 3 for dithionite-oxidized cytochrome bc_1 complexes, Curve 4 for the spectrum derived from Curve 1 minus Curve 2. The absence of signals of reduced ISP defines the fully oxidized state of the complex. For mutant H111N, the signal intensities were reduced to 1/3 to fit in the figure.

intensity of the spectrum was reduced to one third of the original in order to compare the signals in the g=2.00 region, of the three complexes.

Superoxide production in mutant bc_1 complexes during catalysis- Since there is no heme b_L in the H198N and no heme b_H in the H111N, it should be easier for oxygen to get electrons, from either semiquinone or the reduced heme b_L, in these mutant complexes than in the wild type. Figure II-8 shows superoxide production by mutant and wild type complexes under different conditions. In the absence of antimycin, production of superoxide anion by mutant complexes of H198N and H111N is much greater than by the wild type. At the point of strongest chemiluminescence output, superoxide production by H198N and H111N is about 5 times that of the wild type complex (red tracings in Figure II-8). Antimycin significantly increases superoxide production but decreases its production rate in the wild type complex (blue tracing in Figure II-8A). Antimycin has little effect on the amount of superoxide production the production rate in mutants H198N and H111N (blue tracings Figure II-8B and C). This lack of effect of antimycin on superoxide production by H198N and H111N indicates that superoxide is produced at the Q_P site, not at the Q_N site. Thus during bc_1 catalysis, oxygen can only get electrons from reduced heme b_L or from semiquione at the Q_P site.

In bc_1 complexes with fully reduced ISP and cytochrome c_1, no chemiluminescence (O_2^-) is observed upon the addition of quinol (black tracings in Figure II-8), indicating that superoxide production is dependent on ISP reduction by quinol. Therefore, quinol at the Q_P

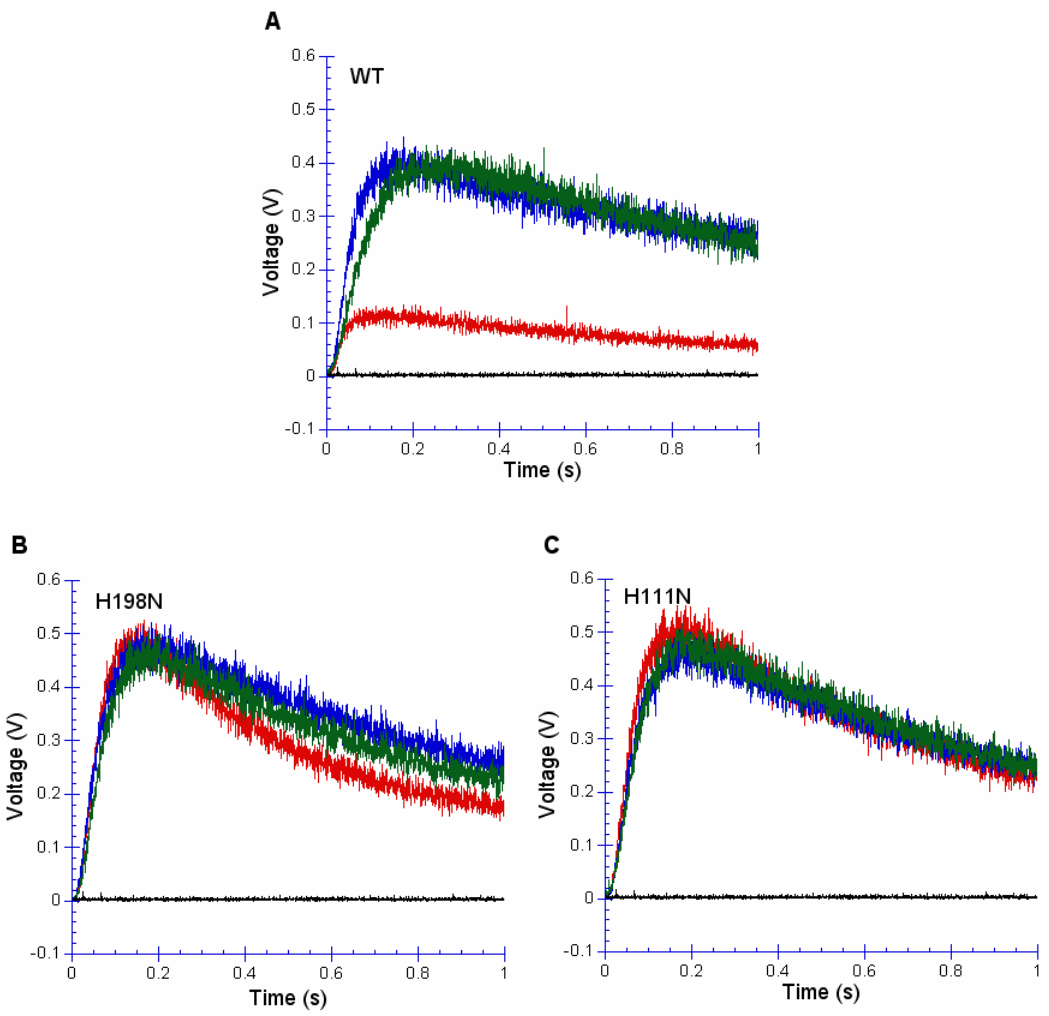

Figure II-8. Superoxide production of wild type and mutant H198N and H111N cytochrome bc_1 complexes. Superoxide production was measured as described in "Experimental Procedures." Red tracings represent complexes without any treatment. Blue, green and black tracings are for complexes with antimycin, Proteinase K and ascorbate treatment, respectively.

site transfers its first electron to iron-sulfur cluster; the second electron, either transferred to heme b_L or retained as semiquinone, reacts with oxygen to produce superoxide. Since there is no detectable semiquinone radical at the Q_P site, molecular oxygen may share quinol electrons with ISP when heme b_L is not available. Normally reduced heme b_L may leak its electron to oxygen. This leakage increases when the low potential electron transfer chain is blocked by antimycin.

Superoxide production requires no electron transfer proteins- The high superoxide production by heme b_H or b_L knock-out mutant and antimycin inhibited wild type bc_1 complexes indicates that this activity may not be directly related to the normal electron transfer. Addition of ascorbate to the bc_1 complex abolishes its ability to produce superoxide, suggesting that some electron acceptor, such as iron-sulfur cluster or other oxidants with comparable redox potentials, is needed (black tracings in Figure II-8). When bc_1 complexes were incubated with proteinase K, all protein subunits were digested to polypeptide with molecular weight less than 10,000 (see Figure II-1). Treatment with proteinase K completely abolished the electron transfer activity of wild type bc_1 complexes, but increase superoxide production to the same level of that in the presence of antimycin. However, treatment with proteinase K has little effect on superoxide production by H111N and H198N mutant complexes (green tracings in Figure II-8). Although mixing quinol and high potential oxidant, such as cytochrome *c* or ferricyanide, in aqueous solution, yields only trace amounts of superoxide, addition of quinol and cytochrome *c* or

ferricyanide to proteinase K treated complex increases superoxide production (data not shown). This increase is directly proportional to the amount of oxidant added, suggesting that generation of superoxide from quinol requires only a hydrophobic environment and a high potential oxidant such as ferricyanide, cytochrome *c* or ISC. Since reduction of ISC is the first reaction in both superoxide generation and cytochrome *c* reduction catalyzed by bc_1 complex, the similar activation energy (60) for these reactions seems reasonable, if the reduction of ISC is rate limiting.

REFERENCE

1. Trumpower, B. L., and Gennis, R. B. (1994) *Annu. Rev. Biochem.* **63**, 675-716
2. Erecinska, M., Chance, B., Wilson, D. F., and Dutton, P. L. (1972) *Proc Natl Acad Sci U S A* **69**, 50-54
3. Wikstrom, M. K. F., and Berden, J. A. (1972) *Biochim. Biophys. Acta - Bioenergetics* **283**, 403-420
4. Alexandre, A., and Lehninger, A. L. (1979) *J Biol Chem* **254**, 11555-11560
5. Mitchell, P. (1976) *J Theor Biol* **62**, 327-367
6. Brandt, U., and Trumpower, B. (1994) *Crit Rev Biochem Mol Biol* **29**, 165-197
7. Crofts, A. R. (2004) *Annu Rev Physiol* **66**, 689-733
8. Link, T. A. (1997) *FEBS Letters* **412**, 257
9. Junemann, S., Heathcote, P., and Rich, P. R. (1998) *J. Biol. Chem.* **273**, 21603-21607
10. Zhang, H., Osyczka, A., Dutton, P. L., and Moser, C. C. (2007) *Biochim. Biophys. Acta - Bioenergetics* **1767**, 883-887
11. De Vries, S., Albracht, S. P., Berden, J. A., and Slater, E. C. (1981) *J. Biol. Chem.* **256**, 11996-11998

12. Cape, J. L., Bowman, M. K., and Kramer, D. M. (2007) *Proc. Natl. Acad. Sci. U.S.A* **104**, 7887-7892

13. Zhu, J., Egawa, T., Yeh, S.-R., Yu, L., and Yu, C.-A. (2007) *Proc. Natl. Acad. Sci. U.S.A* **104**, 4864-4869

14. Snyder, C. H., Gutierrez-Cirlos, E. B., and Trumpower, B. L. (2000) *J. Biol. Chem.* **275**, 13535-13541

15. Crofts, A. R., Holland, J. T., Victoria, D., Kolling, D. R. J., Dikanov, S. A., Gilbreth, R., Lhee, S., Kuras, R., and Kuras, M. G. (2008) *Biochim. Biophys. Acta - Bioenergetics* **1777**, 1001-1019

16. Xia, D., Yu, C.-A., Kim, H., Xia, J.-Z., Kachurin, A. M., Zhang, L., Yu, L., and Deisenhofer, J. (1997) *Science* **277**, 60-66

17. Zhang, Z., Huang, L., Shulmeister, V. M., Chi, Y.-I., Kim, K. K., Hung, L.-W., Crofts, A. R., Berry, E. A., and Kim, S.-H. (1998) *Nature* **392**, 677-684

18. Iwata, S., Lee, J. W., Okada, K., Lee, J. K., Iwata, M., Rasmussen, B., Link, T. A., Ramaswamy, S., and Jap, B. K. (1998) *Science* **281**, 64-71

19. Hunte, C. (2001) *FEBS Letters* **504**, 126-132

20. Lange, C., and Hunte, C. (2002) *Proc. Natl. Acad. Sci. U.S.A* **99**, 2800-2805

21. Tian, H., Yu, L., Mather, M. W., and Yu, C.-A. (1998) *J. Biol. Chem.* **273**, 27953-27959

22. Kim, H., Xia, D., Yu, C.-A., Xia, J.-Z., Kachurin, A. M., Zhang, L., Yu, L., and Deisenhofer, J. (1998) *Proc. Natl. Acad. Sci. U.S.A* **95**, 8026-8033

23. Tian, H., White, S., Yu, L., and Yu, C.-A. (1999) *J. Biol. Chem.* **274**, 7146-7152

24. Xiao, K., Yu, L., and Yu, C.-A. (2000) *J. Biol. Chem.* **275**, 38597-38604

25. Darrouzet, E., Valkova-Valchanova, M., and Daldal, F. (2000) *Biochemistry* **39**, 15475-15483

26. Darrouzet, E., Valkova-Valchanova, M., Moser, C. C., Dutton, P. L., and Daldal, F. (2000) *Proc. Natl. Acad. Sci. U.S.A* **97**, 4567-4572

27. Darrouzet, E., and Daldal, F. (2002) *J. Biol. Chem.* **277**, 3471-3476

28. Brandt, U., and von Jagow, G. (1991) *Eur J Biochem* **195**, 163-170

29. Crofts, A. R., Hong, S., Zhang, Z., and Berry, E. A. (1999) *Biochemistry* **38**, 15827-15839

30. Xia, D., Esser, L., Yu, L., and Yu, C.-A. (2007) *Photosynth. Res.* **92**, 17-34

31. Brandt, U., Haase, U., Schagger, H., and von Jagow, G. (1991) *J. Biol. Chem.* **266**, 19958-19964

32. Cen, X., Yu, L., and Yu, C.-A. (2008) *FEBS Letters* **582**, 523-526

33. Yu, C.-A., Cen, X., Ma, H.-W., Yin, Y., Yu, L., Esser, L., and Xia, D. (2008) *Biochim. Biophys. Acta - Bioenergetics* **1777**, 1038-1043

34. Muller, F., Crofts, A. R., and Kramer, D. M. (2002) *biochemistry* **41**, 7866-7874

35. Zhang, L., Yu, L., and Yu, C.-A. (1998) *J. Biol. Chem.* **273**, 33972-33976

36. Sun, J., and Trumpower, B. L. (2003) *Arch. Biochem. Biophys* **419**, 198-206

37. Turrens, J. F., Alexandre, A., and Lehninger, A. L. (1985) *Arch. Biochem. Biophys* **237**, 408-414

38. Nohl, H., and Jordan, W. (1986) *Biochem. Bioph. Res. Co* **138**, 533-539

39. Yu, C. A., and Yu, L. (1982) *Biochemistry* **21**, 4096-4101

40. Xiao, K., Liu, X., Yu, C.-A., and Yu, L. (2004) *Biochemistry* **43**, 1488-1495

41. Mather, M. W., Yu, L., and Yu, C.-A. (1995) *J. Biol. Chem.* **270**, 28668-28675

42. Berry, E. A., and Trumpower, B. L. (1987) *Anal. Biochem* **161**, 1-15

43. Dutton, P. L. (1978) *Methods Enzymol.* **54**, 411-435

44. Liu, X., Yu, C.-A., and Yu, L. (2004) *J. Biol. Chem.* **279**, 47363-47371

45. Nakano, M. (1990) *Methods Enzymol.* **186**, 585-591

46. Denicola, A., Souza, J., Gatti, R. M., Augusto, O., and Radi, R. (1995) *Free Radical Bio. Med.* **19**, 11-19

47. Gong, X., Yu, L., Xia, D., and Yu, C.-A. (2005) *J. Biol. Chem.* **280**, 9251 - 9257

48. Yu, L., Mei, Q. C., and Yu, C. A. (1984) *J. Biol. Chem.* **259**, 5752-5760

49. Yu, C.-A., and Yu, L. (1980) *Biochim. Biophys. Acta (BBA) - Bioenergetics* **591**, 409-420

50. Elberry, M., Xiao, K., Esser, L., Xia, D., Yu, L., and Yu, C.-A. (2006) *Biochim. Biophys. Acta - Bioenergetics* **1757**, 835-840

51. Esser, L., Elberry, M., Zhou, F., Yu, C.-A., Yu, L., and Xia, D. (2008) *J. Biol. Chem.* **283**, 2846-2857

52. Yun, C. H., Crofts, A. R., and Gennis, R. B. (1991) *Biochemistry* **30**, 6747-6754

53. Covian, R., Gutierrez-Cirlos, E. B., and Trumpower, B. L. (2004) *J. Biol. Chem.* **279**, 15040-15049

54. King, T. E., Yu, C. A., Yu, L., and Chiang, Y. L. (1975) Electron Transfer Chains and Oxidative Phosphorylation. North-Holland Publishing Company, Amsterdam, Oxford, American Elsevier Publishing Company, Inc., New York, 1975. pp 105-118

55. De Vries, S., Albracht, S. P. J., Berden, J. A., and Slater, E. C. (1982) *Biochim. Biophys. Acta - Bioenergetics* **681**, 41-53

56. De Vries, S., Albracht, S. P. J., Berden, J. A., Marres, C. A. M., and Slater, E. C. (1983) *Biochim. Biophys. Acta - Bioenergetics* **723**, 91-103

57. Snyder, C. H., and Trumpower, B. L. (1999) *J. Biol. Chem.* **274**, 31209-31216

58. Crofts, A. R., Shinkarev, V. P., Kolling, D. R. J., and Hong, S. (2003) *J. Biol. Chem.* **278**, 36191-36201

59. Rotsaert, F. A. J., Ding, M. G., and Trumpower, B. L. (2008) *Biochim. Biophys. Acta - Bioenergetics* **1777**, 211-219

60. Forquer, I., Covian, R., Bowman, M. K., Trumpower, B. L., and Kramer, D. M. (2006) *J. Biol. Chem.* **281**, 38459-38465

CHAPTER III

PROTEIN COMPONENTS OF THE CYTOCHROME BC_1 COMPLEX IS NOT ESSENTIAL FOR ITS SUPEROXIDE GENERATION UPON OXIDATION OF UBIQUINOL

Abstract

In addition to its main functions of the electron transfer and proton translocation, cytochrome bc_1 complex also catalyzes generation of superoxide upon oxidation of ubiquinol in the presence of molecular oxygen. The superoxide generating activity seems to inversely proportional to the electron transfer activity. Complexes with less complexity in subunit structure tend to have higher superoxide generating activity. When cytochrome bc_1 complex is treated with proteinase K, the electron transfer activity decreases and the superoxide generating activity increases as the incubating time increases. The maximum superoxide generating activity maintain when the protein components of the complex is completely digested, indicating that proteins play little role in superoxide generating activity. It is speculated that the hydrophobic environment and the availability of a high potential electron acceptor from the complex is responsible for the superoxide generating activity. This speculation is confirmed by the detection of superoxide formation upon oxidation of ubiquinol by a high potential oxidant such as cytochrome c or fericyanide in the presence of phospholipid vesicles or micellar solution

of detergents. No superoxide formation was observed when ubiquinol is oxidized under the hydrophilic conditions.

Introduction

There is a continuous release of electrons from the electron transfer chain to molecular oxygen (O_2) to form superoxide anion ($O_2^{\cdot -}$) during mitochondrial respiration (1-3). The $O_2^{\cdot -}$ subsequently dismutates to H_2O_2 spontaneously or by the action of superoxide dismutases (SOD) (4). Isolated mitochondria in state 4 generate 0.6-1.0 nmol of H_2O_2/min/mg protein, accounting for about 2% of O_2 uptake under physiological conditions (5). Production of $O_2^{\cdot -}$ during mitochondrial respiration is closely related to mitochondrial coupling efficiency.

Two segments of the respiratory chain have been demonstrated to be responsible for generation of dioxygen to $O_2^{\cdot -}$. The one located in NADH-Q oxidoreductase is cyanide-insensitive. Production of $O_2^{\cdot -}$ is either via auto-oxidation of the flavine radical in the NADH dehydrogenase (6) or from bound ubiquinone redical (7) or center N2 (8) of complex I . The other one is located at the bc_1 complex (ubiquinol-cytochrome *c* reductase). Two redox components of the bc_1 complex, ubisemiquinone (9) and the reduced cytochrome b_{566} (10,11), have been implicated to be the electron donor for molecular oxygen to generate $O_2^{\cdot -}$. The $O_2^{\cdot -}$ producing activity of cytochrome bc_1 complex is enhanced by antimycin (11-13).

In the past, most information concerning mitochondrial $O_2^{\cdot -}$ generation was obtained from studies with intact heart mitochondria and electron transfer inhibitors by measuring H_2O_2 concentration in the suspending medium (9,10). More recently, studies

of $O_2^{\cdot -}$ formation are carried out with purified electron transfer complexes, such as NADH-ubiquinone reductase (6,7), succinate cytochrome c reductase (11) or cytochrome bc_1 complex (14). Although results obtained from purified complex should be less ambiguous, the detail of the generating site of $O_2^{\cdot -}$ remains controversial. Evidences supporting flavin (6) radical and ubiquinone radical (7) as the electron donor for the $O_2^{\cdot -}$ generation in complex I are both available. Argument between the reduced cytochrome b_L and ubisemiuquinone radical as the electron donors for molecular oxygen to generate $O_2^{\cdot -}$ continues. Based on the observation of similar activation energy for both the reactions of electron transfer and $O_2^{\cdot -}$ production, investigators believed that both reaction share the common intermediate (15). A systematic comparison of electron transfer activities and $O_2^{\cdot -}$ generating activities of cytochrome bc_1 complexes from different sources or mutant strains, a conclusion can be made: that is the complex with less electron transfer activity and less subunit complexity tends to have a higher $O_2^{\cdot -}$ generating activity. Heat inactivation of electron transfer activity resulted in an increase in $O_2^{\cdot -}$ generating activity. Treating the complex with proteinase K resulted in an inactivation of electron transfer activity of complex but enhance $O_2^{\cdot -}$ generating activity suggesting that protein components of the complex are not directly involved $O_2^{\cdot -}$ generating activity. It is highly likely that the hydrophobic environment and the high potential redox components, such as iron-sulfur cluster and cytochrome c_1 available in the digested cytochrome bc_1 complex is responsible for $O_2^{\cdot -}$ generation. To test this speculation, recently we have followed the $O_2^{\cdot -}$ generation in a system containing only

phopholipid vesicles and ubiquinol using cytochrome c or fericyanide as an oxidant. The $O_2^{\cdot -}$ generation in these system is concentration dependent both on ubiquinol and the oxidant used. A similar result was obtained with detergent, higher than critical micelle concentration, being used instead of phospholipids vesicles.

Herein we report the production of $O_2^{\cdot -}$ during oxidation of ubiquinol by a high potential electron acceptor in the hydrophobic environments under various conditions. The results obtained show clearly that the hydrophobic environment and high potential oxidant but not intact cytochrome bc_1 are required for superoxide generation.

Experimental Procedures

Materials- Cytochrome *c* (horse heart, type III) was purchased from Sigma. Proteinase K was purchased from Invitrogen. *N*-Dodecyl-D-Maltopyranoside (DM) and *N*-octyl- D-Gluocopyranoside (OG) were from Anatrace. Nickel nitrilotriacetic acid gel and a Qiaprep spin Miniprep kit were from Qiagen. 2-Methyl-6- (4 methoxyphenyl)-3, 7-dihydroimidazol[1, 2-α] pyrazin-3-one, hydrochloride (MCLA) was from Molecular Probes, Inc. 2,3-Dimethoxy-5-methyl -6-(10-bromodecyl)-1,4-benzoquinol($Q_0C_{10}BrH_2$) was prepared as previously reported (16). All other chemicals were of the highest purity commercially available.

Enzyme Preparations and Activity Assays- Chromatophores, intracytoplasmic membrane and the His_6-tagged cytochrome bc_1 complexes, wild-type (17) and mutants (15 Yang, jbc) were prepared as previously reported. Bovine heart mitochondrial cytochrome bc_1 complex was prepared according to the method developed in our lab (18).

To assay cytochrome bc_1 complex activity, chromatophores or purified cytochrome bc_1 complexes were diluted with 50 mM Tris-Cl, pH 8.0, containing 200 mM NaCl and 0.01% DM to a final concentration of cytochrome c_1 of 1 μM. Appropriate amounts of the diluted samples were added to 1 ml of assay mixture containing 100 mM Na^+/K^+ phosphate buffer, pH 7.4, 300 μM EDTA, 100 μM cytochrome *c*, and 25 μM $Q_0C_{10}BrH_2$. Activities were determined by measuring the reduction of cytochrome *c* (the increase of absorbance at 550 nm) in a Shimadzu UV 2101 PC spectrophotometer at 23 °C, using a millimolar extinction coefficient of 18.5 for calculation. The non-enzymatic oxidation of $Q_0C_{10}BrH_2$, determined under the same conditions in the absence of enzyme, was subtracted from the assay.

Digestion of cytochrome bc_1 by proteinase K: Stock solution of proteinase K, 2%, was made in 10 mM Tris-Hcl, pH 7.5, containing 20 mM CaCl, 50% glycerol. 2 μl of proteinase K solution was added into 200 ul of 200uM of cytochrome bc_1 complexes in 50 mM Tris-Cl, pH 8.0, containing 200 mM NaCl and 0.01% DM. The mixture was incubated at the room temperature. The electron transfer and $O^{\cdot-}$ generating activities were measured during the course of incubation until all electron transfer activity is gone. The digested bc1 complex was then subjected to SDA-PAGE to confirm that all subunits are digested.

Preparation of phospholipids vesicles: Phospholipid (PL) vesicles was prepared by the cholate-dialysis method(19) (17). Azolectin was dissolved in chroform and dry as a thin film against tube by flushing with nitrogen gas while the tune is rotating. The phospholipid was than suspended in buffer containing 1 % sodium cholate. The mixture was subjected to sonification

intermittently for 10 min until the solution become clear. The solution was than dialyzed against buffer over night with three changes of buffer.

Determination of Superoxide Production: Superoxide anion generation was determined by measuring the chemiluminescence of MCLA-$O^{\cdot -}$ adduct (20), in an Applied Photophysics stopped-flow reaction analyzer SX.18MV (Leatherhead, England), by leaving the excitation light off and registering light emission (21). Reactions were carried out at 23 °C by mixing 1:1 solutions A and B. For the determination of superoxide production in the presence of native, heat deactivated or Proteinase K digested cytochrome bc_1, Solutions A contains 100 mM Na^+/K^+ phosphate buffer, pH 7.4, 1 mM EDTA, 1 mM KCN, 1 mM NaN_3, 0.1% bovine serum albumin, 0.01% DM, and 5.0 μM of cytochrome bc_1 or other systems. Solution B contains 125 μM $Q_0C_{10}BrH_2$ and 4 μM MCLA in the same buffer. For the determination of superoxide production in the presence of detergents, Solutions A contains 100 mM Na^+/K^+ phosphate buffer, pH 7.4, and 5.0 μM of cytochrome *c* and appropriate amount of detergent. Solution B contains 125 μM $Q_0C_{10}BrH_2$ and 4 μM MCLA in the same buffer. Once the reaction starts, the produced fluorescence, in voltage, was consecutively monitored for 2 seconds.

Results and Discussion

Superoxide generating activity in cytochrome bc_1 complex is inversely proportional to its normal electron transfer activity: Table III-1 summarizes the electron transfer and $O_2^{\cdot -}$ generating activities of various preparations of cytochrome bc_1 complexes from various source. Cytochrome bc_1 complex from bovine heart mitochondria has the most complicated subunit structure. It contains 11 subunits and is

Table III-1. Comparison of electron transfer and superoxide generating activities of various cytochrome bc1 complexes.

Preparation	Activity	
	Electron Transfer (μmoles c red/ min/nmoles c)	$O2^{\cdot -}$ generating (XO unit / nmoles c)
Mitochondrial bc1	43	1.5×10^{-3}
Rs bc1	3.5	0.089
ΔIV, Rs bc1	0.8	0.22
Δb_L, Rs bc1, H198N	0.4	0.51
Δb_H, Rs bc1, H111N	0.3	0.51

the most active complex among the known complex. Yeast enzyme is composed of 10 subunits and has about half of the activity of bovine complex. Bacterial complex which has much simpler subunit structure has only about one tenth of the electron transfer activity and has higher $O_2^{\cdot -}$ generating activity. In *Rhodobacter sphaeroides*, the 3-subunit core bacterial complex has only one quarter of the electron transfer activity of its wild-type, 4-subunit, complex, but with much higher $O_2^{\cdot -}$generating activity. When the 3-subunit core complex is reconstituted with the 4^{th} subunit protein, the electron transfer activity restores and the $O_2^{\cdot -}$ generating activity decreases. The fact that cytochrome bc_1 complex with less structural integrity has higher $O_2^{\cdot -}$ generating activity would suggest that $O_2^{\cdot -}$ is generated inside the complex, perhaps in the hydrophobic environment of the Qo packet, and protein subunits may play a role of preventing the release of $O_2^{\cdot -}$ from its production site to aqueous environment.

Superoxide generating activity in the heat inactivated cytochrome bc_1 complex: Figure III-1 shows the relationship between the electron transfer activity and superoxide generating during temperature inactivation of cytochrome bc_1 complex. When cytochrome bc_1 complex is incubated at 37ºC, the electron transfer activity of the complex decreases gradually whereas the $O_2^{\cdot -}$ generating activity increases as the incubation time increases and reaches the maximum before the electron transfer activity is completely inactivated, suggesting that an intact structure is not needed for superoxide generating activity and a totally denaturation of protein is not necessary for the $O_2^{\cdot -}$ generating activity to reach maximal.

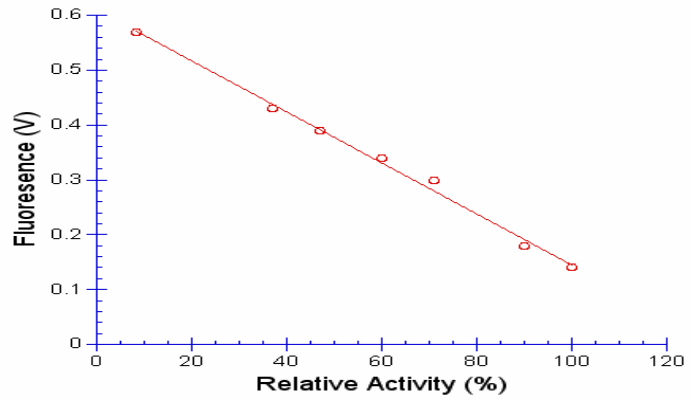

Figure III-1. The relationship between electron transfer activity and superoxide generating during temperature inactivation of cytochrome bc1 complex. 200 µl of cytochrome bc1complex, 200 µM in 50 mM Tris-Cl, pH 8.0, containing 200 mM NaCl and 0.01% DM, was incubated at 37˚C. Superoxide production and electron transfer activities were determined at various incubation times. Electron transfer activity and the superoxide production were measured as described in "Experimental Procedures." Solution A contains 100 mM Na^+/K^+ phosphate buffer, pH 7.4, 1 mM EDTA, 1 mM KCN, 1 mM NaN_3, 0.1% bovine serum albumin, 0.01% DM, and 5.0 µM of incubated cytochrome bc_1. Solution B was the same as A with bc_1 complex being replaced with 125 µM $Q_0C_{10}BrH_2$ and 4 µM MCLA.

Cytochrome bc_1 complex lacking heme b_L or heme b_H has higher $O_2^{\cdot -}$ generating activity than the intact complex: Recently we have generated and characterized several heme *b* deleted mutants by replacing one of its heme ligands residues. Mutants, H198N and H111N, lacking heme b_L and heme b_H, respectively, have very little electron transfer activity but show high $O_2^{\cdot -}$ generating activity (Table III-I). Apparently a much loosen structure around the Qp pocket is present in these two mutants. Further denaturation of these complexes, as expected, does not further increase the $O_2^{\cdot -}$generating activity (15,yang, JBC).

Proteinase-K treated cytochrome bc_1 increase superoxide production ability- The well established fact, that antimycin inhibits electron transfer activity of cytochrome bc_1 complex and stimulates $O_2^{\cdot -}$generating activity, led investigators to believe that both activities share, at least, a common intermediate. It is speculated that during catalytic reaction of the cytochrome bc_1complex, QH_2 transfers its first electron to ISP and become low potential ubisemiquione that reduced cytochrome b_L instantly. One way to test this is to destroy the electron catalytic reaction of transfer activity by hydrolyzing the proteins that house redox components by proteinase digestion. A side by side loss of both activities upon the hydrolysis of protein would indicate that both activities share the common pathway. Figure III-2 shows activity tracing of electron transfer and $O_2^{\cdot -}$ generation during the course of proteinase K digestion. The electron transfer activity diminishes as the protein hydrolysis progress. The $O_2^{\cdot -}$ generating activity is, on the other hand, not dependent of the presence of intact protein subunits and show activity enhancement during the course of digestion. In contrast to the intact complex, the $O_2^{\cdot -}$

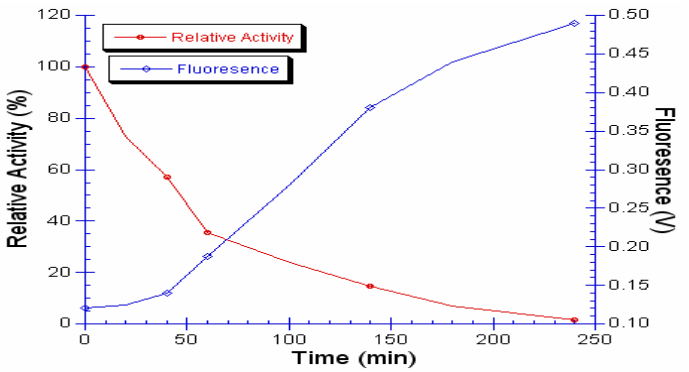

Figure III-2. Activity tracing of electron transfer and *$O_2^{\cdot -}$ generation* during the course of proteinase k digestion of the complex. The superoxide production was measured as described in "Experimental Procedures." Solution A contains 100 mM Na^+/K^+ phosphate buffer, pH 7.4, 1 mM EDTA, 1 mM KCN, 1 mM NaN_3, 0.1% bovine serum albumin, 0.01% DM, and 5.0 µM of proteinse K treated cytochrome bc_1. Solution B was the same as A with bc_1 complex being replaced with 125 µM $Q_0C_{10}BrH_2$ and 4 µM MCLA. The red trace is for electron transfer activity and the blue trace is for superoxide generation activity.

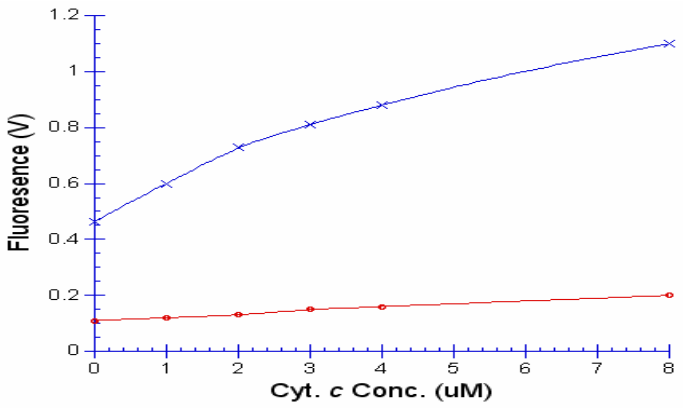

Figure III-3. Comparison of the effect of cytochrome c on the $O_2^{\cdot-}$ generating activities of the intact and proteinase k treated cytochrome bc1 complex. The superoxide production was measured as described in "Experimental Procedures." Except intact or Proteinase K digested complex and various amounts of cytochrome c were used in solution A and various amounts of cytochrome c were present in the solution B in addition to 125 µM $Q_0C_{10}BrH_2$ and 4 µM MCLA.

generating activity of the proteinase K treated complex increases further upon addition of cytochrome c indicating that the system has become oxidant limited. No significant increase in $O_2^{\cdot -}$ generating activity is observed in the intact complex because cytochrome c is not directly accessible to the ubiquinol oxidation site. Figure III-3 compares the effect of cytochrome *c* on the $O_2^{\cdot -}$ generating activity of the intact and proteinase K treated complex.

Since SDS-PAGE pattern shows (see Figure III-4) that there are no intact subunits of cytochrmes *b*, c_1 or ISP in the proteinase treated complex, the protein components of the complex plays no direct role in $O_2^{\cdot -}$ generation. The $O_2^{\cdot -}$ generating activity of the proteinase treated complex reach the same level as that of the antimycin treated complex (15,Yang, JBC). Addition of cytochrome *c* or fericyanide to the proteinase treated complex increase the superoxide production. These results indicate that hydrophobic environment and the high potential oxidant contributes to the superoxide production from QH_2. In the absence of added oxidant, iron-sulfur cluster serves as the high potential oxidant for QH_2 and molecular oxygen act as low potential electron acceptor. The reduction of high potential oxidant at hydrophilic region is coupled to reduction of low potential oxidant in the hydrophobic environment to generate $O_2^{\cdot -}$.

Generation of $O_2^{\cdot -}$ upon oxidation of ubiquinol by cytochrome c or fericyanide in the presence of phospholipids vesicles: When ubiquinol reacted with fericytochrome *c* or fericyanide in the aqueous solution at neutral pH only very slow oxidation take place and no $O_2^{\cdot -}$ formation is detected. Addition of phospholipids vesicles to the system, formation of $O_2^{\cdot -}$ is observed and amount $O_2^{\cdot -}$ generation is proportional to the amount

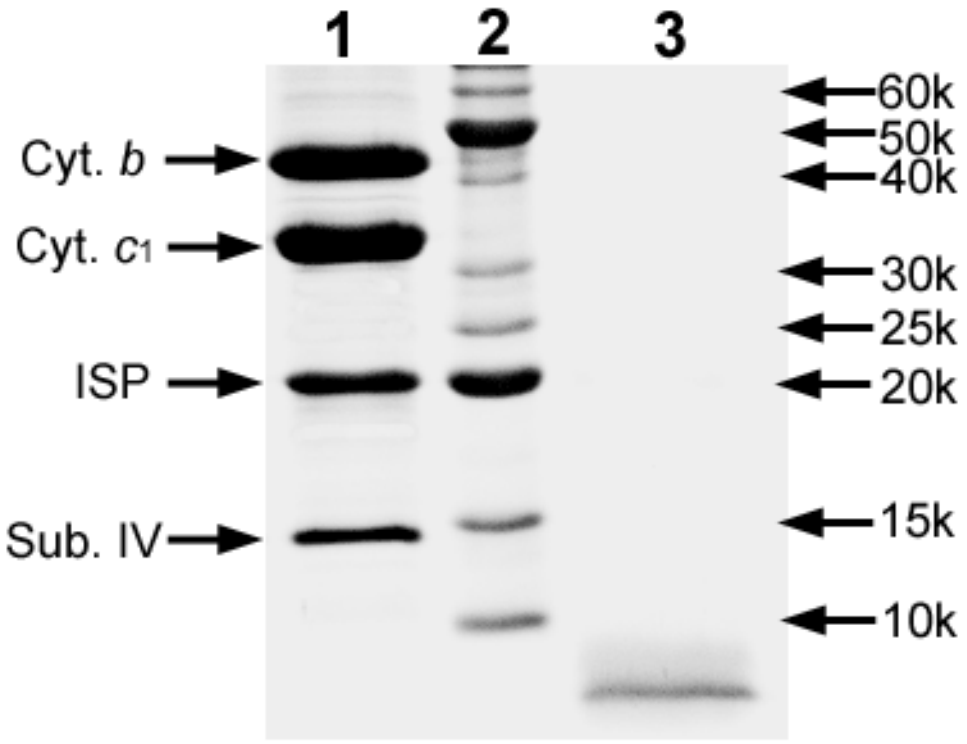

Figure III-4. Sodium dodeceyl sulfate gel electrophoresis of cytochrome bc_1 complex and its proteinase K digested products. Lane 1: standard polypeptide. Lane 2: intact wild type cytochrome bc1; Lane 3: proteinase K-treated wild type. Aliquots of of purified bc_1 complexes samples were incubated with 1% SDS with 0.4% β-ME at 37 ℃ for 20 minutes. Digested samples containing around 200 pmoles of cytochrome c_1 were subjected to electrophoresis.

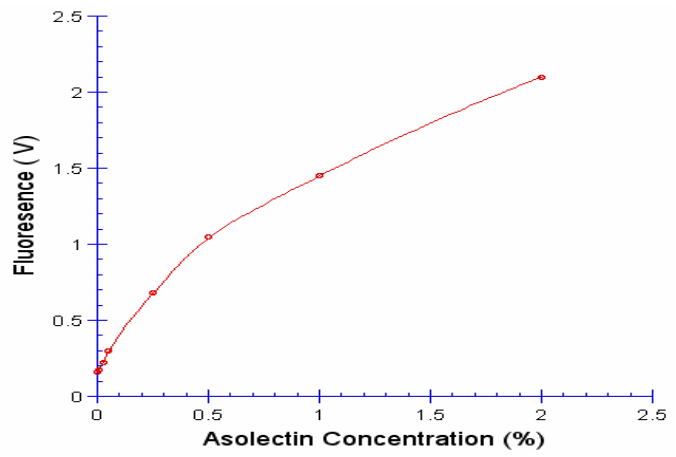

Figure III-5. Generation of superoxide is phopholipid vesicle concentration dependent under the constant amounts of cytochrome c and ubquinol. The superoxide production was measured as described in "Experimental Procedures." Solution A contains 100 mM Na^+/K^+ phosphate buffer, pH 7.4, and 5.0μM of cytochrome c, different concentrations of asolectin. Solution B contains 100 mM Na^+/K^+ phosphate buffer, pH 7.4, 125 uM of QH_2 and 4 uM of MCLA.

of vesicles added (see Figure III-5). This result clearly indicate that formation of $O_2^{\cdot -}$ take place in the hydrophobic environment.

Detergents can facilitate superoxide production by QH_2 and cytochrome c: Since phospholipids vesicles environment can facilitate $O_2^{\cdot -}$ generation, micellar solution of detergent should do the same. To test the effects of detergents on the $O_2^{\cdot -}$ production by QH_2 and cytochrome *c*, both non-ionic detergents, (OG, DM) and ionic detergent (sodium cholate) were used to replace phospholipids vesicles. It is expected little $O_2^{\cdot -}$ generation will be observed if the concentration of detergent used is below its critical micelle concentrations (CMC) because no hydrophobic environment is available. When the concentration of detergent used is higher than CMC, generation of $O_2^{\cdot -}$ is proportional to concentration and reach the maximum which is limited by the amount of QH_2, or high potential oxidant available in the system. Figure III-6 shows the detergent concentration dependent $O_2^{\cdot -}$ generation. The CMCs of OG, DM and sodium cholate are 25, 0.15 and 4 mM respectively. These results confirm the idea that the hydrophobic environment plays a key role in $O_2^{\cdot -}$ generation on the oxidation of QH2 by a high potential oxidant.

Superoxide anion generation is ubiquinol and oxidant concentration dependent: Generation of $O_2^{\cdot -}$ requires ubiquinol, high potential oxidant such as ISC, cytochrome c or fericyanide. To test the oxidant, cytochrome *c,* concentration dependency of $O_2^{\cdot -}$ generation, different concentrations of cytochrome *c* was added to reaction mixture containing fixed amount of QH_2, 125 μM, and 8 mM sodium cholate (Figure III-7A). It

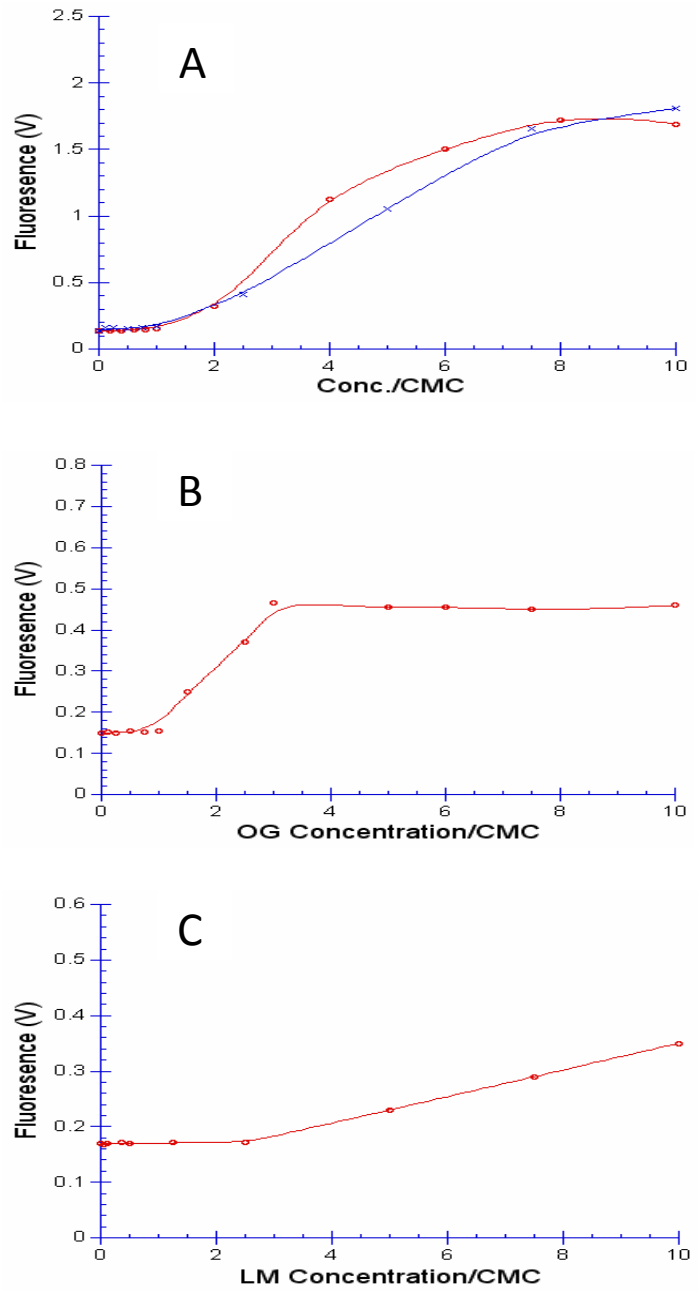

Figure III-6. Effect of detergents on the superoxide production under constant amount of cytochrome c and QH_2. The superoxide production was measured as described in "Experimental Procedures." Solution A contains 100 mM Na^+/K^+ phosphate buffer, pH 7.4, and 5.0μM of cytochrome c, different concentrations of detergent, Sodium cholate (blue), Deoxycholate (red) (A) Octyl glucoside (B) and Dodeoxymaltoside (C). Solution B contains 100 mM Na^+/K^+ phosphate buffer, pH 7.4, 125 uM of QH2 and 4uM of MCLA

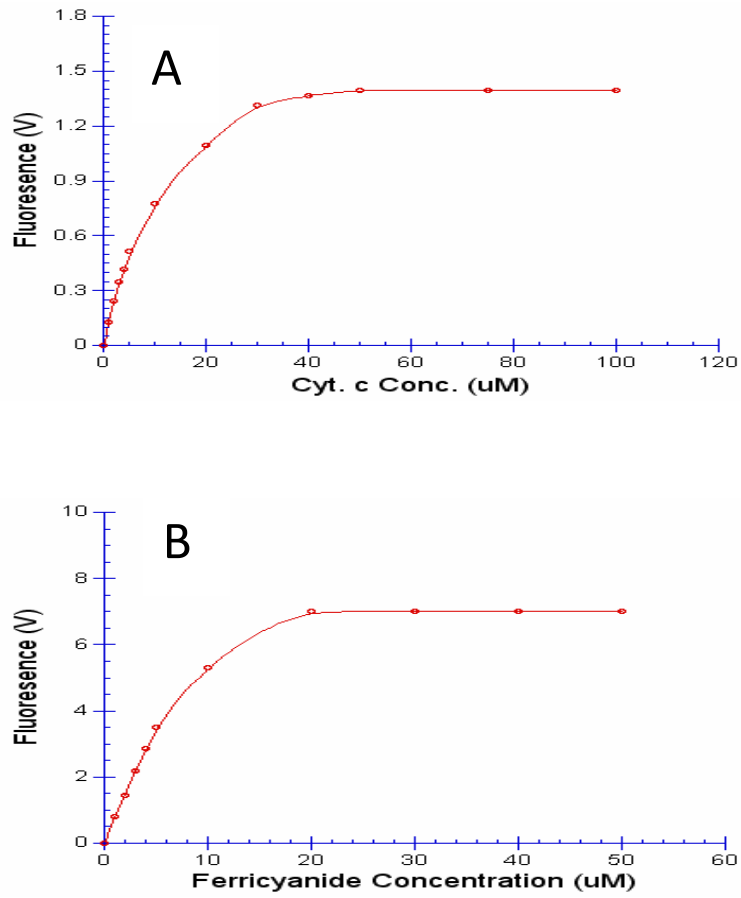

Figure III-7. Superoxide generation is high potential oxidant (cytochrome c and fericyanide) concentration dependent. The superoxide production was measured as described in "Experimental Procedures." For panel A, solution A contains 100 mM Na^+/K^+ phosphate buffer, pH 7.4, 16 mM of sodium cholate, and different concentration of cytochrome c; For panel B, solution A contains 100 mM Na^+/K^+ phosphate buffer, pH 7.4, 4 mM of sodium cholate, and different concentration of fericyanide. Solution B contains 100 mM Na^+/K^+ phosphate buffer, pH 7.4, 125 μM of QH_2 and 4 μM of MCLA

is clear that the superoxide production is proportional to the concentration of cytochrome *c*. Figure III-7B shows the titration of fericyanide on the $O_2^{\cdot -}$ generation under the fixed amount of QH_2, 25 μM, and 2 mM sodium cholate. The reason for using less amount of sodium cholate is due to the better efficiency of ferricyanide than cytochrome c in promoting the $O_2^{\cdot -}$ generation.

The effect of QH_2 concentration was also studied. Under the constant concentration of cytochrome *c* (2.5 μM) and sodium cholate (8 mM), superoxide production increased with QH_2 concentration increased until it is saturated (See Figure III-8).

Reaction mechanism of $O_2^{\cdot -}$ generation: In the intact, native cytochrome bc_1 complex, there is a hydrophobic domain surround by cytochrome *b* subunit and a part of iron-sulfur protein, generally referred as quinol oxidation pocket. Quinol undergoes bifurcated oxidation by simultaneously transfer its two electrons to ISC and heme b_L. It is generally believed that one of the electrons goes to ISC and the other goes to heme b_L. Molecular oxygen can either withdraw electron from reduced heme b_L or compete with heme b_L to obtain electron directly from quinol to generate $O_2^{\cdot -}$. Two possible reasons to explain why only a fraction of $O_2^{\cdot -}$ is generated in the intact bc_1 complex. Firstly, molecular oxygen is not a good electron acceptor for reduced heme b_L, thermodynamically. Secondly $O_2^{\cdot -}$ generated with the Qo pocket may not be easy to escape. When heme b_L is not available, ISC and molecular oxygen will share the two electrons from quinol and resulting in generation of superoxide. The structure surround the Qo pocket in the mutant complex is looser than that of the wild-type complex thus

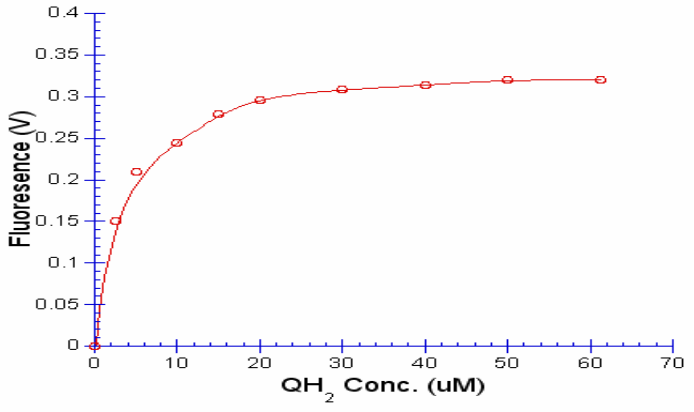

Figure III-8: Correlation between superoxide production and QH_2 under constant amount of sodium cholate. The superoxide production was measured as described in "Experimental Procedures." Solution A contains 100 mM Na^+/K^+ phosphate buffer, pH 7.4, 16 mM of sodium cholate, and 5.0 μM of cytochrome c. Solution B contains 100 mM Na^+/K^+ phosphate buffer, pH 7.4, 4uM of MCLA and different concentrations of QH_2.

generated $O_2^{\cdot -}$ is easier to release and be detected. Proteinase k digested or heat denatured complexes show higher $O_2^{\cdot -}$ generating activity can also be explained by the less structural restriction.

REFERENCE

1. Loschen, G., Azzi, A., and Floh, L. (1973) *FEBS Letters* **33**, 84-88
2. Loschen, G., Azzi, A., Richter, C., and Floh, L. (1974) *FEBS Letters* **42**, 68-72
3. Boveris, A., and Chance, B. (1973) *Biochem. J.* **134**, 707-716
4. McCord, J. M., and Fridovich, I. (1969) *J. Biol. Chem.* **244**, 6049-6055
5. Boveris, A., Oshino, N., and Chance, B. (1972) *Biochem. J.* **128**, 617-630
6. Galkin, A., and Brandt, U. (2005) *J. Biol. Chem.* **280**, 30129-30135
7. Ohnishi, S. T., Ohnishi, T., Muranaka, S., Fujita, H., Kimura, H., Uemura, K., Yoshida, K.-i., and Utsumi, K. (2005) *Journal of Bioenergetics and Biomembranes* **37**, 1-15
8. Genova, M. L., Ventura, B., Giuliano, G., Bovina, C., Formiggini, G., Parenti Castelli, G., and Lenaz, G. (2001) *FEBS Letters* **505**, 364-368
9. Turrens, J. F., Alexandre, A., and Lehninger, A. L. (1985) *Archives of Biochemistry and Biophysics* **237**, 408-414
10. Nohl, H., and Jordan, W. (1986) *Biochemical and Biophysical Research Communications* **138**, 533-539
11. Zhang, L., Yu, L., and Yu, C.-A. (1998) *J. Biol. Chem.* **273**, 33972-33976
12. Muller, F., Crofts, A. R., and Kramer, D. M. (2002) *biochemistry* **41**, 7866-7874
13. Sun, J., and Trumpower, B. L. (2003) *Archives of Biochemistry and Biophysics* **419**, 198

14. Sun, J., and Trumpower, B. L. (2003) *Archives of Biochemistry and Biophysics* **419**, 198-206

15. Forquer, I., Covian, R., Bowman, M. K., Trumpower, B. L., and Kramer, D. M. (2006) *J. Biol. Chem.* **281**, 38459-38465

16. Yu, C. A., and Yu, L. (1982) *Biochemistry* **21**, 4096-4101

17. Tian, H., Yu, L., Mather, M. W., and Yu, C.-A. (1998) *J. Biol. Chem.* **273**, 27953-27959

18. Yu, C.-A., and Yu, L. (1980) *Biochimica et Biophysica Acta (BBA) - Bioenergetics* **591**, 409-420

19. Kagawa, Y., and Racker, E. (1971) *J. Biol. Chem.* **246**, 5477-5487

20. Nakano, M. (1990) *Methods Enzymol.* **186**, 585-591

21. Denicola, A., Souza, J., Gatti, R. M., Augusto, O., and Radi, R. (1995) *Free Radical Biology and Medicine* **19**, 11-19

CHAPTER IV

FORMATION OF AN INTERSUBUNIT DISULFIDE BOND BETWEEN CYTOCHROME C_1 AND IRON-SULFUR PROTEIN IN CYTOCHROME BC_1 COMPLEXES

Abstract

Head domain movement of iron-sulfur protein plays an essential role in the bifurcated oxidation of ubiquinol catalyzed by the cytochrome bc_1 complex. To better understand the electron transfer mechanism of the bifurcated ubiquinol oxidation at Qp site, we fixed the head domain of ISP at the cyt c_1 position by creating an intersubunit disulfide bond between two genetically engineered cysteine residues: one at position 141 of ISP and the other one at position 180 of cyt c_1 [S141C(ISP)/G180C(cyt c_1)]. The formation of a disulfide bond between ISP and cyt c_1 in this mutant complex is confirmed by SDS-PAGE and Western blot. In this mutant complex, the disulfide bond formation is concurrent with the loss of the electron transfer activity of the complex. When the disulfide bond is released by treatment with β-mercaptoethanol, the activity is restored. These results further support the hypothesis that the mobility of the head domain of ISP is functionally important in the cytochrome bc_1 complex. Formation of the disulfide bond between ISP and cyt c_1 shortens the distance between the [2Fe–2S] cluster and heme c_1, hence the rate of intersubunit electron transfer between these two redox prosthetic groups induced by pH change is increased. This intersubunit disulfide bond formation also decreases the rate of stigmatellin

induced reduction of ISP in the fully oxidized complex, suggesting that an endogenous electron donor comes from the vicinity of the *b* position in the cytochrome *b*.

Introduction

The cytochrome bc_1 complex (also known as ubiquinol-cytochrome *c* oxidoreductase or complex III) is a multi-subunit dimeric integral protein complex. It is an essential segment of cellular energy-conserving electron transport chains in animals, plants, and photosynthetic bacteria(1). This complex catalyzes electron transfer from ubiquinol to cytochrome *c* (or cytochrome c_2 in bacteria) and concomitantly translocates protons across inner membrane to generate a membrane potential and pH gradient for ATP synthesis. Although the cytochrome bc_1 complexes from different sources vary in their polypeptide compositions, they all contain four redox prosthetic groups: two *b*-type cytochromes (b_L and b_H), one *c*-type cytochrome (c_1), and one high potential Rieske iron–sulfur cluster [2Fe–2S] [reviewed from(2)]. Structural information obtained from X-ray crystallographic studies has revealed the arrangement of the redox centers, transmembrane helices, inhibitor binding sites and the intertwined dimeric structure (3-6). The longer than expected distance between [2Fe–2S] and heme c_1 and the less defined structure of the head domain of the iron–sulfur protein suggest a domain movement of ISP during the electron transfer in bc_1 complex. The domain movement hypothesis was further supported by the observation of various positions of the [2Fe–2S] cluster in different crystal forms (5,7) and in complexes loaded with different inhibitors(7,8).

Structurally, the iron–sulfur protein (ISP) in cytochrome bc_1 complex can be divided into three domains: the soluble C-terminal extramembrane domain (head), which houses the [2Fe–2S] cluster at its tip, the membrane-spanning N-terminal domain (tail), and the flexible linking domain (neck), which links the head and tail domains(9,10). Bending of the neck is required for movement of the ISP head domain between the two positions ("*b*"

and "c_1"). This movement is essential for electron transfer (11-14). Due to its movement between cytochrome *b* interface and cytochrome c_1 interface, the head domain of ISP is considered to have two docking positions: "*b*" position and "c_1" position(13). When oxidized ISP at "*b*" position, it will take electron from QH_2 at Q_P pocket. After then, reduced ISP will move to "c_1" position and pass its electron to oxidized heme c_1.

Since 1997, The X-ray crystallographic structures from a variety of sources have been solved (3-5,7). Unfortunately, so far, there is no any X-ray crystallographic structure with QH_2 at Q_P pocket available. Also, with the binding of P_f inhibitors, ISP head domain can be fixed at "*b*-position", which is proved by the crystallographic structures with either UHDBT or stigmatellin(8,15). In the native or P_m inhibitor bound bc_1 crystallographic structures, the electron density of ISP head domain is anomalous. X-ray structures with ISP at "c_1" position have not been available yet.

Presumably, the reason why it is hard to get bc_1 X-ray structure with QH_2 at Q_P pocket is that QH_2 will be immediately oxidized by ISP and heme b_L once it enters Q_P pocket. Oxidized QH_2 will leave Q_P pocket so that the second QH_2 can get into Q_P pocket. To make QH_2 stay at Q_P pocket, its oxidation at Q_P pocket has to be prevented. To prevent QH_2 oxidation at Q_P pocket, we constructed a mutant S141C(ISP)/G180C (cyt c_1), in which ISP is fixed at c_1-position. Since ISP is far away from *b*-position, theoretically, ISP in this mutant shouldn't take electron from QH_2 at Q_P pocket anymore. Therefore, with this mutant, we can try to get an X-ray crystallographic structure with QH_2 at Q_P pocket. Meanwhile, with this mutant, we also can try to see if we can get X-ray structures of bc_1 with ISP at c_1-position. Herein, we report our evidences that ISP is fixed at c_1-position in this mutant.

Experimental Procedures

Materials — Cytochrome *c* (horse heart, type III) was purchased from Sigma. . *N*-Dodecyl- β -D-Maltopyranoside (DM) and *N*-octyl-β-D-Gluocopyranoside (OG) were from Anatrace. 2,3-Dimethoxy-5-methyl-6-(10-bromodecyl)-1,4-benzoquinol ($Q_0C_{10}BrH_2$) was prepared in our laboratory as previously reported (16). Ni-NTA gel, Qiaprep Spin Miniprep kit and PCR purification kit were from Qiagen. All other chemicals were of the highest purity commercially available.

Growth of Bacteria — Escherichia coli cells were grown at 37 °C in LB medium. *Rb. sphaeroides* BC17 cells (17) were grown photosynthetically at 30 °C in an enriched Siström's medium containing 5 mM glutamate and 0.2% casamino acids. Photosynthetic growth conditions for *Rb. sphaeroides* were essentially as described previously (18). The concentrations and antibiotics used were: ampicillin, 125 μg/ml; kanamycin sulfate, 30 μg/ml; tetracycline, 10 μg/ml for *E. coli*, and 1 μg/ml for *Rb. sphaeroides*; and trimethoprim, 100 μg/ml for *E. coli* and 30 μg/ml for *Rb. sphaeroides*.

Generation of Rb. sphaeroides Strains Expressing the His_6-tagged bc_1 Complexes with Single or Pair of Cysteine Substitutions on Cytochrome c_1 and ISP — The QuickChange™ XL site-directed mutagenesis kit from Stratagene was used for mutagenesis. The oligonucleotides used for mutagenesis were as follows: S141C (ISP), F-5' CCGATCGGCGGCGTGT GCGGTGACTTCGGGGGC 3'; R-5' GCCCCCGAAGTCACCGCACACGCCGCCGATCGG 3'; G180C (cyt c_1), F-5' GCCTGCTCGTGGAT CGCCATG 3'; R-5' CTAGGCGATCCACGAG CAGGC 3'.

The double-stranded plasmid pGEM-7Zf(+)-*fbcFB* was used as the template for mutagenesis. Forward and reverse primers were used for PCR amplification. The

pGEM-7Zf(+)-*fbc*FB plasmid was constructed by ligating the *Eco*R I-*Xba* I fragment from pRKD*fbc*FBC$_H$Q (17) into *Eco*R I and *Xba* I sites of the pGEM-7Zf(+) plasmid. After the mutagenesis, the fragment containing the mutant from pGEM-7Zf(+)-*fbc*F$_m$B was inserted into pRKD418-*fbc*FB$_{Km}$C$_H$Q by *Eco*R I and *Nsi* I double digestion and ligation reaction. Loss of kanamycin resistance was then used to screen for the recombinant cloning containing the mutant ISP gene (pRKD418-*fbc*F$_m$BC$_H$Q). A similar process was used to get the clones with the mutant cytochrome c_1 gene (pRKD418-*fbc*FBC$_{Hm}$Q) and double mutant pRKD418-*fbc*F$_m$BC$_{Hm}$Q.

The pRKD418-*fbc*F$_m$BC$_{Hm}$Q plasmid in *Escherichia coli* S17-1 cells was mobilized into *Rb. sphaeroides* BC17 cells by the plate-mating procedure (17). The presence of engineered mutations was confirmed by DNA sequencing before and after photosynthetic or semi-aerobic growth of the cells as previously reported (13,17). Expression plasmid pRKD418-*fbc*F$_m$BC$_{Hm}$Q was purified from an aliquot of a photosynthetic or semi-aerobic culture using the Qiagen Plasmid Mini Prep kit. Because *Rb. sphaeroides* cells contain more than one type of endogenous plasmids (13), the isolated plasmids lack the purity and concentration needed for direct sequencing. Therefore, the DNA segments containing the mutation sequence in ISP and cytochrome c_1 were amplified from the isolated plasmids by the polymerase chain reaction. The PCR products were purified with an extraction kit from Sigma. The DNA sequencing was performed by the Recombinant DNA/Protein Core Facility at the Oklahoma State University.

Enzyme Preparations and Assay of Cytochromes — Chromatophore membranes were prepared from frozen cell paste and cytochrome bc_1 complexes with a His$_6$ tag placed at the C-terminus of cytochrome c_1 were purified from chromatophores as

described previously (18) and stored at -80 °C in the presence of 10% glycerol. Protein concentrations were determined by the absorbance at 280 nm, using a converting factor of 1 OD_{280} = 0.56 mg/ml. The concentrations of cytochromes *b* and c_1 were determined spectrophotometrically using published molar extinction coefficients (19-21).

Activity Assay of the Cytochrome bc_1 Complex — To assay ubiquinol-cytochrome *c* reductase activity, chromatophores or purified cytochrome bc_1 complexes were diluted with 50 mM Tris-Cl, pH 8.0, containing 200 mM NaCl and 0.01% N-dodecyl-β-D-maltoside (LM) to a final concentration of cytochrome *b* of 1 μM unless otherwise specified. Appropriate amounts of the diluted samples (2, 4, or 6 μl) were added to 1 ml of assay mixture containing 100 mM Na^+/K^+ phosphate buffer, pH 7.4, 0.3 mM EDTA, 100 μM cytochrome *c*, and 25 μM $Q_0C_{10}BrH_2$. Activities were determined by measuring the reduction of cytochrome *c* (the increase of the absorbance at wavelength 550 nm) in a Shimadzu UV 2101 PC spectrophotometer at 23 °C, using a millimolar extinction coefficient of 18.5 for calculation. The non-enzymatic oxidation of $Q_0C_{10}BrH_2$, determined under the same conditions, in the absence of enzyme, was subtracted during specific activity calculations. Although the chemical properties of $Q_0C_{10}BrH_2$ are comparable with those of $Q_0C_{10}H_2$, the former is a better substrate for the cytochrome bc_1 complex (16).

Gel Electrophoresis and Western Blot Preparation — SDS-polyacrylamide gel electrophoresis was performed according to the method of Laemmli (22) using a Bio-Rad Mini-Protean dual slab vertical cell. Samples were digested with 10 mM Tris-Cl buffer, pH 6.8, containing 1% SDS and 3% glycerol in the presence or absence of 0.4% β-mercaptoethanol (β-ME) for 10 min at room temperature before being subjected to

electrophoresis. Western blotting was performed with polyclonal rabbit antibodies against cytochrome c_1 or ISP of the *Rb. Sphaeroides* bc_1 complex. The polypeptides separated by SDS-PAGE gel were transferred to 45 Micron nitrocellulose membrane for immunoblotting. Protein A conjugated to horseradish peroxidase (HRP) was used as the second antibody. Color development was carried out using a HRP color development solution.

Determination of the Redox Potential of Cytochromes c_1 in the Wild Type and the Mutant Cytochrome bc_1 Complexes — Redox titrations of cytochromes c_1 in the wild type and the mutant bc_1 complexes were determined essentially according to the previously published method (23,24). 3 ml aliquots of the bc_1 complex (7 μM cytochrome c_1) in 0.1 M Na^+/K^+ phosphate buffer, pH 7.0, containing 25 μM 1,4-benzoquinone (Em, 293 mV), 25 μM 2,3,5,6-tetramethyl-p-phenylenediamine (Em, 260 mV), 25 μM 1,2-naphthoquinone (Em, 143 mV), 20 μM phenazine methosulfate (Em, 80 mV), 20 μM phenazine ethosulfate (Em, 55 mV), 25 μM 1,4-naphthoquinone (Em, 36 mV) and 25 μM duroquinone (Em, 5 mV) were used. Reductive titrations were carried out by addition of sodium dithionite solution to the ferricyanide-oxidized sample. Oxidative titrations were carried out by addition of ferricyanide solution to the dithionite-reduced sample. At indicated Eh values during the redox titration absorption spectra, 600 to 500 nm, were taken with a Shimadzu model UV-2100 spectrophotometer. The optical density at 552 nm, minus that at 535 nm, was used for cytochrome c_1 measurement. The midpoint potential of cytochrome c_1 was calculated by fitting the redox titration data, obtained for cytochrome c_1, using the Nernst equation for a one-electron carrier (n = 1) by Kaleidagraph (23).

Determination of pH-induced Reduction and Oxidation of ISP and Cytochrome c_1 in the Partially Reduced Wild Type and Mutant bc_1 Complexes — The wild type or mutant bc_1 complex was diluted in 3 ml of 20 mM Tris-Cl buffer, pH 8.0, containing 200 mM NaCl and 0.01% LM. The concentration of cytochrome c_1 was adjusted to about 10 μM. Different amounts of NaOH or HCl were added to give the indicated pHs. Fully oxidized or reduced cytochrome c_1 and ISP were obtained by addition of $K_3Fe(CN)_6$ or sodium ascorbate. Reduction of cytochrome c_1 was followed by measuring the increase of the α-absorption (553-535 nm) in a Shimadzu UV 2101 PC spectrophotometer. Reduction of ISP was followed by measuring the negative CD peak at 500 nm of partially reduced ISP minus fully oxidized complex in a JASCO J-715 spectropolarimeter (13,25,26). The same samples were used for the absorption and CD measurement. Instrument settings for the spectropolarimeter were: scan speed, 100 nm/min; step resolution, 1 nm; accumulation, 10 traces for averaging; response, 1 s; bandwidth, 2.0 nm; sensitivity, 10 mdeg; and slit width, 500 μm.

Determination of the pH induced Electron Transfer Rates between the [2Fe-2S] Cluster and Heme c_1 in the Wild Type and the Mutant bc_1 Complexes — The method used is essentially the same as that previously reported (13,26). The cytochrome bc_1 was diluted in 20 mM Tris-Cl buffer, pH 8.0, containing 200 mM NaCl and 0.01% LM to a cytochrome c_1 concentration around 10 μM. The percentage of cytochrome c_1 reduction in the sample was adjusted to around 50% at pH 8.0 by adding sodium ascorbate or ferricyanide. For the electron transfer from the [2Fe-2S] cluster to heme c_1, the pH of the sample was decreased to pH 6.9 by adding HCl. This solution was rapidly mixed with an equal volume of the same buffer but containing enough NaOH to cause the pH change

from 6.9 to 8.9 in the stopped flow spectrophotometer at room temperature. Increased reduction of cytochrome c_1 was monitored spectrophotometrically. The reaction was monitored at 553nm-540nm. Complex mixed with an equal volume of the same buffer at pH 6.9 was used as a baseline.

Stigmatellin Induced Reduction Rate of ISP in the Absence of Exogenous Electron Donor in the Fully Oxidized Complex — In order to know whether position of [2Fe-2S] cluster in ISP was pulled toward the cytochrome c_1, far away from the Qp site by the formation of the disulfide bond between cyt c_1 and ISP, stigmatellin is used to induce the reduction of ISP in the absence of exogenous electron donor in the fully oxidized complex. The bc_1 complexes from wild type, S141C(ISP)/G180C(cyt c_1), and A185C(cyt *b*)/ K70C(ISP) (13) were diluted to 10 μM of cytochrome c_1 in 3 ml of 20 mM Tris-Cl buffer, pH 8.0, containing 200 mM NaCl and 0.01% LM. $K_3Fe(CN)_6$ was used to fully oxidize the bc_1 complexes, and the fully oxidized state of complexes was confirmed by measuring CD from 450 nm to 550nm in a JASCO J-715. Stigmatellin induced reduction of ISP were measured after incubating the fully oxidized bc_1 complexes with 50 μM inhibitor for 5 min, 1 hr and 2hr, respectively. Fully reduced ISP spectrum was obtained after the bc_1 complex was reduced by sodium ascorbate. The reduction of ISP was calculated by the negative CD peak at 500 nm of reduced ISP minus fully oxidized spectrum.

Stigmatellin Induced Oxidation Rate of Cytochrome c_1 in the Partially Reduced Complex — It is well known that binding of stigmatellin to cytochrome bc_1 complex causes substantial elevation of the mid-point potential of ISP (27,28). As a result, an inter-subunit electron transfer between the [2Fe-2S] cluster and heme c_1 is expected to

take place after stigmatellin is added into the complex. The bc_1 complex was diluted to cytochrome c_1 5 μM in the buffer containing 20 mM Tris-Cl buffer, pH 8.0, containing 200 mM NaCl and 0.01% LM. Sodium ascorbate was used to adjust the reduction of cyt c_1 to around 50%. Stigmatellin was added to the complex to a final concentration 25 μM. The redox state of cytochrome c_1 was monitored (553-545 nm).

Flash Photolysis Experiments: Flash photolysis experiments were carried out on 300 μL solutions contained in a 1-cm glass semimicrocuvette using the detection system described by Heacock et al(29). A Phase R model DL1400 flash lamp-pumped dye laser using coumarin LD 490 produced a 480 nm light flash of < 0.5 μs duration. Samples typically contained 5 μM cyt bc_1, 20 μM Ru_2D, 5 mM $[Co(NH_3)_5Cl]^{2+}$, in 20 mM sodium borate, pH 9.0, 0.01% dodecylmaltoside. The $[Co(NH_3)_5Cl]^{2+}$ was used as a sacrificial electron acceptor. The cyt bc_1 was treated with 10 μM $Q_oC_{10}BrH_2$, 1 mM succinate, and 50 nM SCR to completely reduce [2Fe2S] and cyt c_1, and reduce cyt b_H by 30%. The photooxidation and reduction of cyt c_1 was monitored at 552 nm, while the reduction of cyt b_H was monitored at 561 – 569 nm. Under the conditions used the reoxidation of cyt b_H by Q in the Q_N site was much slower than reduction because of the low concentration of oxidized Q.

Results and Discussion

Construction of mutant bc_1 complexes in which ISP is fixed in c_1 position- To generate a mutant in which ISP is fixed at c_1-position, mutants (ISP/cyt*b*) S141C/H111C, S141C/G112C, S141C/G180C, S141C/M114C were constructed. Meanwhile, mutants of H111C, G112C, M114C, G180C in cytochrome c_1 and S141C in ISP were also constructed, respectively. Substitution of S141C in ISP of *R.S.* bc_1 complex is a good choice for our

purpose (Figure IV-1): A). Residue S141 is not a conserved residue but an extra residue, though most of residues in the head domain are conserved. B). It is located on the head domain of ISP, close to iron-sulfur cluster spatially. C) High structural similarity between Cysteine and Serine. Due to the lack of X-ray crystallographic structure in which ISP is at c_1 position, the choosing of residues on cytochrome c_1 is a little bit arbitrary. However, there were still two rules we have to follow: A). Substituted residues should not be conserved and substitution cannot cause significant activity damage B). They are located around heme c_1 and face the head domain of ISP.

The locations of these substituted residues are shown in Figure IV-2. In Figure IV-2, His111, Gly112, Met114, and G180C are substituted by cysteines. The distances between engineered cysteines in cytochrome c_1 and S141C in ISP are also shown in this Figure IV-2. The distances from H111C, G212C, M114C, G180C in cytochrome c_1 to S141C in ISP are 24.26 Å, 24.43 Å, 22.96 Å, 12.01Å, respectively. All of these distances are much longer than the distance (1.8 - 2.3 Å) required for the formation of disulfide bond. However, the head domain of ISP is at *b*-position in this X-ray graphic structure. During catalysis, the head domain of ISP will rotate through ~23 Å to cytochrome c_1 for electron delivery (30). Therefore, if orientation is right, all of these four mutants have possibilities to form inter-subunit disulfide bonds. However, eventually, the inter-subunit disulfide bond is only formed in mutant S141C/G180C. We'll describe our evidences in the following parts.

Photosynthetic Growth Behaviors of the Wild Type and Mutants — Since cytochrome bc_1 complex is absolutely required for photosynthetic growth of *Rb.*

Figure IV-1: Part of Sequence alignment of ISP subunits between beef and *R.S.* bc_1 complexes. Residue S141 is in red color. It is not a conserved residue but an extra residue, though most of residues in the head domain are conserved.

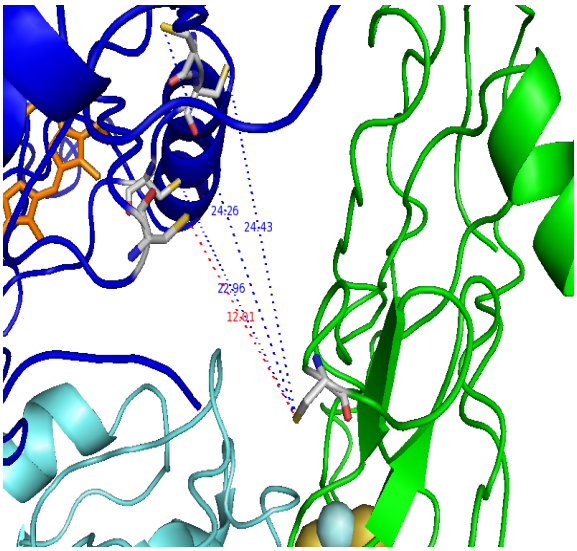

Figure IV-2: Diagram of the locations of substituted residues in cytochrome c_1 and ISP. All subunits are displayed as cartoon style. ISP is in green, and cytochrome c_1 in blue and cytochrome *b* in cyan. Iron-sulfur cluster are displayed as spheres and hemes are displayed as sticks in orange. Residues H111C, G112C, M114C and G180C in cytochrome c_1 and S141C are displayed as sticks. The distances from H111C, G212C, M114C, G180C in cytochrome c_1 to S141C in ISP are 24.26 Å, 24.43 Å, 22.96 Å, 12.01Å, respectively

sphaeroides, a mutant with cysteine substitution at a critical position will not grow photosynthetically, whereas mutants with substitution at noncritical positions will grow. Thus, observing the photosynthetic growth behavior, one can determine whether the engineered cysteines are at critical positions. In mid-log phase, semi-aerobically dark grown wild type and mutant cells were inoculated into enriched Siström's medium and subjected to anaerobic photosynthetic growth conditions. All the single and double mutants grew at rates comparable with that of the wild type (Table IV-1), indicating that the engineered cysteine positions are noncritical to the complex. However, mutants G180C(cty c_1) and S141C(ISP)/G180C(cyt c_1) grew at a retarded rate (80% of the wild type), suggesting that the small effect on photosynthetic growth is caused by the substitution of G180 with cysteine. It also suggests that few disulfide bonds form in the S141C(ISP)/G180C(cyt c_1) mutant intact cell system.

Formation of a Disulfide Bond between the ISP Head Domain and Cytochrome c_1 in the S141C(ISP)/G180C(cyt c_1) Mutant bc_1 Complex — Chromatophores freshly prepared from the S141C(ISP), G180C(cyt c_1), and S141C(ISP)/ G180C(cyt c_1) mutant cells have, 100, 78, and 26% of the bc_1 activity found in the wild type chromatophores (Table IV-1), respectively. The purified His_6-tagged bc_1 complexes isolated from freshly prepared chromatophore have, 100, 80, and 8% of the wild type bc_1 activity respectively (Table IV-1), based on cytochrome *b* content. Both of the single mutants, S141C(ISP) and G180C(cyt c_1) have a comparable activity with wild type bc_1, indicating these two single substituions have little effect on mutant bc_1's catalytic activity. It is not controversial that mutant S141C/G180C can grow photosynthetically well whereas purified protein has only 8% of wild type's bc_1. As we know, formation of a disulfide

Table IV-1: Characterization of mutants

Strains	P.S.[a]	Activity[b]	
		chromatophore	Purified protein
Wild type	+++	2.3 (100%)	2.5 (100%)
S141C(ISP)	+++	2.3 (100%)	2.5 (100%)
G180C(cyt c_1)	+++	1.8 (78%)	2.0 (80%)
S141C(ISP)/G180C(cyt c_1)	++	0.6 (26%)	0.2[c] (8%)
H111C(cyt c_1)	+	0.2 (9%)	0.6 (24%)
S141C(ISP)/H111C(cyt c_1)	+	0.2 (9%)	0.6 (24%)
G112C(cyt c_1)	+	0.8 (35%)	0.9 (36%)
S141C(ISP)/G112C(cyt c_1)	+	0.8 (35%)	0.9 (36%)

The cytochrome bc_1 complexes were in 50 mM Tris–Cl, pH 8.0, containing 200 mM NaCl, 200 mM histidine, 0.5% octyl glucoside and 10% glycerol.
[a] Ps = photosynthetic growth.[b] The enzymatic activity is expressed as μmol of cytochrome *c* reduced/min/nmol cytochrome *b* at room temperature.
[c] If purification is carried out in the presence of β-ME, this value will be 2.0.

bond is an oxidative process, so no disulfide bond can be formed in anaerobic conditions, even though two cysteines are in favorable positions. Since photosynthetic growth is under strict anaerobic conditions, disulfide bond formation between these two engineered cysteines in mutant S141C(ISP)/G180C(cyt c_1) is not possible. However, during preparation of chromatophores and purification of the bc_1 complex, these two engineering cysteines are exposed to air and the formation of the disulfide bond takes place, resulting in a decrease of activity. To see whether or not the loss of the bc_1 complex activity observed in the mutant S141C(ISP)/G180C(cyt c_1) results from disulfide bond formation during the purification, SDS-PAGE patterns of the purified mutant complexes, with and without β-ME treatment, were examined (Figure IV-3). The purified complexes were treated with SDS in the absence or presence of β-ME (Figure IV-3) at room temperature for 10 min and subjected to electrophoresis. The same process was done with bc_1 of the wild type, S141C(ISP), and G180C(cyt c_1) mutants. When the β-ME was present, all bc_1 complexes showed same patterns in SDS-PAGE: 4 protein bands, cyt *b* (41 kDa), cyt c_1 (30.4 kDa), ISP (21 kDa), and subunit IV (14 kDa). However, in the absence of β-ME, mutant S141C/G180C showed different patterns from the others: (i) An adduct protein band of the cross-link protein was present and its molecular weight was around 51 kDa, the sum of cyt c_1 (30.4 kDa) and ISP (21 kDa); (ii) The density of cyt c_1 and ISP bands decreased significantly, indicating that most cyt c_1 and ISP are present in the cross-link protein. The inter-subunit disulfide bond linked adduct protein from the mutant S141C(ISP)/G180C(cyt c_1) was identified as a smear protein band in SDS-PAGE (Figure IV-3), consistent with the characteristic of cytochrome c_1 which also shows as a smear band in SDS-PAGE in the absence of β-ME(31). Western blot analysis with antibodies

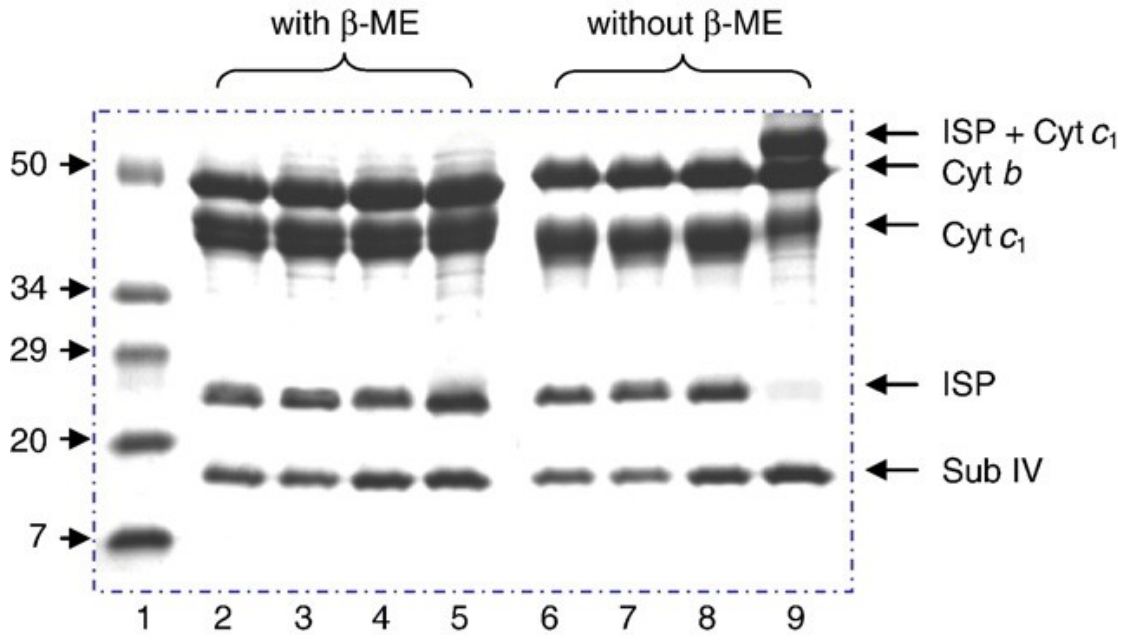

Figure IV-3: SDS-PAGE of the wild type and the cysteine mutant cytochrome bc_1 complexes. Lane 1, protein standard (Std); Lane 2 & 6, the wild type; Lane 3 & 7, S141C(ISP); Lane 4 & 8, G180C(cyt c_1); Lane 5 & 9, S141C(ISP)/G180C(cyt c_1). Adduct cross-link protein bond (ISP + Cyt c_1, lane 9) is disappeared when treated with β-ME (lane 5). Moreover, the intensity of ISP and cyt c_1 bands are obviously decreased compared to the corresponding bonds in the lane 5.

against *R. sphaeroides* cytochrome c_1 or ISP was done to characterize the adduct protein band (Figure IV-4). The results show that the adduct protein band can be blotted by both anti-cyt c_1 and anti-ISP antibodies, indicating that the adduct protein contains both cyt c1 and ISP. Trace amount of cytochrome c1 and ISP was also observed in the Western blot analysis of the double mutant complex.

Effect of β-ME on the Activity of Cytochrome bc_1 Complex — To confirm that formation of a disulfide bond between ISP and cytochrome c_1 in the S141C(ISP)/G180C(cyt c_1) mutant causes activity loss, the effect of β-ME on bc_1 complex activity and the degree of disulfide bond formation were examined. When purified S141C(ISP)/G180C(cyt c_1) mutant complex was incubated at 4ºC with β-ME, activity increased as incubation proceeded (Figure IV-5). Activity was restored to that of single mutant G180C(cyt c_1) after a 24 hour incubation. No adduct protein of ISP and cytochrome c_1 was detected in the β-ME treated S141C(ISP)/G180C(cyt c_1) mutant complex. When this complex was purified from freshly prepared chromatophores in the presence of 100 mM β-ME, it had the same activity as that found in the G180C(cyt c_1) and no ISP- cytochrome c_1 adduct was detected. All these results show that the loss of enzymatic activity is caused by the formation of a disulfide bond between S141C(ISP) and G180C(cyt c_1). It must be emphasized that the observed activity restoration is not due to nonenzymatic reduction of cytochrome *c* by added β-ME (13), nor to long term exposure to 4ºC, because the same treatment has little effect on the wild type complex.

Effect of the Mutations on Redox Potential of Cytochrome c_1 in the bc_1 Complex — The redox potential of cyt c_1 in the S141C(ISP)/G180C(cyt c_1) mutant complex is 220 mV (Figure IV-6), slightly lower than 235 mV observed in the wild type bc_1 complex (31), indicating the formation of a disulfide bond does not affect the redox potential of

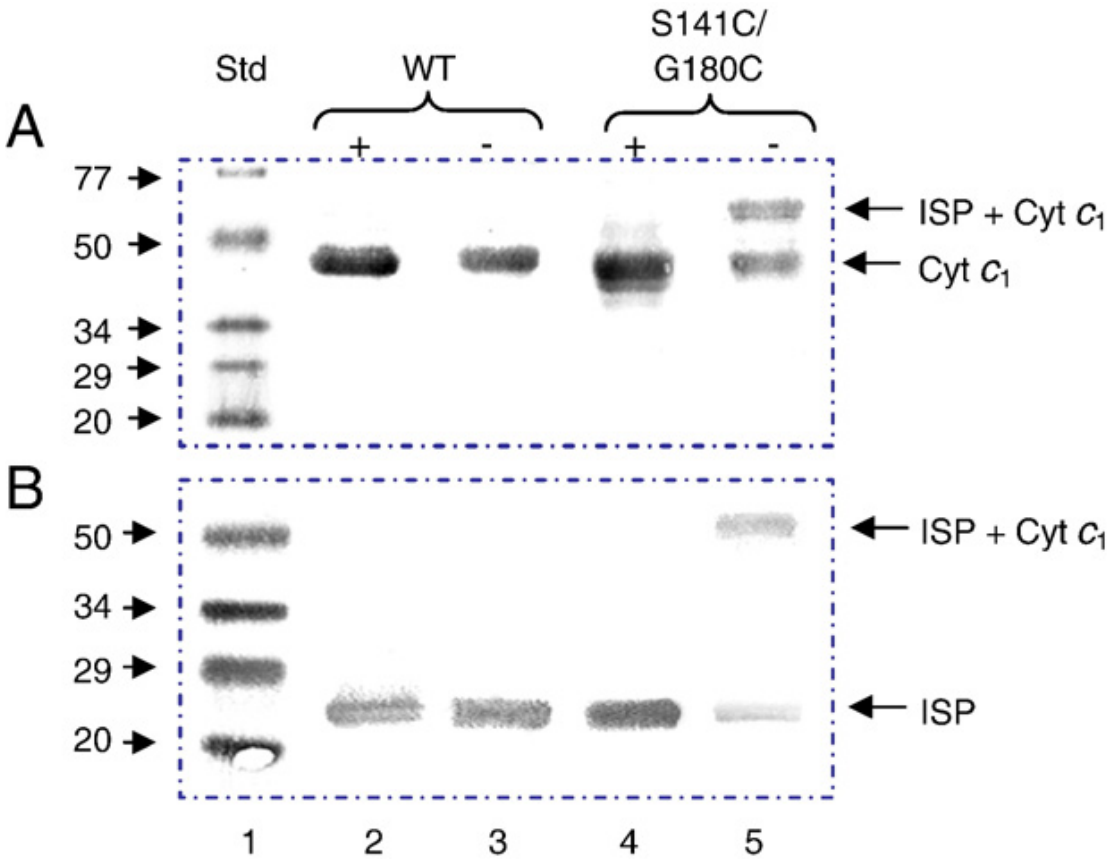

Figure IV-4: Western blot analysis of ISP or cytochrome c_1 in cytochrome bc_1 complexes from the wild type and S141C(ISP)/G180C(cyt c_1). Aliquots of the wild type and S141C(ISP)/G180C(cyt c_1) were incubated in the loading buffer containing 1% SDS with (+) or without (-) 0.4% β-ME at room temperature for 10 min. Digested samples containing 200 pmol of cytochrome *b* were subjected to electrophoresis. Samples in the gel were transferred to 45 micron nitrocellulose membrane and treated with antibody against *Rb. sphaeroides* cytochrome c_1 (A) or ISP (B). Protein A-horseradish peroxide conjugate was used as a second antibody. Std, protein standard. WT, wild type.

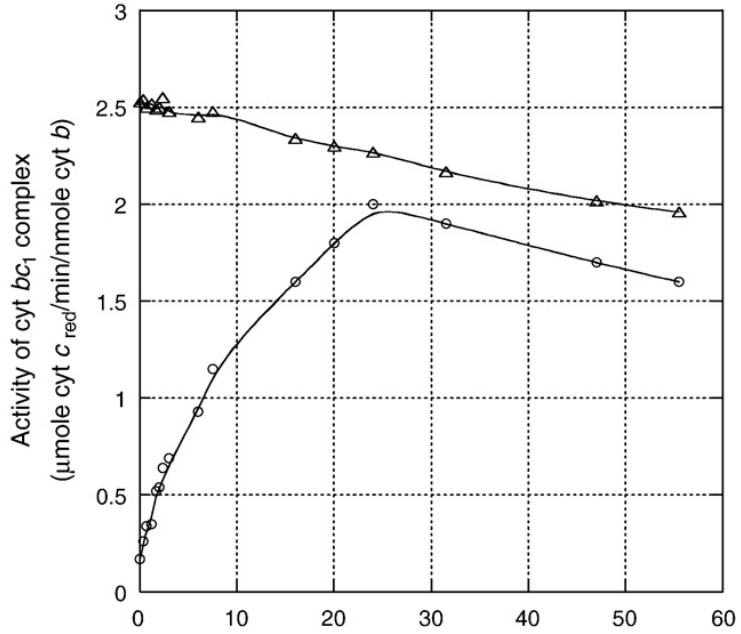

Figure IV-5: Effect of β-ME on the cytochrome bc_1 activity in purified complexes from the wild type (triangle) and the mutant S141C/G180C (circle) at 4ºC. 10 µM cytochrome bc_1 was incubated at 4ºC with 15mM β-ME.

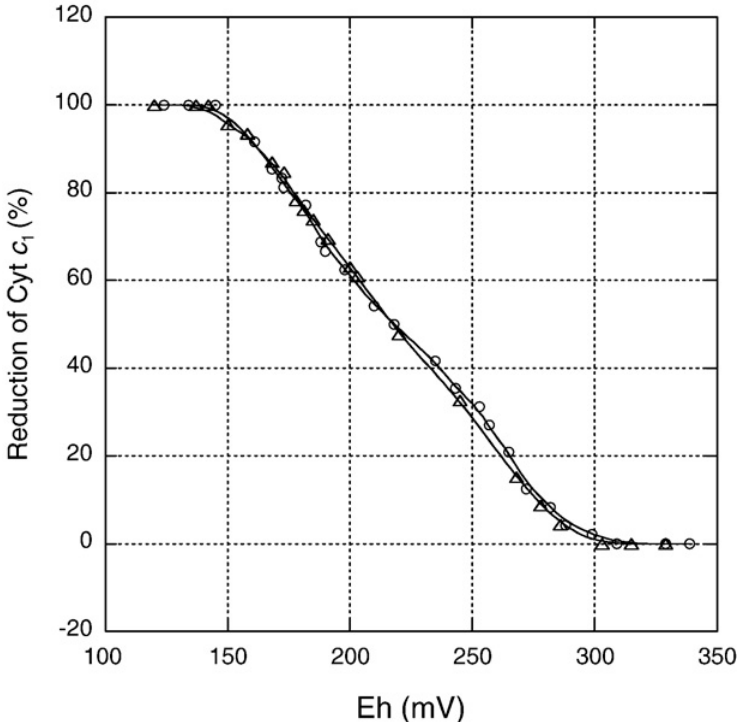

Figure IV-6: Redox potential titration of cytochrome c_1 in S141C(ISP) /G180C(cyt c_1) bc_1 complex. Oxidative and reductive titrations were performed as described in "Experimental Procedures." Triangle curve shows oxidative titration by ferricyanide and the circle shows reductive titration by dithionite. The data were fit to the Nernst equation when $n = 1$

cyt c_1 significantly, and the loss of bc_1 activity cannot be attributed to a redox potential change.

pH-dependent Oxidation of ISP and Reduction of Cytochrome c_1 in the Purified Cytochrome bc_1 Complex — It has been reported that intra-molecular electron transfer between the [2Fe-2S] cluster and heme c_1 in both bovine and *Rb. sphaeroides* cytochrome bc_1 complexes can be induced by pH change of the enzyme solution (13,26). This is based on the fact that the redox potential of heme c_1 is independent of pH, whereas the redox potential of the [2Fe-2S] cluster is pH-dependent (negative correlation). A similar phenomenon is observed in the S141C(ISP)/ G180C(cyt c_1) mutant complex, as shown in Figure IV-6. Both ISP and cytochrome c_1 are 52% reduced at pH 8.0, indicating that they have the same redox potential at the given pH. However, when the pH is increased to 9.0, cytochrome c_1 reduction increases to 78% and ISP reduction decreases to 28%. When the pH is increased, the redox potential of ISP decreases while that of cytochrome c_1 remains unchanged. As a result, electrons transfer from ISP to cytochrome c_1. Similarly, when the pH is decreased from pH 8.0 to 7.0, cytochrome c_1 reduction decreases from 52% to 30%, whereas ISP reduction increases from 52% to 82%. A linear relationship between ISP oxidation and cytochrome c_1 reduction is observed (Figure IV-7). These results suggest that formation of an inter-subunit disulfide bond does not alter the pH dependency of midpoint potentials of either ISP or cytochrome c_1.

Stigmatellin Induced Reduction Rate of ISP in the Absence of Exogenous Electron Donor in the Fully Oxidized Complex — Stigmatellin is a tightly bound Qp site inhibitor (32). The [2Fe-2S] cluster in the mutant S141C(ISP)/G180C(cyt c_1) bc_1 complex is

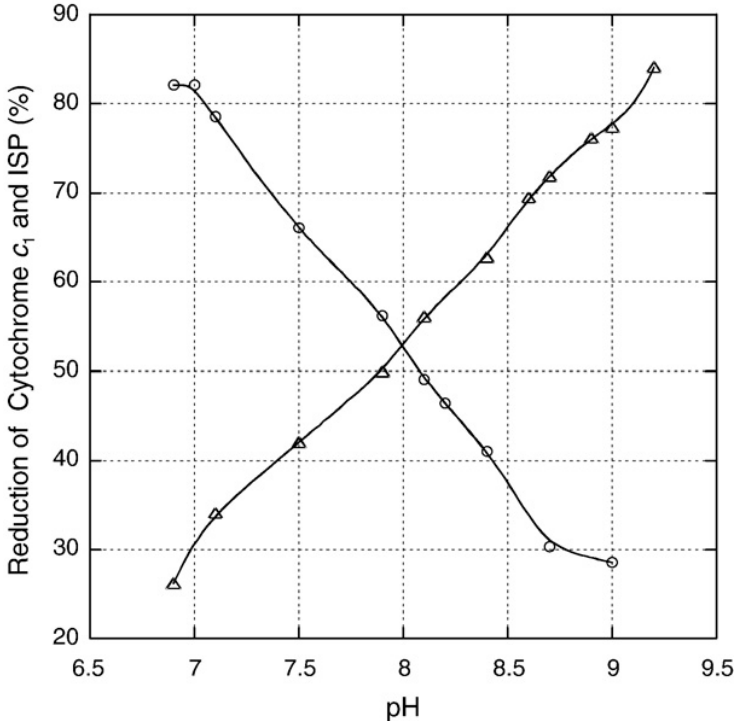

Figure IV-7: pH induced reduction and oxidation of ISP (circle) and cytochrome c_1 (triangle) in the partially reduced cytochrome bc_1 complex from S141C(ISP)/G180C(cyt c_1) mutant. The experimental conditions and instrument settings are detailed under "Experimental Procedures."

further from bound stigmatellin than those in the wild type and A185C(cyt *b*)/K70C(ISP). As a result, its reduction rate induced by stigmatellin is the slowest in these three bc_1 complexes (Table IV-2) with only a small portion of ISP, in the mutant S141C(ISP)/G180C(cyt c_1) complex, being reduced. On the contrary, the reduction rate of the [2Fe-2S] cluster in the mutant A185C(cyt *b*)/K70C(ISP) bc_1 complexes, induced by stigmatellin, is the fastest. The slow reduction rate of ISP in mutant S141C(ISP)/G180C(cyt c_1) bc_1 complex shows that formation of a disulfide bond between S141C and G180C pulls the [2Fe-2S] cluster away from the Qp site, while the fast reduction rate of ISP in A185C(cyt *b*)/K70C(ISP) complex shows the [2Fe-2S] cluster is pulled close to the Qp site. Since there is no reducing compound present in the ferricyanide oxidized complex, the source of the electron donor is unknown; it might come from amino acid residues located near Qp site. The possibility that the reducing compound is ferricyanide has been ruled out because similar reduction is observed in a complex oxidized by cytochrome *c* oxidase and cytochrome *c*.

Stigmatellin Induced Oxidation of Cytochrome c_1 in the Partially Reduced Cytochrome bc_1 Complex — In the partially reduced wild type complex, a rapid oxidation of cytochrome c_1 is observed upon addition of stigmatellin. This oxidation is the result of an elevation of the mid-point potential of ISP by stigmatellin bound at the Qp site and the fixation of the head domain of ISP at the *b*-position. Because the head domain of ISP is linked to the c_1 position through inter-subunit disulfide bond, the effect of stigmatellin on the mid-point potential of ISP is diminished. The binding of stigmatellin is no longer able to fix the head domain of ISP at the *b* position, a condition that requires for the elevation of the mid-point potential of ISP. Thus cytochrome c_1 in the mutant S141C(ISP)/G180C(cyt c_1) complex will not be oxidized by ISP in spite of the short distance between heme c_1 and the

Table IV-2: Reduction of ISP induced by stigmatellin in the absence of exogenous electron donor.

Strain	Reduction percentage of ISP		
	5 min	1 hr	2 hr
Wild type	54%	81%	100%
S141C/G180C	43%	59%	76%
K70C/A185C	91%	98%	100%

The bc_1 complexes from the wild type, S141C(ISP)/G180C(cyt c_1), and A185C(cyt *b*)/K70C(ISP) were diluted to 10 μM in 3 ml of 20 mM Tris-Cl buffer, pH 8.0, containing 200 mM NaCl and 0.01% dodecylmaltoside. After incubated with 50 μM stigmatellin for 5 min, 1 hr, and 2 hr, the bc_1 complexes was subjected to the CD to measure the reduction of ISP.

[2Fe-2S] cluster. Figure IV-8 compares the stigmatellin induced oxidation of cytochrome c_1 in the partially reduced bc_1 complexes of wild type and mutant S141C(ISP)/G180C(cyt c_1). Only a small portion of cytochrome c_1 in the mutant complex is oxidized upon the addition of stigmatellin and the rate of oxidation is much smaller than in the wild type. Although the rate of stigmatellin induced cytochrome c_1 oxidation in the wild type complex is much faster than that in the mutant complex, this rate is still much smaller than that induced by pH. The reason is that, in the case of pH induced oxidation, ISP potential is directly affected by pH, regardless of the location of head domain of ISP. In stigmatellin induced reduction, the potential change of iron-sulfur cluster is due to the fixation of the head domain of ISP at the *b*-position. Protein conformation plays an important role in the electron transfer. Since stigmatellin can no longer fix head domain of ISP at the *b*-position in the mutant complex, little potential elevation is expected. Therefore, little oxidation of cytochrome c_1 occurs, in spite of the short distance between the two redox centers.

The determination of electron transfer rate between ISP and c_1 in WT and mutant bc_1 complexes- The kinetics of electron transfer within *R. sphaeroides* cytochrome bc_1 can be studied using the ruthenium dimer Ru_2D to photoinitiate the reaction(33). The 4+ charge on Ru_2D allows it to bind with high affinity to the negatively charged domain on cyt c_1(33). Laser flash photolysis of a solution containing Ru_2D and cyt bc_1 with cyt c_1 and [2Fe2S] initially reduced resulted in rapid photooxidation of cyt c_1. The metal-to-ligand charge-transfer excited state of Ru_2D is a strong oxidant and oxidizes cyt c_1 within 1 μs. The sacrificial electron acceptor $[Co(NH_3)_5Cl]^{2-}$ was present in the solution to oxidize Ru^{II*} and/or Ru^{I}. With this method, the rate constant of electron transfer between ISP and c_1 in mutant S141C/G180C was determined to be more than 1,000,000/s (Table IV-3). This rate is much higher than that in wild type bc1 complexes,

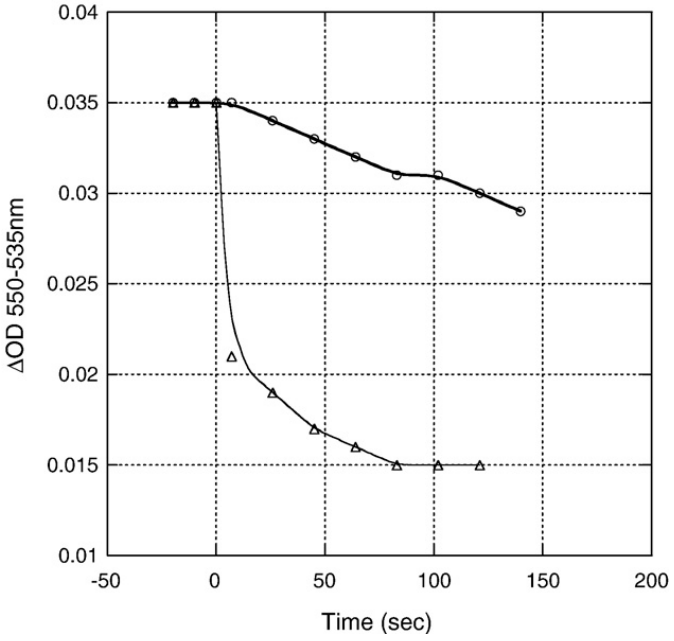

Figure IV-8: Time trace of stigmatellin induced oxidation of cytochrome c_1 in the partially reduced cytochrome bc_1 complex. 5 μM of the wild type (circle) and the mutant S141C(ISP)/G180C(cyt c_1) (triangle) cytochrome bc_1 complexes were treated with 25 μM stigmatellin. The oxidation of cytochrome c_1 is followed spectrophotometrically.

Table IV-3: Comparison of electron transfer rates between cytochrome c_1 and ISP in mutant and WT bc_1 complexes

	Docking site of ISP	ET Rate Constant (ISP-c_1)
WT	Randomly	60,000/s
WT (in the presence of famoxadone)	*b*-position	6,800/s[34]
S141G/G180C	c_1-position	>1,000,000/s

which is 80,000/s(34). It should be noted that the rate of 1,000,000/s is the maximal rate constant can by measured with the instrument used. When ISP of wild type bc_1 complex is fixed at b-position by famoxadone, this rate will become around 6,800/s(34). This experiment further demonstrates that in mutant S141G/G180C, ISP is really fixed at c_1-position through engineered inter-subunit disulfide bond.

All in all, from all experimental evidences above, we can conclude that in mutant bc_1 protein S141C/G180C, ISP is fixed at c_1-position through engineered cysteines of S141C and G180C. This mutant bc_1 complexes will provides us an opportunity to grow bc1 crystals with QH_2 at Qo pocket, which will help us to locate the exact Qo pocket in cytochrome bc_1 complexes. Meanwhile, with this crystal structure, we can learn how ISP interacts with heme c_1 in its c_1-position, which will benefit our further understanding on the bc_1 catalytic mechanism.

REFERENCE

1. Trumpower, B. L., and Gennis, R. B. (1994) *Annu. Rev. Biochem.* **63**, 675-716
2. Berry, E. A., Guergova-Kuras, M., Huang, L.-s., and Crofts, A. R. (2000) *Annual Review of Biochemistry* **69**, 1005-1075
3. Lange, C., and Hunte, C. (1999) *Proc. Natl. Acad. Sci. U.S.A* **99**, 2800-2805
4. Hunte, C. (2001) *FEBS Letters* **504**, 126
5. Iwata, S., Lee, J. W., Okada, K., Lee, J. K., Iwata, M., Rasmussen, B., Link, T. A., Ramaswamy, S., and Jap, B. K. (1998) *Science* **281**, 64-71
6. Xia, D., Yu, C.-A., Kim, H., Xia, J.-Z., Kachurin, A. M., Zhang, L., Yu, L., and Deisenhofer, J. (1997) *Science* **277**, 60-66
7. Zhang, Z., Huang, L., Shulmeister, V. M., Chi, Y.-I., Kim, K. K., Hung, L.-W., Crofts, A. R., Berry, E. A., and Kim, S.-H. (1998) *Nature* **392**, 677
8. Kim, H., Xia, D., Yu, C.-A., Xia, J.-Z., Kachurin, A. M., Zhang, L., Yu, L., and Deisenhofer, J. (1998) *Proc. Natl. Acad. Sci. U.S.A* **95**, 8026-8033
9. Iwata, S., Saynovits, M., Link, T. A., and Michel, H. . (1996) *Structure* **4**, 567-579
10. Link, T. A., Saynovits, M., Assmann, C., Iwata, S., Ohnishi, T., and Von Jagow, G. . (1996) *Eur J Biochem* **237**, 71-75
11. Tian, H., White, S., Yu, L., and Yu, C.-A. (1999) *J. Biol. Chem.* **274**, 7146-7152
12. Esser, L., Gong, X., Yang, S., Yu, L., Yu, C.-A., and Xia, D. (2006) Surface-modulated motion switch: Capture and release of iron-sulfur protein in the cytochrome bc1 complex.

13. Xiao, K., Yu, L., and Yu, C.-A. (2000) *J. Biol. Chem.* **275**, 38597-38604

14. Tian, H., Yu, L., Mather, M. W., and Yu, C.-A. (1998) *J. Biol. Chem.* **273**, 27953-27959

15. Esser, L., Quinn, B., Li, Y.-F., Zhang, M., Elberry, M., Yu, L., Yu, C.-A., and Xia, D. (2004) *Journal of Molecular Biology* **341**, 281

16. Yu, C.-A., and Yu, L. (1982) *Biochemistry* **21**, 4096-4101

17. Mather, M. W., Yu, L., and Yu, C.-A. (1995) *J. Biol. Chem.* **270**, 28668-28675

18. Tian, H., Yu, L., Mather, M. W., and Yu, C.-A. (1997) *J. Biol. Chem.* **272**, 23722-23728

19. Berden, J. A., and Slater, E. C. (1970) *Biochim. Biophys. Acta* **216**, 237-249

20. Yu, C. A., Yu, L., and King, T. E. (1972) *J. Biol. Chem.* **247**, 1012-1019

21. Yu, L., Dong, J. H., and Yu, C.-A. (1986) *Biochim. Biophys. Acta* **852**, 203-211

22. Wilson, D. F., Erecinska, M., Dutton, P. L., and Tsudzuki, T. (1970) *Biochemical and Biophysical Research Communications* **41**, 1273

23. Liu, X., Yu, C.-A., and Yu, L. (2004) *J. Biol. Chem.* **279**, 47363-47371

24. Dutton, P. L. (1978) *Methods in enzymology* **54**, 411-435

25. Ugulava, N. B., and Crofts, A. R. (1998) *FEBS Letters* **440**, 409

26. Zhang, L., Tai, C.-H., Yu, L., and Yu, C.-A. (2000) *J. Biol. Chem.* **275**, 7656-7661

27. von Jagow, G., and Ohnishi, T. (1985) *FEBS Letters* **185**, 311-315

28. Bowyer, J. R., Dutton, P. L., Prince, R. C., and Crofts, A. R. (1980) *Biochimica et Biophysica Acta (BBA) - Bioenergetics* **592**, 445

29. Heacock, D. H. d., Liu, R. Q., Yu, C. A., Yu, L., Durham, B., and Millett, F. (1993) *J. Biol. Chem.* **268**, 27171-27175

30. Crofts, A. R. (2004) *Photosynthesis Research* **80**, 223

31. Elberry, M., Yu, L., and Yu, C.-A. (2006) *Biochemistry* **45**, 4991-4997

32. Covian, R., Gutierrez-Cirlos, E. B., and Trumpower, B. L. (2004) *J. Biol. Chem.* **279**, 15040-15049

33. Robert C. Sadoski, G. E., Hua Tian, Li Zhang, Chang-An Yu, Linda Yu, Bill Durham, and Francis Millett. (2000) *Biochemistry* **39**, 4231-4236

34. Kunhong Xiao, G. E., Sany Rajagukguk, Chang-An Yu, Linda Yu, Bill Durham, and Francis Millett. (2003) *Journal of biological chemistry* **278**, 25731 - 25737

CHAPTER V

EFFECT OF MUTATIONS IN THE CYTOCHROME *B EF* LOOP ON THE ELECTRON TRANSFER REACTIONS OF THE RIESKE IRON-SULFUR PROTEIN IN THE CYTOCHROME BC_1 COMPLEX

Abstract

Long range movement of the iron-sulfur protein (ISP) between the cytochrome *b* (cyt *b*) and cyt c_1 redox centers plays a key role in electron transfer within the cyt bc_1 complex. An important question is how this domain movement is controlled to allow bifurcated electron transfer to both the low and high potential chains, and prevent short-circuit reactions. A series of mutants in the cyt *b ef* loop of *Rhodobacter sphaeroides* cyt bc_1 were prepared to examine the role of this loop in controlling the capture and release of the ISP from cyt *b*. Electron transfer in the cyt bc_1 complex was studied using the ruthenium dimer, Ru_2D, to rapidly photooxidize cyt c_1 and initiate the reaction. Flash photolysis of a solution containing reduced wild-type cyt bc_1 and Ru_2D results in photooxidation of cyt c_1 within 1 μs, followed by electron transfer from the iron-sulfur center [2Fe2S] center to cyt c_1 with a rate constant of $k_1 = 60{,}000\ s^{-1}$. Famoxadone binding to the $Q_{P\ pocket}$ decreases k_1 to $5{,}400\ s^{-1}$, indicating that a conformational change on the surface of cyt *b* decreases the rate of release of the ISP from cyt b. The mutation I292A on the surface of the ISP binding crater decreased k_1 to $4{,}400\ s^{-1}$, while addition of

famoxadone further decreased it to 3,000 s^{-1}. The mutation L286A at the tip of the *ef* loop decreased k_1 to 33,000 s^{-1}, but famoxadone binding caused no further decrease, suggesting that this mutation blocked the conformational change induced by famoxadone. Studies on all the mutants examined provide further evidence that the *ef* loop plays an important role in regulating the domain movement of the ISP to facilitate productive electron transfer and to prevent short-circuit reactions.

Introduction

The cytochrome bc_1 complex (ubiquinol:cytochrome c reductase) is an integral membrane protein in the electron transport chains of mitochondria and many respiratory and photosynthetic prokaryotes (1, 2). The complex contains the Rieske iron-sulfur protein (ISP), cyt c_1, and two b-type hemes (b_L and b_H) in the cyt *b* subunit (1, 2). The complex translocates four protons to the positive side of the membrane as two electrons are transferred from ubiquinol (QH_2) to cyt c using a widely-accepted Q-cycle mechanism (2). In a key bifurcated reaction, QH_2 binds to the $Q_{P\ pocket}$ located near the outside of the membrane, and transfers its first electron to the Rieske iron-sulfur center ([2Fe2S]), and then to cyt c_1 and cyt c (1-3). The second electron is transferred from semiquinone in the $Q_{P\ pocket}$ to cyt b_L and then to cyt b_H, leading to reduction of ubiquinone in the Q_N pocket to the semiquinone. This cycle is repeated to reduce the semiquinone at the Q_N pocket to QH_2. X-ray crystallographic studies have shown that the conformation of the ISP depends on the presence of inhibitors in the $Q_{P\ pocket}$ as well as the crystal form (4-7). An anomalous signal for [2Fe2S] is found close to cyt b_L in native $I4_122$ bovine crystals, but its intensity is small, indicating that the ISP is conformationally mobile (4,7). In beef, chicken and yeast cyt bc_1 crystals grown in the presence of stigmatellin, the ISP is in a conformation with [2Fe2S] proximal to the cyt b_L heme, called the *b* state (5-8). However, in native chicken or beef $P6_522$ crystals in the absence of $Q_{P\ pocket}$ inhibitors, the ISP is in a conformation with [2Fe2S] close to cyt c_1, called the c_1 state (5,6). A novel shuttle mechanism for the ISP has been proposed based on these structural studies (4-7). With the ISP initially in the *b* state, QH_2 in the $Q_{P\ pocket}$ transfers an electron to the oxidized [2Fe2S] center. The ISP then rotates by 57^o to the

c_1 state where reduced [2Fe2S] transfers an electron to cyt c_1. The main features of this mobile shuttle mechanism have been supported by a variety of experimental studies using mutation and/or cross-linking to immobile the ISP or alter the conformation of the neck region (9-20).

An important question regarding the Q-cycle mechanism is how QH_2 at the $Q_{P\ pocket}$ can deliver two electrons sequentially to the high and low potential chains, even though thermodynamics would favor delivery of both electrons to the high potential chain (1,2). A number of mechanisms have been proposed in which the conformations of the ISP and/or the quinone substrates are controlled to favor the reversible oxidation of QH_2 and minimize short circuit reactions (21-29). Studies of the effects of $Q_{P\ pocket}$ inhibitors have indicated that there is a linkage between the occupant of the $Q_{P\ pocket}$ and the conformation and dynamics of the ISP. Stigmatellin forms a hydrogen bond with the His-161 ligand of the [2Fe2S] center, thus increasing its redox potential by 200-250 mV and immobilizing the ISP in the *b* conformation (5-8, 30). Famoxadone binding to the $Q_{P\ pocket}$ leads to significant conformational changes on the surface of cyt *b* which trigger a long-range conformational change in the ISP from the mobile state to a state with [2Fe2S] proximal to cyt *b* (31). The *ef* loop plays an important role in relaying conformational changes in the Q_P pocket to surface domains that control the binding of the ISP. Moreover, molecular dynamics simulations have shown that residues 263-268 of the ef loop are displaced by up to 2 Å as the ISP rotates from the *b* state to the c_1 state (32). In this paper, the effects of mutations of *ef* loop residues on electron transfer from QH_2 to the iron-sulfur center and then to cyt c_1 are studied using the binuclear ruthenium complex, Ru_2D, to rapidly photooxidize cyt c_1 and initiate the reaction (9, 17). The

ruthenium photooxidation method provides a unique way to measure the dynamics of the ISP domain movement from the *b* state to the c_1 state (9, 17, 33).

Experimental Procedures

Materials. A modification of the method of Downard et al. (34) was used to prepare Ru_2D. Succinate, *p*-benzoquinone and antimycin A were obtained from Sigma Chemical Co., stigmatellin was purchased from Fluka Chemical Co., and N-Dodecyl-β-D-maltoside was obtained from Anatrace. $[Co(NH_3)_5Cl]^{2+}$ was synthesized as described in reference (35), and 2,3-dimethoxy-5-methyl-6-(10-bromodecyl)-1,4-benzoquinol, $Q_0C_{10}BrH_2$, was prepared as previously reported (36). Succinate cytochrome c reductase (SCR) was purified as previously described (37).

Generation of R. sphaeroides strains expressing the his6-tagged bc_1 complexes: The Quickchange™ XL site-directed mutagenesis kit from Stratagene was employed for mutagenesis. Plasmid pGEM7Zf(+)-fbcB was used as a template and forward and reverse primers were used for PCR amplification. Template plasmid pGEM7Zf(+)-fbcB was constructed by ligating the fragment between NsiI and XbaI in the plasmid pRKDfbcFBC$_{6H}$Q into NsiI and XbaI sites of the pGEM7ZF(+) plasmid. The primers used are listed in the Table V-1.

After mutagenesis, NsiI-XbaI fragment from the pGEM7Zf(+)-fbcBm was ligated into NsiI and XbaI sites of the pRKDfbcFB$_{bpKm}$C$_{6H}$ plasmids which contained Kanamycin-resistant gene in the BstI and pinA sites (38). Strains containing recombinant plasmid will be sensitive to antibiotics kanamycin. The pRKDfbcFBmC$_{6H}$Q plasmid in E.*coli* S17-1 cells was mobilized into R. sphaeroides BC-17 through conjugation (38).

The engineered mutations were confirmed by DNA sequencing before and after photosynthetic growth as previously reported (38), which was performed by the Recombinant DNA/Protein Core Facility at Oklahoma State University.

Mutant cytochrome bc_1 was purified as described by Xiao et al.(39).The steady-state activity of bc_1 complexes was determined as described by Liu et al.(40).

Flash Photolysis Experiments: Flash photolysis experiments were carried out on 300 μL solutions contained in a 1-cm glass semimicrocuvette using the detection system described by Heacock et al. (41). A Phase R model DL1400 flash lamp-pumped dye laser using coumarin LD 490 produced a 480 nm light flash of < 0.5 μs duration. Samples typically contained 5 μM cyt bc_1, 20 μM Ru_2D, 5 mM $[Co(NH_3)_5Cl]^{2+}$, in 20 mM sodium borate, pH 9.0, 0.01% dodecylmaltoside. The $[Co(NH_3)_5Cl]^{2+}$ was used as a sacrificial electron acceptor. The cyt bc_1 was treated with 10 μM $Q_oC_{10}BrH_2$, 1 mM succinate, and 50 nM SCR to completely reduce [2Fe2S] and cyt c_1, and reduce cyt b_H by 30%. The photooxidation and reduction of cyt c_1 was monitored at 552 nm, while the reduction of cyt b_H was monitored at 561 – 569 nm. Under the conditions used the reoxidation of cyt b_H by Q in the $Q_{N\ pocket}$ was much slower than reduction because of the low concentration of oxidized Q.

Table V-1: Primers used during mutagenesis operation

Mutant (in the cytochrome b)	Primers
H276A (D252)	5'-GCCGAACTACCTCGGCGCCCCCGACAACTACATCG-3' 3'-CGGCTTGATGGAGCCGCGGGGGCTGTTGATGTAGC-5'
P277A (P253)	5'-CGAACTACCTCGGCCACGCCGACAACTACATCGAGG-3' 3'-GCTTGATGGAGCCGGTGCGGCTGTTGATGTAGCTCC-5'
D278A (D254)	5'-CTACCTCGGCCACCCCGCCAACTACATCGAGGCGAAC-3' 3'-GATGGAGCCGGTGGGGCGGTTGATGTAGCTCCGCTTG-5'
D278N	5'-CTACCTCGGCCACCCCAACAACTACATCGAGGCGAAC-3' 3'-GATGGAGCCGGTGGGGTTGTTGATGTAGCTCCGCTTG-5'
D278E	5'-CTACCTCGGCCACCCCGAAAACTACATCGAGGCGAAC-3' 3'-GATGGAGCCGGTGGGGCTTTTGATGTAGCTCCGCTTG-5'
D278I	5'-CTACCTCGGCCACCCCATCAACTACATCGAGGCGAAC-3' 3'-GATGGAGCCGGTGGGGTAGTTGATGTAGCTCCGCTTG-5'
D278V	5'-CTACCTCGGCCACCCCGTCAACTACATCGAGGCGAAC-3' 3'-GATGGAGCCGGTGGGGCAGTTGATGTAGCTCCGCTTG-5'
D278H	5'-CTACCTCGGCCACCCCCACAACTACATCGAGGCGAAC-3' 3'-GATGGAGCCGGTGGGGGTGTTGATGTAGCTCCGCTTG-5'
N279A (N255)	5'-CTCGGCCACCCCGACGCCTACATCGAGGCGAACCC-3' 3'-GAGCCGGTGGGGCTGCGGATGTAGCTCCGCTTGGG-5'
Y280A (Y256)	5'-GGCCACCCCGACAACGCCATCGAGGCGAACCCGC-3' 3'-CCGGTGGGGCTGTTGCGGTAGCTCCGCTTGGGCG-5'
L286A (L262)	5'-CATCGAGGCGAACCCGGCCTCGACGCCCGCGCAC-3' 3'-GTAGCTCCGCTTGGGCCGGAGCTGCGGGCGCGTG-5'
L286V	5'-CATCGAGGCGAACCCGGTCTCGACGCCCGCGCAC-3' 3'-GTAGCTCCGCTTGGGCCAGAGCTGCGGGCGCGTG-5'
L286R	5'-CATCGAGGCGAACCCGAGGTCGACGCCCGCGCAC-3' 3'-GTAGCTCCGCTTGGGCTCCAGCTGCGGGCGCGTG-5'
L286E	5'-CATCGAGGCGAACCCGGAGTCGACGCCCGCGCAC-3' 3'-GTAGCTCCGCTTGGGCCTCAGCTGCGGGCGCGTG-5'
L286I	5'-CATCGAGGCGAACCCGATCTCGACGCCCGCGCAC-3' 3'-GTAGCTCCGCTTGGGCTAGAGCTGCGGGCGCGTG-5'
S287A (N263)	5'-CGAGGCGAACCCGCTCGCCACGCCCGCGCACATCG-3' 3'-GCTCCGCTTGGGCGAGCGGTGCGGGCGCGTGTAGC-5'
A290S (A266)	5'-CCGCTCTCGACGCCCTCGCACATCGTGCCGG-3' 3'-GGCGAGAGCTGCGGGAGCGTGTAGCACGGCC-5'
H291A (H267)	5'-GCTCTCGACGCCCGCGGCCATCGTGCCGGAATGG-3' 3'-CGAGAGCTGCGGGCGCCGGTAGCACGGCCTTACC-5'
I292A (I268)	5'-CTCGACGCCCGCGCACGCCGTGCCGGAATGGTACTTC-3' 3'-GAGCTGCGGGCGCGTGCGGCACGGCCTTACCATGAAG-5'
I292L	5'-CTCGACGCCCGCGCACCTGGTGCCGGAATGGTACTTC-3' 3'-GAGCTGCGGGCGCGTGGACCACGGCCTTACCATGAAG-5'
I292M	5'-CTCGACGCCCGCGCACATGGTGCCGGAATGGTACTTC-3' 3'-GAGCTGCGGGCGCGTGTACCACGGCCTTACCATGAAG-5'
I292V	5'-CTCGACGCCCGCGCACGTCGTGCCGGAATGGTACTTC-3' 3'-GAGCTGCGGGCGCGTGCAGCACGGCCTTACCATGAAG-5'
I292E	5'-CTCGACGCCCGCGCACGAGGTGCCGGAATGGTACTTC-3' 3'-GAGCTGCGGGCGCGTGCTCCACGGCCTTACCATGAAG-5'
I292R	5'-CTCGACGCCCGCGCACCGCGTGCCGGAATGGTACTTC-3' 3'-GAGCTGCGGGCGCGTGGCGCACGGCCTTACCATGAAG-5'

Results

The kinetics of electron transfer within *R. sphaeroides* cytochrome bc_1 were studied using the ruthenium dimer Ru_2D to photoinitiate the reaction (9). The 4+ charge on Ru_2D allows it to bind with high affinity to the negatively charged domain on cyt c_1 (9). Laser flash photolysis of a solution containing Ru_2D and cyt bc_1 with cyt c_1 and [2Fe2S] initially reduced resulted in rapid photooxidation of cyt c_1, as indicated by the decrease in absorbance at 552 nm (Figure IV-1). The metal-to-ligand charge-transfer excited state of Ru_2D is a strong oxidant and oxidizes cyt c_1 within 1 μs. The sacrificial electron acceptor $[Co(NH_3)_5Cl]^{2-}$ was present in the solution to oxidize Ru^{II*} and/or Ru^{I} according to the mechanism shown in Scheme 1. Cyt c_1 is subsequently reduced by [2Fe2S] in a biphasic reaction with rate constants of $k_1 = 60{,}000\ s^{-1}$ and $k_2 = 2{,}300\ s^{-1}$, as indicated by the increase in absorbance at 552 nm (Figure V- 1A). The fast phase k_1 has been assigned to direct electron transfer from [2Fe2S] to cyt c_1 (9). The slow phase of reduction of cyt c_1 has the same rate constant as the reduction of cyt b_H observed at 562 nm (Figure V- 1B), indicating rate-limiting electron transfer from QH_2 to [2Fe2S] with rate constant k_2 followed by rapid electron transfer from [2Fe2S] to cyt c_1, and from the semiquinone to cyt b_L and cyt b_H (Scheme 2) (9).

It has been demonstrated that the measured rate constant k_1 for electron transfer from [2Fe2S] to cyt c_1 is controlled by the rate of the conformational change of the ISP from the *b* state to the c_1 state, rather than by true electron transfer (17). Therefore, the value of k_1 provides a direct measure of the rate of this conformational change. Binding stigmatellin to the $Q_{P\ pocket}$ completely inhibits the reduction of both cyt c_1 and cyt b_H in the ruthenium kinetics experiment (Figure V- 1A) (9), consistent with the X-ray

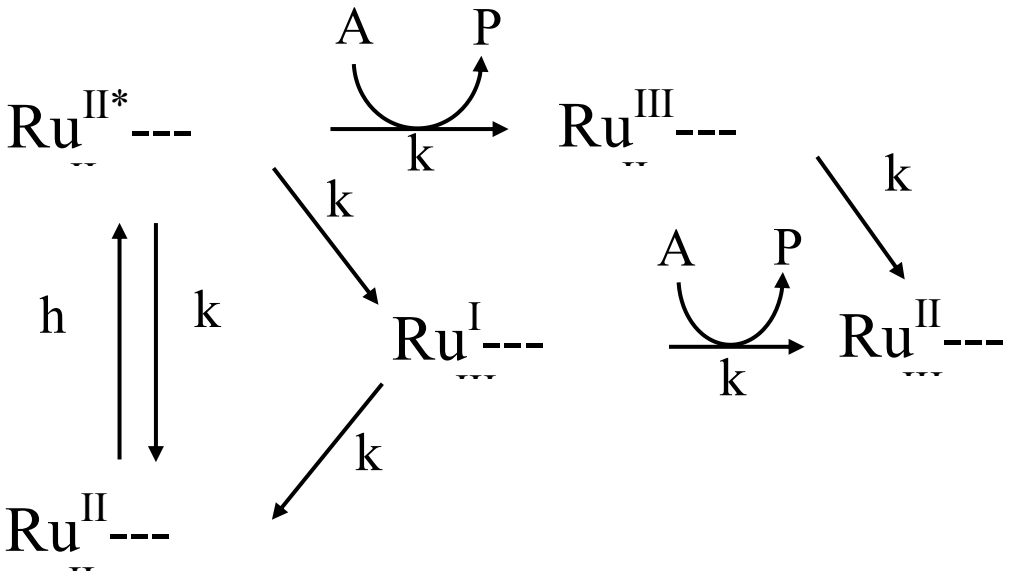

Scheme V-1. Photooxidation of cyt c_1 by ruthenium complex. A: sacrificial electron acceptor. P: products.

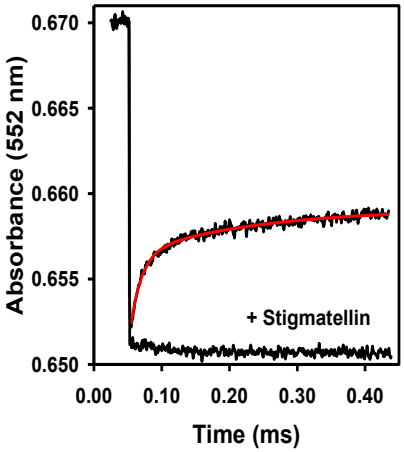

Figure 1A

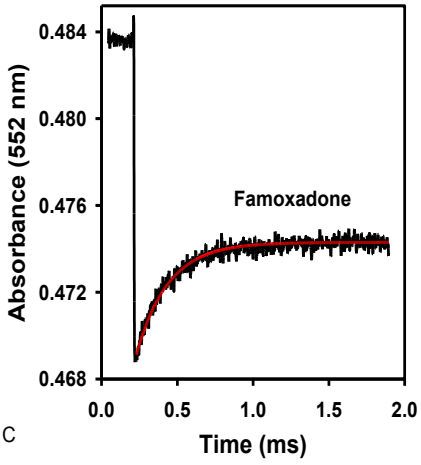

Figure 1C

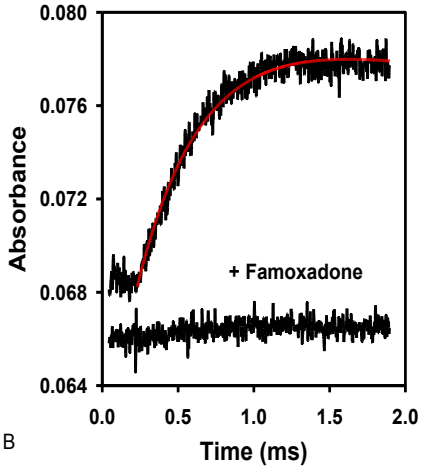

Figure 1B

Figure V-1: **Electron transfer within wild-type *R. sphaeroides* cyt bc_1 following photooxidation of cyt c_1.** The 300 μL sample contained 5 μM cyt bc_1, 20 μM Ru_2D, 5 mM $[Co(NH_3)_5Cl]^{2+}$, in 20 mM sodium borate, pH 9.0 with 0.01% dodecylmaltoside. The cyt bc_1 was treated with 10 μM $Q_oC_{10}BrH_2$, 1 mM succinate, and 50 nM SCR to completely reduce [2Fe2S] and cyt c_1, and reduce cyt b_H by about 30%. The sample was then excited with a 480 nm laser flash to photooxidize cyt c_1 within 1 μs. (A) The 552 nm transient indicates that cyt c_1 was photooxidized within 1 μs, and then reduced in a biphasic reaction with rate constants of 60,000 s^{-1} and 2,000 s^{-1}. The lower transient was obtained from the same sample treated with 20 μM stigmatellin. (B) The rate constant for the reduction of cyt b_H measured at 561 – 569 nm was 2,300 s^{-1} in the absence of inhibitor. Addition of 30 μM famoxadone eliminated reduction of cyt b_H, as shown in the lower curve. (C) When the original sample was treated with 30 μM famoxadone, the reduction of cyt c_1 was monophasic with a rate constant of 5,400 s^{-1}. (C)

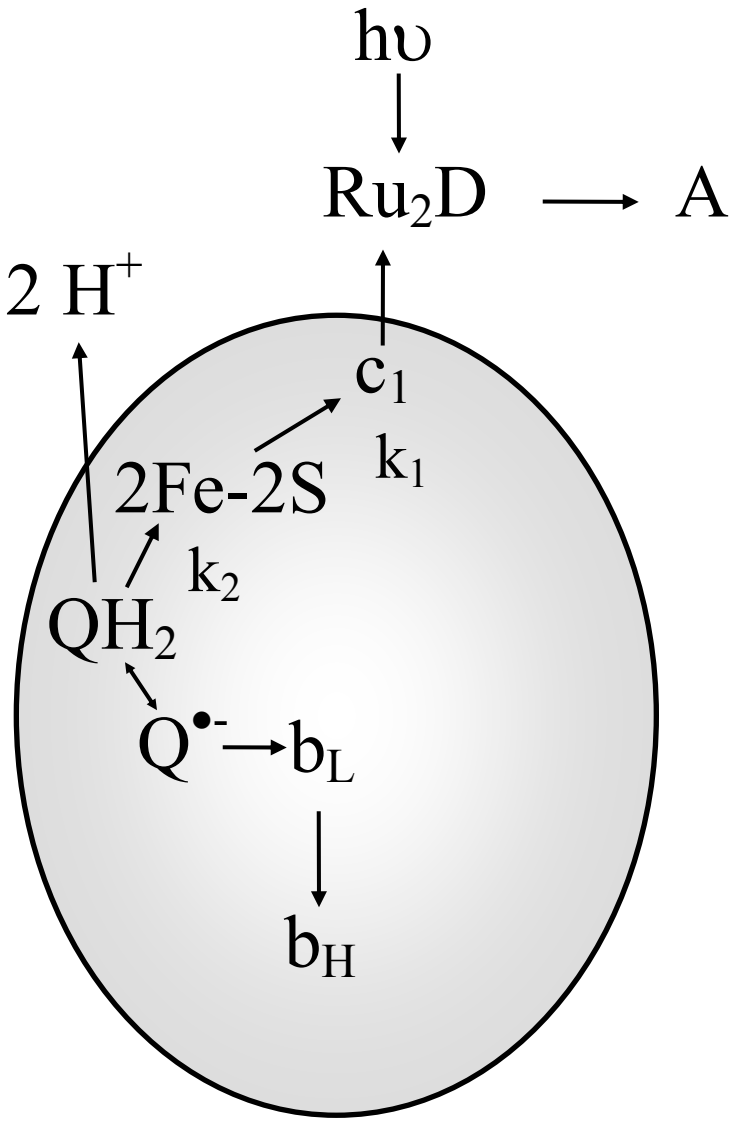

Scheme V-2

crystallographic studies showing that stigmatellin forms a hydrogen bond with the histidine ligand of the reduced [2Fe2S] center, and locks the ISP in the *b* conformation (5-8). In contrast, binding famoxadone to the $Q_{P\ pocket}$ does not prevent electron transfer from [2Fe2S] to cyt c_1, but instead decreases the rate constant from 80,000 s^{-1} to 5,000 s^{-1} (Figure IV-1C) (33). Famoxadone does not lock the ISP in the *b* conformation, but instead decreases the rate of the conformational change of the ISP from the *b* state to the c_1 state. Since famoxadone binding affected the conformation of the *ef* loop in cyt b, it was suggested that the *ef* loop might play a role in controlling the conformation of the ISP protein (31, 33). In order to examine this conformational link further, a series of mutants in which *ef* loop residues were substituted with Ala were prepared. These included the *ef* loop residues H276, P277, D278, N279, Y280, L286, S287, A290, H291, and I292 (Figure V-2 and V-3). The steady-state activity and the values of the rate constants k_1 and k_2 were measured for each of these mutants, both in the presence and absence of famoxadone. A number of the mutants caused relatively small decreases in the rate constant k_1, but the largest changes were seen for the mutants D278A, Y280A, L286A, and I292A (Table V-2). Additional mutants at residues D278, L286 and I292 were prepared to further explore the roles of these residues.

The D278A mutation decreased the steady-state activity from 2.35 to 1.43, and the rate constant k_1 from 60,000 s^{-1} to 26,000 s^{-1}, but did not affect the rate constant k_2. Famoxadone binding decreased the rate constant k_1 to 2,300 s^{-1}. The mutants D278N, D278E, D278I, and D278H did not have as large an effect on k_1 or k_2 as the D278A mutation. In contrast, the D278V mutation led to a 4.1-fold decrease in the steady-state activity, and a complete loss in the signal for electron transfer from [2Fe2S] to cyt c_1.

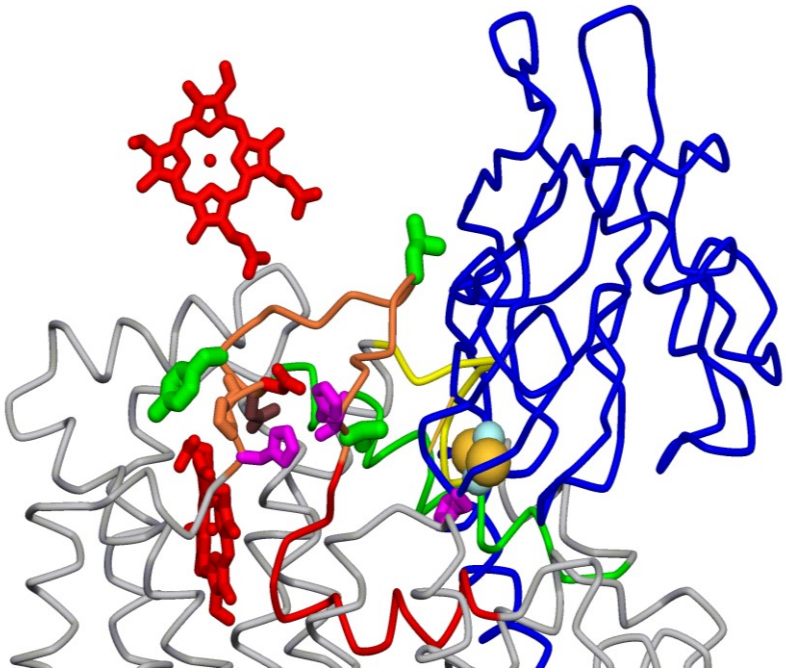

Figure V-2: X-ray crystal structure of *R. sphaeroides* cyt bc_1. The cyt c_1 and cyt b_L hemes are colored red, the 2Fe-2S center is represented by a CPK model, the ISP is blue, and cyt *b* is grey. Residues 276-292 in the *ef* loop are colored orange while residues 293-307 are red. Residues 152-170 in the cd1 helix are green and residues 179-187 in the neck-contacting domain are colored yellow. The residues in cyt *b* that were mutated are shown as sticks.

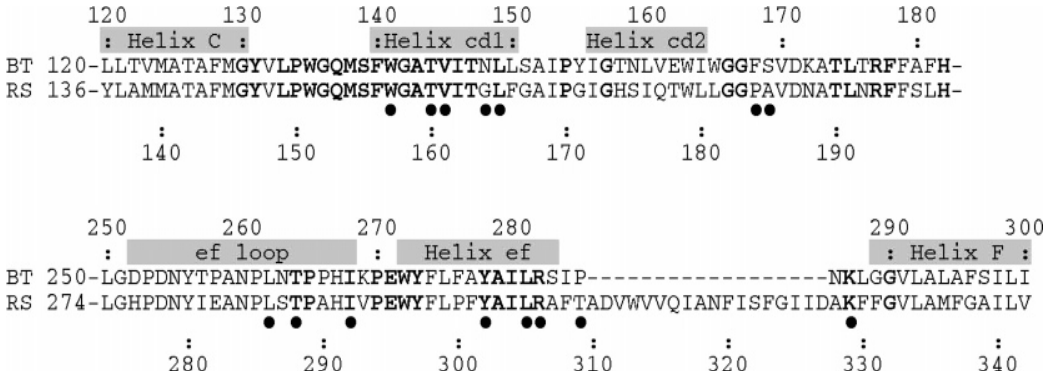

FIGURE V- 3: Sequence alignment of residues near the Qo pocket of the cyt *b* subunit in cyt bc_1 complexes from bovine (BT) and *R. sphaeroides*(RS). Residues with a high sequence similarity are in bold font. Helices determined crystallographically are indicated by gray rectangles.Residues in direct contact with the ISP are indicated with a black dot. Adopted from ref *21*.

Table V-2. Effect of the mutations in the *ef* loop of cyt *b* on the kinetics of electron transfer within *R. sphaeroides* cyt bc_1.

Cyt bc_1	Specific	k_1 (s^{-1})	Famoxadone	k_2 (s^{-1})	Δ CA (Å)
WT	2.35	60,000	5,400	2,300	
H276A (D252)	1.56	42,000	2,800	2,200	3.3
P277A (P253)	1.10	35,000	4,500	1,700	3.0
D278A (D254)	1.43	26,000	2,300	2,300	2.9
D278N	1.88	35,000	2,500	2,400	
D278E	1.6	51,000	6,700	2,900	
D278I	2.41	38,000	4,300	2,000	
D278V	0.57	-	-	-	
D278H	1.49	36,000	4,100	1,500	
N279A (N255)	2.43	37,000	4,300	1,900	1.5
Y280A (Y256)	1.34	7,900	3,200	2,800	0.5
L286A (L262)	0.78	33,000	35,000	740	
L286V	0.8	-	-	-	
L286R	0.75	-	-	-	
L286E	0.88	17,000	12,000	1,900	
L286I	2.4	18,000	2,900	2,300	
S287A (N263)	2.16	55,000	5,700	1,000	0.7
A290S (P266)	2.65	49,000	5,600	1,900	0.9
H291A (H267)	2.54	51,000	4,100	2,000	1.4
I292A (I268)	0.81	4,400	3,000	350	1.4
I292L	1.3	10,000	4,700	1,500	
I292M	0.92	6,200	2,800	1,700	
I292V	0.92	33,000	3,500	1,300	
I292E	0.12	-	-	-	
I292R	0.56	10,000	2,500	1,700	

The rate constants k_1 for electron transfer from [2Fe2S] to cyt c_1, and k_2 for electron transfer from QH_2 to [2Fe2S] were measured in a solution containing 5 μM cyt bc_1, 20 μM Ru_2D, 5 mM $[Co(NH_3)_5Cl]^{2+}$, in 20 mM sodium borate, pH 9.0, 0.01% dodecylmaltoside. The cyt bc_1 was treated with 10 μM $Q_PC_{10}BrH_2$, 1 mM succinate, and 50 nM SCR to completely reduce [2Fe2S] and cyt c_1, and reduce cyt b_H by about 30%. Famoxadone (30 μM) was added where indicated. ΔCA is the

The Y280A mutation decreased the steady-state activity from 2.35 to 1.34, and the rate constant k_1 from 60,000 s^{-1} to 7,900 s^{-1}, without significantly affecting the rate constant k_2. Famoxadone did bind well to this mutant, as indicated by the complete inhibition of reduction of cyt b_H, but it only decreased the rate constant k_1 from 7,900 s^{-1} to 3,200 s^{-1}.

The mutation L286A decreased the steady-state rate by 3-fold, k_1 to 33,000 s^{-1}, and k_2 to 740 s^{-1}. Most surprisingly, famoxadone binding did not significantly affect the rate constant k_1, but it did completely inhibit reduction of cyt b_H. The L286E mutant decreased k_1 to 17,000, while addition of famoxadone only decreased k_1 to 12,000. The conservative mutation L286I decreased k_1 to 18,000, but famoxadone binding decreased k_1 by a larger factor, to 2,900. No electron transfer between [2Fe2S] and cyt c_1 was observed for the mutant L286R.

The mutation I292A decreased the steady-state activity by 2.9-fold, and decreased k_1 to 4,400 s^{-1} and k_2 to 350 s^{-1}. Famoxadone binding had a relatively small effect on k_1, decreasing it only to 3,000 s^{-1}. All of the mutations at I292 led to significant decreases in k_1 and k_2 (Table IV-2). The largest effect was observed for the I292E mutation, which decreased the steady-state activity to 0.12, and eliminated all electron transfer transients in the ruthenium photooxidation experiment. Famoxadone binding eliminated the reduction of cyt b_H observed at 561 nm for all of the mutants, indicating that famoxadone binding was not affected.

Discussion

Changes in the conformation of the ISP play an essential role in the mechanism of cyt bc_1, and it is important to understand how the dynamics of these conformational

changes control electron transfer within the complex. The ruthenium photooxidation technique provides a unique method to measure the rate constants for electron transfer from the [2Fe2S] center to cyt c_1, as well as from QH_2 to the [2Fe2S] center. A number of experiments have indicated that the measured rate constant k_1 for electron transfer from [2Fe2S] to cyt c_1 is rate-limited by a conformational gating mechanism (33). If k_1 was rate-limited by true electron transfer from [2Fe2S] to cyt c_1, then Marcus theory would predict a large dependence on the driving force of the reaction, which depends on the difference in redox potentials of [2Fe2S] and cyt c_1. However, k_1 is independent of pH over the range pH 7.0 to 9.5 where the redox potential of the [2Fe2S] decreases significantly due to deprotonation of His-161 (33). Moreover, the rate constant is not affected by ISP mutations which decrease the redox potential of [2Fe2S] by up to 160 mV (33). Since reduced ISP is predominantly in the *b* state at the beginning of the kinetics experiment (42), the rate constant k_1 provides a direct measure of the dynamics of the conformational change of the ISP from the b-state to the c_1 state.

A number of mechanisms have been proposed for the bifurcated electron transfer reaction at the $Q_{P\ pocket}$ in which the first electron is transferred from QH_2 to [2Fe2S], while the second electron is transferred from semiquinone to cyt b_L (21-29). An important requirement for these mechanisms is that they account for the reversibility of the reaction, as well as minimization of short circuit reactions, such as the delivery of both electrons from QH_2 to [2Fe2S]. Double gating mechanisms have been proposed in which QH_2 only reacts at the active $Q_{P\ pocket}$ when the ISP is in the b-state and both [2Fe2S] and cyt b_L are oxidized (23, 25-29). It has been proposed that the semiquinone anion moves from the distal site near [2Fe2S] to a position near oxidized cyt b_L to favor

electron transfer to the latter (22, 27). Coulombic repulsion would prevent the motion of the semiquinone anion towards reduced cyt b_L, thus preventing a potential short circuit reaction (27). Concerted mechanisms have also been proposed in which QH_2 transfers both electrons to [2Fe2S] and cyt b_L simultaneously without formation of a semiquinone intermediate (23, 26, 28, 29).

It has been proposed that a structural linkage between the quinol substrate in the Q_P binding $_{pocket}$ and the conformation of the ISP might play an important role in the mechanism of bifurcated electron transfer (21). Unfortunately, it has not been possible to experimentally detect QH_2, semiquinone, or Q in the Q_P binding pocket. Nevertheless, $Q_{P\ pocket}$ inhibitors have many similarities to the natural ubiquinol substrate, and it has been suggested that the effects of these inhibitors on the conformational linkage between cyt *b* and the ISP might provide insight into the catalytic mechanism of the bifurcation reaction (21). X-ray crystallographic studies have shown that $Q_{P\ pocket}$ inhibitors including stigmatellin, UHDBT, famoxaodone, and JG-144 displace both the cd1 helix and the PEWY sequence in the ef helix outward to expand the Q_P pocket (21, 43). These changes in the Q_P pocket are relayed to the surface of cyt *b* to form a binding crater which will capture the ISP in the b-state conformation. Stigmatellin binding leads to the largest changes in the Q_P pocket, and forms a hydrogen bond with the His-161 ligand of the reduced [2Fe2S] center, thus increasing its redox potential by 200 – 250 mV, and completely immobilizing the ISP in the *b* conformation (5-8, 30). It has been proposed that QH_2 might bind in a conformation similar to that of stigmatellin, with a hydrogen bond to His-161 to facilitate proton-coupled electron transfer to [2Fe2S] (21, 22).

Famoxadone binds somewhat deeper in the Q_P pocket than stigmatellin, and does

not form a hydrogen bond with His-161 (31). It binds in a U-shaped conformation with a network of interactions between the three aromatic groups on famoxadone and aromatic residues in the Q_P binding pocket (31). Extensive conformational changes on the surface of cyt *b* accompany famoxadone binding to the Q_P pocket (31). These include one domain between residues 160-175 (bovine numbering) that contacts the neck region of the ISP, another domain between residues 262 and 268 which forms the docking crater for the iron-sulfur domain at the end of the *ef* loop, and the middle of the *ef* loop (residues 252-256) which connects the Q_P pocket with the other two surface domains (Figure V-2). The *ef* loop appears to relay conformational changes in the Q_P pocket to the ISP docking crater and neck contact domain. These conformational changes on the surface of cyt *b* trigger a long-range conformational change in the ISP from the loose state to a state with [2Fe2S] proximal to cyt *b* (31). Famoxadone binding to the $Q_{P\ pocket}$ decreases the rate constant k_1 for electron transfer from [2Fe2S] to cyt c_1 from 60,000 s^{-1} to 5,000 s^{-1} (33). Therefore, famoxadone does not completely lock the ISP in the *b* conformation, but instead significantly decreases the rate of release of the ISP from the *b* state to the c_1 state.

In order to further explore the role of the *ef* loop in regulating the dynamics of the ISP, a series of mutants at residues in the *ef* loop were constructed. *R. sphaeroides* cyt *b* residues 276 – 280 correspond to bovine residues 252 – 256 which are in the middle of the *ef* loop on the surface of cyt *b* (Figure IV-2). These residues undergo large displacements upon famoxadone binding, leading to the suggestion that they might relay conformational changes in the Q_P pocket to the ISP docking crater. Surprisingly, mutation of residues H276, P277, D278, and N279 led to relatively small changes in k_1

and k_2, suggesting that if these residues do help relay conformational changes, that function is not sensitive to substitution of individual amino acid side changes. The D278A mutation led to the largest decrease in k_1 for this group, from 60,000 s^{-1} to 26,000 s^{-1}, but no significant change in rate constant k_2. Famoxadone binding to this mutant decreased k_1 to 2,300 s^{-1}, which is similar to the percent reduction observed in wild-type cyt bc_1, suggesting that this mutant does not modulate the effect of famoxadone. The mutation Y280A led to a substantial decrease in k_1 to 7,900 s^{-1}, while famoxadone binding only caused a further decrease to 3,200 s^{-1}. This mutation might cause a conformational change similar to that of famoxadone, limiting the additional effect of famoxadone binding.

R. sphaeroides cyt *b* residues 286 – 292 correspond to bovine residues 262 – 268 in the *ef* loop which forms part of the ISP docking crater. Mutation of residues S287, A290, and H291 had relatively little effect on k_1, which is surprising in the case of H291 since the histidine side chain moves 9.3 Å upon famoxadone binding (31). However, mutations at I292 located in the ISP docking crater near the [2Fe2S] center had a large effect on electron transfer activity (Table 2). The I292A mutation decreased k_1 to 4,400 s^{-1} while famoxadone binding only further decreased it to 3,000 s^{-1}. The rate constant k_2 for QH_2 oxidation was decreased to 350 s^{-1}, indicating that this mutation had an effect on the conformation of QH_2 reaction site. Substitution of I292 with a basic arginine residue was tolerated with a decrease in k_1 to 10,000 s^{-1} and only a modest change in k_2. In contrast, substation of I292 with an acidic glutamate nearly completely eliminated both steady-state activity and electron transfer activity measured by the ruthenium photooxidation method. It is apparent that I292 plays an important role in controlling the

conformation of the ISP.

The effects of mutation of L286 at the tip of the *ef* loop are particularly interesting. The mutation L286A decreases the rate constant k_1 to 33,000 s^{-1} and k_2 to 740 s^{-1}. However, famoxadone binding does not lead to any further decrease in k_1, suggesting that this mutation might block the famoxadone-induced conformational change in the wild-type protein which decreases the rate constant k_1 by such a large factor. The L286E mutation also led to a significant decrease in the rate constant k_1, to 17.000 s^{-1}, while famoxadone binding did not cause much further decrease. The importance of L286 is also illustrated in experiments by Darrouzet and Daldal (14, 19). They found that insertion of one alanine at residue 46 in the neck region of the ISP decreased the rate of the domain movement from the *b* state to the c_1 state to a half time of 10 ms, which could be measured in *R. capsulatus* chromatophores. A second revertant mutation substituting Leu for Phe at residue 286 restored rapid domain movement, which was too fast to measure in chromatophores (19). This finding is particularly remarkable given that cyt *b* residue 286 is more than 25 Å from the neck region of the ISP. Revertant mutations were also found in the ISP neck region for a primary mutation at T288 in the *ef* loop (24). A possible mechanism for this linkage between the *ef* loop and ISP neck region is suggested by the effect of famoxadone binding, which causes coordinated conformational changes in both the *ef* loop region and the cyt *b* residues 179 -187 which contact the ISP neck region. It appears likely that the conformational linkage between the ISP neck region and the cyt *b ef* loop is mediated by the cyt *b* protein using structural linkages similar to those caused by famoxadone binding.

It has been proposed that the conformation of the ISP plays an important role in

several different stages of the mechanism of cyt bc_1 (21). First, it is proposed that binding QH_2 to the active Q_P pocket displaces the cd1 helix and the *ef* loop outwards to capture the oxidized ISP in the *b* state conformation. The formation of a hydrogen bond between QH_2 and His-161 would stabilize the active site conformation, and allow proton-coupled electron transfer from QH_2 to oxidized [2Fe2S]. After the second electron is transferred from semiquinone to cyt b_L and cyt b_H, oxidized Q would leave the Q_P binding pocket and the cd1 helix and the *ef* loop would relax to their original positions, releasing the ISP and allowing it to rotate to the c_1 position and transfer an electron to cyt c_1 (21). An important question about this mechanism is whether ISP is released from the *b* state after the first electron is transferred to [2Fe2S] and the hydrogen bond to His-161 is broken, or remains locked in the *b* state until cyt b_H is reduced. Famoxadone binding is informative in this regard, because it leads to many of the same conformational changes in the ISP binding crater as stigmatellin, but does not form a hydrogen bond to His-161. The rate of release of the ISP from the b-state is decreased from 60,000 s^{-1} to 5,000 s^{-1} by famoxadone binding, but the ISP is not completely locked in the b-state (33). Once the ISP is released from the *b* state and rotates to the cyt c_1 state, there may be conformational linkages that prevent its return to the *b* state under conditions that would lead to short-circuit reactions. When cyt b_H is reduced in the presence of antimycin, an electron is not transferred back to the ISP on a long time scale, suggesting that the ISP does not return to the *b* state in the absence of QH_2. The *ef* loop presents a barrier to the rotation of the ISP between the *b* and c_1 states (19, 32), and this barrier might regulate the rotation in both directions. The present studies have provided additional evidence that the *ef* loop plays an important role in regulating the domain movement of the ISP to facilitate

productive electron transfer and prevent short-circuit reactions.

REFERENCE

1. Trumpower, B. L. and Gennis, R. B. (1994) *Annu. Rev. Biochem.* **63**, 675-716.
2. Trumpower, B. L. (1990), *J. Biol. Chem.* **265**, 11409-11412.
3. Brandt, U. (1998) *Biochim. Biophys. Acta* **1364**, 261-268.
4. Xia, D., Yu, C.-A., Kim, H., Xia, J.-Z., Kachurin, A. M., Zhang, L., Yu, L., and Deisenhofer, J. (1997) *Science* **277**, 60-66.
5. Zhang, Z., Huang, L., Shulmeister, V. M., Chi, Y.-I., Kim, K. K., Hung, L.-W., Crofts, A. R., Berry, E. A., and Kim, S.-H. (1998) *Nature* **392**, 677-684.
6. Iwata, S., Lee, J. W., Okada, K., Lee, J. K., Wata, M., Rasmussen, B., Link, T. A., Ramaswamy, S., and Jap, B. K. (1998) *Science* **281**, 64-71.
7. Kim, H., Xia, D., Yu, C.-A., Xia, J.-Z., Kachurin, A. M., Zhang, L., Yu, L., and Deisenhofer, J. (1998) *Proc. Natl. Acad. Sci. U.S.A.* **95**, 8026-8033.
8. Hunte, C., Koepke, J., Lange, C., Rossmanith, T., and Michel, H. (2000) *Stucture Fold Des*. **8**, 669-84.
9. Sadoski, R. C., Engstrom, G., Tian, H., Zhang, L., Yu, C.-A., Yu, L., Durham, B., and Millett, F. (2000) *Biochemistry* **39**, 4231-4236.
10. Tian, H., Yu, L, Mather, M., and Yu, C. A. (1998) *J. Biol. Chem.* **273,** 27953-27959.
11. Xiao, K., Yu, L., and Yu, C.-A. (2000 *J. Biol. Chem.* **275**, 38597-38604.
12. Tian, H., White, S., Yu, L., and Yu, C.-A. (1999) *J. Biol. Chem.* **274**, 7146-7152.
13. Darrouzet, E., Valkova-Valchanova, M. and Daldal, R. (2000) *Biochemistry* **39**, 15475-15483.

14. Darrouzet E, Valkova-Valchanova M, Moser CC, Dutton PL, Daldal F. (2000) *Proc Natl Acad Sci* U S A. 2000 Apr 25;97(9):4567-72.

15. Nett, J. H., Hunte, C., and Trumpower, B. L. (2000) *Eur. J. Biochem.* **267**, 5777-5782.

16. Gosh, M., Wang, C., Ebert, E., Vadlamuri, S., and Beattie, D. S. (2001) *Biochemistry* **40**, 327-335.

17. Engstrom, G., Xiao, K., Yu, C.-A., Yu, L., Durham, B., and Millett, F. (2002) *J. Biol. Chem.* **277,** 31072-31078.

18. Darrouzet, E., Valkova-Valchanova, M, and Daldal, F. (2002) *J. Biol. Chem.* **277**, 3464-3470.

19. Darrouzet, E., and Daldal, F. (2002) *J. Biol. Chem.* **277**, 3471-3476.

20. Brugna, M, Rodgers, S., Schricker, A., Montoya, G., Kazmeier, M, Nitschike, W., and Sinning, I. (2000) *Proc. Nat. Acad. Sc. US.* **97**, 2069-2074.

21. Esser, L., Gong, X., Yang, S., Yu, L., Yu, C.-A., and Xia, D. (2006) *Proc. Nat. Acad. Sci*. **103** 13045-13050.

22. Hong, S., Ugulava, N., Guergova-Kuras, M., and Crofts, A. R. (1999) *J. Biol. Chem*. **274** 33931-33944.

23. Osyczka A, Moser CC, Daldal F, Dutton PL., (2004) *Nature*. **427** 607-12.

24. Darrouzet E, Daldal F. (2003) *Biochemistry*. **42** 1499-507.

25. Rich, P. (2004) *Biochim. Biochphys. Acta* **1658** 165-171

26. Osyczka, A., Moser, C. C., and Dutton, P.L. (2005) *Trends Biochem. Sci.* **30** 176-182

27. Crofts AR, Lhee S, Crofts SB, Cheng J, Rose S.(2006) *Biochim Biophys Acta*.

[Epub ahead of print]

28. Mulkidjanian, A. Y., (2005) *Biochim. Biophys. Acta* **1709** 5-34

29. Osyczka A, Zhang H, Mathe C, Rich PR, Moser CC, Dutton PL. (2006) *Biochemistry*. **45** 10492-503.

30. von Jagow, G., and Ohnishi, T. (1985) *FEBS Lett.* **185**, 311-315.

31. Gao, X., Wen, X., Yu, C.-A., Esser, L., Tsao, S., Quinn B., Zhang, L., Yu, L., and Xia, D., (2002) *Biochemistry* **41**, 11692-11702.

32. Izrailev S, Crofts AR, Berry EA, Schulten K. (1999) *Biophys J*. **77** 1753-68.

33. Xiao, K., Engstrom, G., Rajagukguk, S., Yu, C.-A., Yu, L., Durham, B., and Millett, F. (2003) J. Biol. Chem. **278** 11419-11426.

34. Downard, A. J., Honey, G. E., Phillips, L. F., and Steel, P. J. (1991) *Inorg. Chem.* **30**, 2259-2260.

35. Moeller, T., Ed. (1957) *Inorganic Synthesis*, Vol. V, p. 185, McGraw Hill Book Company, Inc., New York.

36. Yu, C. A., and Yu, L. (1982) *Biochemistry* **21**, 4096-4101.

37. Yu, L., and Yu, C. A. (1982) *J. Biol. Chem*. **257**, 2016-2021.

38. Mather, M. W., Yu, L., and Yu, C.-A. (1995) *J. Biol. Chem.* **270**, 28668-28675

39. Xiao, K., Yu, L., and Yu, C.-A. (2000) *J. Biol. Chem.* **275**, 38597-38604

40. Liu X, Yu CA, Yu L. (2004) *J. Biol. Chem.* **279**, 47363 – 47371

41. Heacock, C., Liu, R., Yu, C.-A., Yu, L., Durham, B., and Millett, F. (1993) *J. Biol. Chem.* **268**, 27171-27175.

42 Yu CA, Wen X, Xiao K, Xia D, Yu L. (2002) *Biochim Biophys Acta*. **1555** 65-70

43. Esser L, Quinn B, Li YF, Zhang M, Elberry M, Yu L, Yu CA, Xia D. (2004) *J Mol*

Biol. **341** 281-302.

VITA

Shaoqing Yang

Candidate for the Degree of

Doctor of Philosophy

Thesis: STUDIES ON THE CATALYSIS MECHANISM OF CYTOCHROME BC_1 COMPLEX

Major Field: Biochemistry and Molecular Biology

Biographical:

Personal Data:

Born in Linzhou, Henan Province, P.R.China

Education:

Bachelor of Science in biochemistry, Jilin University, Jilin Province, P.R.China,1996; Master of Science in biochemistry & Molecular Biology, Nankai University, Tianjin, P.R. China, 1999; Completed the requirements for the Doctor of Philosophy in biochemistry and molecular biology at Oklahoma State University, Stillwater, Oklahoma in July, 2008.

Experience:

Teaching faculty in Nankai University, P.R. China, 1999-2002

Professional Memberships: American Biophysical Society.

Publications:

Shaoqing Yang, He-Wen Ma, Linda Yu and Chang-An Yu, (2008) On the Mechanism of Quinol Oxidation at Qp Site in Cytochrome bc_1 Complex: Studied by Mutants without Cytochrome b_L or b_H, *J. Biol. Chem.* **Submitted;** He-Wen Ma, **Shaoqing Yang**, Linda Yu and Chang-An Yu, (2008) Formation of disulfide bond between ISP and cytochrome c_1 in cytochrome bc_1 complexes, *Biochimica et Biophysica Acta (BBA) – Bioenergetics,* 1777, 317-326;Sany Rajagukguk*, **Shaoqing Yang***, Chang-An Yu, Linda Yu, Bill Durham, and Francis Millett, (2007) Effect of Mutations in the Cytochrome *b ef* Loop on the Electron-Transfer Reactions of the Rieske Iron-Sulfur Protein in the Cytochrome bc_1 Complex, *Biochemistry*, **46** (7), 1791 -1798 **(* Equal contribution);**Lothar Esser, Xing Gong, **Shaoqing Yang**, Linda Yu, Chang-An Yu, and Di Xia, (2006) Surface-modulated motion switch: Capture and release of iron–sulfur protein in the cytochrome bc_1 complex, *Proc. Natl. Acad. Sci. U.S.A*, **103**(35),13045-13050**;**

Name: Shaoqing Yang Date of Degree: July, 2008

Institution: Oklahoma State University Location: Stillwater, Oklahoma

Title of Study: STUDIES ON THE CATALYTIC MECHANISM OF CYTOCHROME BC_1 COMPLEX

Pages in Study: 163 Candidate for the Degree of Doctor of Philosophy

Major Field: Biochemistry and Molecular Biology

Scope and Method of Study:

The purpose of this study is to further investigate the catalytic mechanism of cytochrome bc1 complexes. With site-directed mutagenesis, we constructed a series of mutant cytochrome bc1 complexes, such as mutants lacking heme b_L and b_H, mutant in which ISP is fixed at c_1-position by engineered inter-subunit disulfide bond, and mutants whose mutations are located in the *ef* loop of subunit cytochrome *b*. I have investigated mutant complexes' biochemical and biophysical properties with EPR, stopflow, spectrophotometer, and so on.

Findings and Conclusions:

In mutant H198N of cytochrome b, no heme b_L is formed. Likewise, in mutant H111N, no heme b_H is formed. The loss of either heme b_L or heme b_H will significantly decrease cytochrome *c* and c_1's reduction rates. However, in the mutant H111N, heme b_L reduction rate is pretty close to that of wild type bc_1. Since heme b_L cannot be reduced unless ISP took one electron from QH_2, we can conclude that ISP reduction rate in H111N is also close to that of wild type bc_1. As a consequence, we can conclude that ISP movement is controlled by the electron transfer in low potential chain. Meanwhile, fast kinetics studies show that antimycin can affect QH2 oxidation at Q_P Pocket. EPR spectra from these two mutants doesn't show the presence of antimycin-resistant radical signal, indicating QH_2 oxidation maybe follows concerted mechanism.

Proteinase K digested cytochrome bc_1 increases superoxide production, indicating proteinous component in cytochrome bc_1 is not required for superoxide production. Further investigation shows that hydrophobic environment and high potential oxidant are required for superoxide production by QH_2.

Purified Mutant protein S141C(ISP)/G180C(cyt. c_1) shows very little catalytic activities. However, after treated with β-mecaptoethanol, its activities can be recovered up to 80% of that of wild type bc_1. Electron transfer rate between ISP and cytochrome c_1 in this mutant is 100 times faster than that in wild type bc_1, further indicating ISP head domain is fixed at c_1-position in this mutant.

Two important residues (I192, L286 in the *ef* loop of *R.S.* cytochrome bc_1 were identified through alanine scanning. Analysis of catalytic activities indicated their bulky side chain plays a role during catalysis. Further investigation is needed.

ADVISER'S APPROVAL: Dr. Chang-An Yu